AD-A031 006 THIOKOL CORP HUNTSVILLE ALA HUNTSVILLE DIV F/G 21/9.2
MEAN FLOW/ACOUSTIC INTERACTIONS AND STATISTICAL ANALYSIS OF STE--ETC(U)
JUN 76 R L CLICK
UNCLASSIFIED U-76-18 AFOSR-TR-76-1099 F44620-74-C-0080 NL

1 OF 2
ADA031006

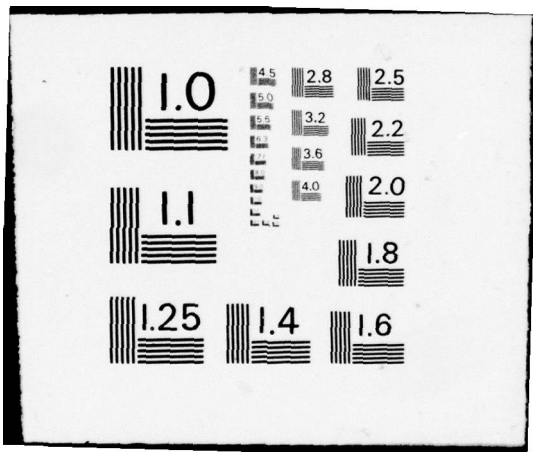
1.0
1.1
1.25
1.4
1.6
1.8
2.0
2.2
2.5
2.8
3.2
3.6
4.0
4.5
5.0
5.5

AFOSR - TR - 76 - 1099

Control No. U-76-18

12

FC

MEAN FLOW/ACOUSTIC INTERACTIONS AND STATISTICAL ANALYSIS OF STEADY STATE COMBUSTION OF NONMETALLIZED COMPOSITE SOLID PROPELLANTS

DR. R. L. GLICK
THIOKOL CORPORATION
HUNTSVILLE, ALABAMA 35807

FINAL REPORT, CONTRACT F44620-74-C-0080

MAY 1, 1974 - JUNE 30, 1976

Prepared for:

Department of the Air Force
Air Force Office of Scientific Research (AFSC)
Bolling Air Force Base, D. C. 20332

NOTICE

Research sponsored by the Air Force Office of Scientific Research (AFSC), United States Air Force, under Contract F44620-74-C-0080. The United States Government is authorized to reproduce and distribute reprints for governmental purposes notwithstanding any copyright notation hereon.

FOREWORD

This is a final report covering the work completed under Contract F44620-74-C-0080 for the period 1 May 1974 through 30 June 1976. Publication of this report does not constitute Air Force approval of the findings or conclusions contained herein. It is published only for the exchange of data and stimulation of ideas.

APPROVED BY:

G. F. Mangum
Project Director

C. C. Lee
Director, Programs

TABLE OF CONTENTS

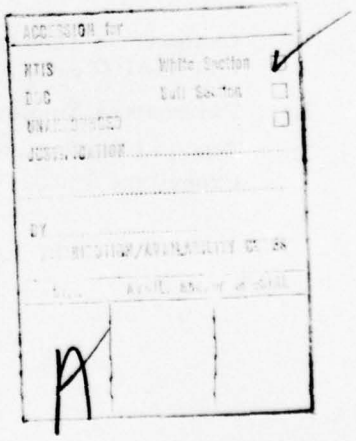

LIST OF FIGURES

LIST OF TABLES

INTRODUCTION

The T-burner has been employed for sometime to define linear response characteristics of solid propellants to fluctuations in environmental conditions. Although qualitative assessment of relative stability is accomplished without undue difficulty, quantitative determinations are complicated by the need for quantitative definition of the bosses. Until 1972 when Culick[1] first deduced the presence of acoustic/mean flow interactions (A/MFI) from the linearized, one-dimensional equations of change, losses were considered determinable from properly executed experiments. However, Culick's analysis introduced the flow turning loss and vent gain. The former is usually negligible in burners configured for pressure coupled measurements. Unfortunately, the latter is not. Because the flow turning gain varies with mass flow rate, it renders direct T-burner loss measurement techniques impotent. Therefore, indirect "measures" of this term were effected by including it within the statistical data correlation procedure. Unfortunately, this indirect procedure is not altogether practical. The lack of precision in the data bits combine with the necessity to define three unknowns to require a very large (and expensive) data base in order to define the vent gain with confidence.

It is well known that qualitative features of nonsteady, two-dimensional flows can be determined by employing the so-called hydraulic analogy. Consequently, the purpose of this portion of the program was to explore the vent region flow field with the hydraulic analogy.

Since 1969, steady-state composite propellant combustion modeling has been dominated by the Beckstead, Derr, Price (BDP) model[2,3]. Subsequent development of the basic model has extended it to bidisperse AP propellants with aluminum[4], polydisperse AP propellants with aluminum[5], and nitramine propellants[6 - 8]. The extensions to bidisperse AP and nitramine propellants were made by assuming all particles burn at the same rate; the extension to a polydispersion was made by "coalescing" all particles above a critical diameter into a single, mean particle (those below the critical diameter were assumed to react in the surface melt); the extension to nitramines was made by introducing a surface melt criteria and different particle surface constraints with and without a surface melt. A major difficulty with these analyses lies with the fact that although mean states are involved the mean states are postulated rather than deduced. In short, "are the mean states employed correct?" In 1973 Glick[9, 10] presented a "complete" statistical analysis of additive free composite propellant combustion that eliminated the need to select a mean state because all possible states were explicitly included in the analysis. This approach appeared to be a viable alternative to the mean state schemes and included true mixed, polydisperse oxidizer capabilities. The purpose of the combustion modeling aspect of this program was to develop the "complete" statistical approach.

TECHNICAL DISCUSSION

COMBUSTION MODELING

Introduction

A revolution, wrought by combat pilot's demands for low missile exhaust signature, has recently occurred in propellant formulations for many tactical applications of solid propellant rockets. This demand for low signature has created demands for new binders, new oxidizers, new additives, and new formulations. Moreover, as significant amounts of condensed phases are verboten because they enhance visible signature, damping of acoustic disturbances in the motor's chamber is decreased relative to that for a similar formulation with condensed phases in the products. Consequently, combustion instability has returned as a real and frequent problem. Unfortunately, there is neither a sufficient base of experience nor adequate understanding of combustion phenomena (this extends to the common AP/hydrocarbon propellants too) to solve low signature propellant formulation problems expeditiously if instability is a factor. As a result, the propellant formulator faces situations in which rate, exponent, temperature sensitivity, physicals, processing, and energetics are constrained* and stability is demanded. In the ballistics arena the formulators "weapons" are strand burner, T-burner, particle collection bomb, and ballistic test motor. Evidence that these "weapons" can prevail exists in every operational motor. Unfortunately, as time progresses, the competition becomes ever fiercer as new ingredients and tighter constraints enter the fray. Consequently, our past successes may be more preliminary than main events. In summary, real formulation problems exist with low signature propellants if stability requirements are imposed.

The overall objective of this work is to construct an analytical model describing steady-state combustion of non-metallized, polydisperse composite propellant. This model can then be employed within a computer aided propellant formulation strategy to assist in the development of propellants capable of meeting the challenging constraints imposed by today's weapons systems. Basically, the parameters in the model would be defined with a small baseline of data for the oxidizer, binder, additive system under consideration. With a viable model this "baselined model" would be capable of accurately predicting ballistic parameters within the baseline propellant(s) family. Consequently, either the propellant formulator could interact directly with the baselined model to satisfy design objectives or non-linear optimization techniques could be employed with the baselined model to define an optimal (to some criteria) formulation for the design constraints.

It is very important to note that a steady-state combustion model can also define nonsteady (linear and nonlinear) combustion characteristics

*As might be expected, the lower bound of these constraints often represents the state-of-the-art!

in the low and mid-frequency regimes through the Z-N procedure.* Therefore, the aforementioned computer aided propellant formulation strategy can include instability constraints as well as steady-state ones. Indeed, extension of the model developed herein into the nonsteady regime via the Z-N procedure is currently underway at Purdue University under AFRPL funding.

It would be extremely satisfying to state that the modeling aspect of this program has satisfied all of its objectives. However, it hasn't. Indeed, we have reversed our field in the combustion modeling area and are now proceeding in a direction considerably different from the original one.

Fundamentals of Statistical Combustion Modeling

The "clay" of the propellant formulator is heterogeneous solid propellant. These propellants are admixtures of solid particles (oxidizers and additives) and binder (polymer and additives) and the total solids content is usually as large as possible because of energetics constraints. Therefore, the solid propellant is literally a packed bed of polydisperse particles "filled" with binder. The admixture is most often formed by blending components in high shear mixers. Therefore, it is expected that the packing is random. This expectation is supported by the isotropy shown by macroscopic properties (ballistic, physical). However, packing fraction measurements indicate a higher percentage of theoretical (an ordered packing) than is apparently** achievable through complete randomization. At first, these bits of evidence appear to conflict; however, harmony is restored by assuming that the solids structure consists of ordered, multiparticle aggregates that are themselves randomly arranged. Therefore, there is order on the scale of particle size, but long range disorder. It is interesting to note that nature has chosen precisely this arrangement for liquid structure (molecules represent short range order but liquid is disordered). Therefore, this structure is common in nature.

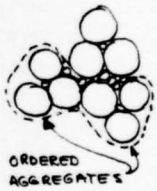

The burning surface traverses the solid. Therefore, the burning surface must reflect characteristics of the solid. Although the chemical discretization wrought by the heterogeneous structure can be softened by the presence of surface melts, there appears little possibility that the random discreteness wrought by the solids internal structure can be completely washed out. Therefore, a random, discrete structure is expected on the burning surface. This means that all states of all particles will be present on the burning surface. By all states it is meant that there is a sequence of states between the state of a particle as it emerges at the burning surface and the state of that particle as it "leaves" the burning surface (either consumed or ejected) and that every one of these sequential states will be represented.

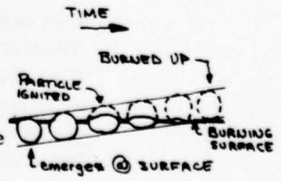

SEQUENCE OF STATES BETWEEN EMERGENCE AND CONSUMPTION

*The Z-N procedure[11, 12] enables one to utilize a steady-state model to predict nonsteady behavior as long as the reactive zones behave in a quasi-steady fashion.

**No one has solved the theoretical problem of the maximum packing fraction obtain able with a random, polydispersion of spheres. Therefore, we don't know if theory/experiment are harmonious or not.

The first thing to note is that the state of a particular particle* on the burning surface is always changing. Therefore, heterogeneous propellant combustion is never steady-state in the classical sense that nothing varies in time. However, rocket motor experience clearly demonstrates that steady-state condition can be closely approximated. Since the whole is the sum of its parts, this demonstrates the following: (1) the motor follows the mean behavior of all particles inhabiting the burning surface and (b) the mean phenomena can be stationary in time. In other words, ballistic performance of a rocket motor and ballistic parameters of heterogeneous propellant depend upon ensemble means of the deflagrating surface's microstates! Therefore, heterogeneous propellant combustion phenomena is a stochastic phenomena. Consequently, successful attacks on heterogeneous propellant phenomena must come from a combination of stochastic and more conventional methods of analysis. Although interest is centered herein on combustion phenomena, this philosophy must also hold for both processing and physical properties.

Ballistic parameters represent ensemble means of microstates. In practical propellants the particulates are polydisperse. Therefore, the burning surface's microstates will be spread among a distribution of distinguishable particles. Ensemble averaging can be accomplished at roughly three levels. The crudest (and hence the least realistic) is to simply average all microstates into a single mean state. This is the one-dimensional approach. Since this means that the multiplicity of distinguishable microstates are "crammed" into a unique mean, this model can predict only gross phenomenological characteristics because all information pertaining to the diversity of the microstructure has been lost in the averaging process. Therefore, these models are inherently incapable of predicting detailed particle size effects. All one-dimensional combustion models are of this type[13 - 19]. The next level of "averaging" involves averaging of the microstates associated with distinguishable particles. In this "petite ensemble" method diversity due to distinguishable particles appears explicitly while diversity due to a distinguishable particle's microstates appears implicitly. Therefore, "petite ensemble" models can predict particle size effects. The statistical combustion model developed under this program and that of Miller, et al.[20, 21] fall into this category. The statistical combustion models of Cohen, et al.[4] and Sammons[5] lie somewhere between this and the former category because they employ an equal rate hypothesis. That is, these models "recognize" distinguishable particles but presume that the distinguishable particles all have the same regression rate. The ultimate reality, because it is what nature does, comes from recognizing all microstates in a grand ensemble. Glick[9, 10] has partially formulated a combustion model of this type.

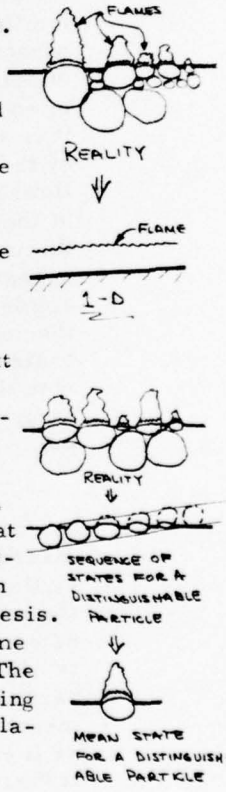

It is important to note that computational effort rapidly escalates with complexity. At the one-dimensional level only one flame structure must be computed; at the "petite ensemble" level one must compute as many flame structures as there are distinguishable particles; at the grand

*Devote the "state of a particular particle" by its "microstate".

ensemble level as many flame structures as there are microstates must be computed. Moreover, at the grand ensemble level each microstate is always nonsteady and there is no reason (other than mathematical necessity) to assume the condensed phase is homogeneous. Thus, at the grand ensemble level one is faced with a virtually overwhelming computational burden. On the other hand, "petite ensemble" averaging provides huer-istic reasons for treating a distinguishable particle's flame structure as ensemble-steady and the condensed phase as homogeneous. Consequently, it appears that the "petite ensemble" approach offers the most quality information per unit cost. For this reason it will prevail for a consider-able period of time. This is the theoretical approach followed in this work; this is the reason that effort on the grand ensemble approach was discontinued.

Because of the random, discrete structure of heterogeneous propellants, the burning surface possesses a random, discrete structure. Attention is focused herein on this structure and, in particular, at the basic "element" of this structure: an oxidizer particle and its "binder". These fuel surfacer/oxidizer particle pairs are the "fundamental parti-cles" of statistical combustion modeling. Because of the random struc-ture of the solid, the population of fuel surface/oxidizer particle pair microstates for any distinguishable pair will be random.

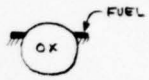

FUEL SURFACE/OX PARTICLE PAIR

The purpose of statistical analysis is to relate mean behavior to individual microstate behavior. Since the whole is the sum of its parts, this is accomplished by summing all microstates on the burning surface. Consider the control volume sketched in Figure 1. For this control volume mass and energy conservation (neglect kinetic and potential energy) give[22]

$$dm/dt = \oint_{S_p} \rho \vec{u} \cdot d\vec{S} + \oint_{S_o} \rho \vec{u} \cdot d\vec{S} \qquad (1)$$

and

$$\oint_{S_o} \vec{q}'' \cdot d\vec{S} - \oint_{S_o+S_p} p\, dV/dt = dE/dt + \oint_{S_o} \rho h \vec{u} \cdot d\vec{S} + \oint_{S_p} \rho h \vec{u} \cdot d\vec{S} \qquad (2)$$

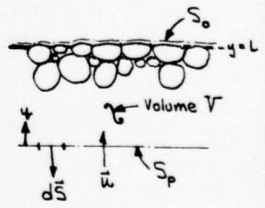

CONTROL VOLUME
FIG. 1

where the fact that $|\vec{q}''| = 0$ on S_p has been employed. Assume that S_p moves such that the volume in the control volume is stationary $[V \neq V(t)]$. Then to an excellent approximation $m \neq m(t)$. The stored energy E is

$$E = \oint_{S_p} \left(\int_0^L \rho e\, dy \right) dS \qquad (3)$$

Since $|\vec{u}| = \bar{r}$, $\rho = \rho_c$, and $h = h_{c,\infty}$ on S_p , Eq. (1) becomes, in the moving coordinate system,

$$\bar{r}\rho_c S_p = \oint_{S_p} m'' dS = \oint_{S_o} m'' dS \tag{4}$$

With this relation, Eq. (3), and the fact that $V \neq V(t)$, Eq. (2) becomes

$$\oint_{S_o} \vec{q}'' \cdot d\vec{S} = d\left[\oint_{S_p}\left(\int_0^L \rho e dy\right) dS\right]/dt + \oint_{S_o} (h_c - h_{c,\infty}) m'' dS \tag{5}$$

Equations (4) and (5) are "integral" equations that constrain the phenomena.

Assume that there are Q microstates (j = 1, Q) on S_o . Then Eqs. (4) and (5) become

$$\bar{r}\rho_c = \sum_{j=1}^{Q} \oint_{\Delta S_{o,j}} m'' dS / S_p \tag{6}$$

and

$$\sum_{j=1}^{Q} \left\{ \oint_{\Delta S_{o,j}} \left[q''_{s} - (h_{c,s} - h_{c,\infty}) m'' - \frac{d}{dt}\left(\int_0^L \rho e dy\right)\right] dS \right\} = 0 \tag{7}$$

On the individual microstate level q''_s, $h_{c,s}$, m'' are functions of time and ρ , e are functions of y and t because of temperature gradients and the discrete structure of the condensed phase. Consequently, if <u>all</u> distinguishable microstates are to be "counted" (grand ensemble method) <u>at least</u> Q simultaneous ordinary differential equations must be solved to define r. Since Q is a <u>very</u> large number, this approach is currently computationally impossible.

There are many more microstates than distinguishable particles. Therefore, to reduce the computational burden define a <u>suitable</u> mean microstate for each distinguishable particle and then "count" distinguishable particles. This is the petite ensemble approach. Let Q_p be the number of particles and N_j the number of microstates for the j^{th} distinguishable particle. Then $Q = \sum_{j=1}^{Q_p} N_j$ and $Q_p << Q$. With this subdivision of microstates Eqs. (6) and (7) become

$$\bar{r}\rho_c = \sum_{j=1}^{Q_p} \left(\sum_{k=1}^{N_j} \oint_{\Delta S_{o,k}} m'' dS \right) / S_p \tag{8}$$

and

$$\sum_{j=1}^{Q_p}\left\{\sum_{k=1}^{N_j}\int_{\Delta S_{o,k}}\left[q''_{fw}-(h_{c,w}-h_{c,\infty})m''-\frac{d}{dt}\left(\int_0^{L_j}\rho e\,dy\right)\right]dS\right\}=0 \qquad (9)$$

In both equations the inner sum represents the sum over all microstates associated with the j^{th} distinguishable particle. Since these microstates are similar to those of an appropriate monodisperse propellant, the inner sums represent ensemble averages* for a sequence of monodisperse pseudo-propellants.** In this fashion one is lead quite naturally to the concept that the combustion phenomena of propellants with mixes, polydisperse oxidizers can be related mathematically to burning rates from monodisperse, psuedo-propellants if the fuel surface/oxidizer particle pairs act independently. In other words, a complex poly-phenomena can be reduced to a sequence of simpler mono-phenomena; the well known divide and conquer strategy.

Other advantages accrue with the petite ensemble strategy. Because ensemble averages do not fluctuate randomly in time (the summation eliminates the "noise" due to the randomness) (a) only temporal fluctuations coherent with environmental fluctuations need be accounted for and (b) all monodisperse pseudo-propellant condensed phase thermophysical properties and thermal wave thicknesses are those for the bulk propellant*** sizes are small compared to the thermal waves thickness. The fact that thermal wave thicknesses are equivalent for all pseudo-monodisperse propellants implies that lateral, conductive energy transport in the condensed phase will be small.

Application of the mean value theorem for integrals to Eqs. (8) and (9) yields

$$\bar{F}\rho_c = \sum_{j=1}^{Q_p}\bar{m}''_j\,\Delta S_{o,j}/S_p \qquad (10)$$

*Term these ensemble averages petite ensemble averages to show that they apply to a particular distinguishable particle.

**This is really a mathematical construction; the pseudo prefix denotes that these monodisperse propellants can not exist in nature.

***Recall that the pseudo-propellant is a mathematical construct. As the condensed phases structure is random, a petite ensemble psuedo-propellant mean for the condensed phase must include all possible arrangements for those particular distinguishable particles. The mean of this sum is the mean of all possible arrangements. In other words, the bulk propellant.

and

$$\sum_{j=1}^{Q_p} \left[\bar{q}''_{t_w} - \overline{(h_{c,w} - h_{c,\infty})\dot{m}''} - \frac{d}{dt}\left(\int_0^{L_j} \rho c \bar{T}\, dy \right) \right] \Delta S_{o,j} = 0 \qquad (11)$$

where the bar over denotes suitable mean values. The integral energy equation is obviously satisfied when each summand is identically zero. Since the summand augmented by lateral condensed phase energy transfer is the mean energy equation for a fuel surface/oxidizer particle pair and lateral energy transport is small in the condensed phase, any valid solution for the mean microstate of a monodisperse pseudo-propellant can be employed with Eq. (10) to compute the mean rate of a polydisperse propellant.

Since $\bar{\dot{m}}''_j \Delta S_{o,j} = \bar{\dot{m}}''_{p,j} \Delta S_{p,j}$ where the subscript p refers to quantities based on the projection of $\Delta S_{o,j}$ on S_p, Eq. (10) can be rewritten as

$$\bar{r}\rho_c = \sum_{j=1}^{Q_p} \bar{\dot{m}}''_{p,j} \Delta S_{p,j} / S_p \qquad (12)$$

If the planar statistics of the burning surface are stationary, differentiation of Eq. (12) yields

$$\partial \bar{r} / \partial ( ) = \rho_c^{-1} \sum_{j=1}^{Q_p} \left[\partial \bar{\dot{m}}''_{p,j} / \partial ( ) \right] \Delta S_{p,j} / S_p \qquad (13)$$

where ( ) denotes any environmental variable (p, T_∞, X flow, etc.). Thus, with some manipulation and the appropriate definitions

$$\bar{v} = \sum_{j=1}^{Q_p} \bar{\dot{m}}''_{p,j} \bar{v}_j \Delta S_{p,j} / (\bar{r}\rho_c S_p) \qquad (14a)$$

$$\bar{\sigma}_p = \sum_{j=1}^{Q_p} \bar{\dot{m}}''_{p,j} \bar{\sigma}_{p,j} \Delta S_{p,j} / (\bar{r}\rho_c S_p) \qquad (14b)$$

$$\bar{\mathcal{R}}_p = \sum_{j=1}^{Q_p} \bar{\dot{m}}''_{p,j} \bar{\mathcal{R}}_{p,j} \Delta S_{p,j} / (\bar{r}\rho_c S_p) \qquad (14c)$$

$$\bar{\mathcal{R}}_v = \sum_{j=1}^{Q_p} \bar{\dot{m}}''_{p,j} \bar{\mathcal{R}}_{v,j} \Delta S_{p,j} / (\bar{r}\rho_c S_p) \qquad (14d)$$

These relations show that all important ballistic parameters can be computed from pseudo-monodisperse values. They also show that if the pseudo-monodisperse propellant mean properties ($\bar{}$) are bounded the polydisperse mean property ($\bar{}$) lies within these bounds.

The central task in the petite ensemble approach is to determine appropriate monodisperse pseudo-propellant means. Since the mean microstate must satisfy the constraints

$$\bar{\dot{m}}''_{p,j} = \oint_{\Delta S_{p,j}} \dot{m}''_{p,j}\, dS \,/\, \Delta S_{p,j} \tag{15}$$

and

$$\bar{\dot{q}}''_{p,j} = \oint_{\Delta S_{p,j}} [(h_{c,w} - h_{c,\infty})\dot{m}''_{p,j} + \frac{d}{dx}\left(\int_0^{L_j} \rho c \bar{T}\, dy\right)]\, dS \,/\, \Delta S_{p,j} \tag{16}$$

These, together with the phenomenological fuel surface/oxidizer particle pair combustion model, represent the major instruments for defining appropriate means. For this purpose these integrands can be interpreted as a value for a particular microstate and dS as the surface area occupied by particles with that microstate. Assume a reasonable functional form for $\dot{m}''_{p,j}(t)$. Then, since temporal and spatial microstates are related by the ergodic surmise (stationary phenomena), the mass flux from any microstate can be determined. The number of specific microstates is defined by assuming a burning surface topography. The oxidizer particle size distribution defines the number density of j^{th} oxidizer particles (dN_j/dV) as only those j^{th} particles lying within $\pm D_j/2$ from the burning surface can intersect it and all "depths" of intersection $-D_j/2 \le y \le D_j/2$ are equally probable, the number of particles in any specific microstate can be determined. By combining these two steps mean values can be defined in terms of parameters in the forms assumed for mass flux and surface topography.

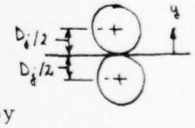

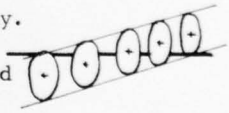

There now appears to be several ways to proceed. They depend upon whether Eq. (16) is employed as a relation for the mean state or as a tool to assist in defining the mean state. In the first approach the mean state is defined by requiring that the mean microstate be an accessible microstate and then Eq. (16) employed with the physiochemical combustion model to define $\bar{\dot{m}}''_{p,j}$, etc. Another approach would be to employ certain aspects of the physiochemical combustion model (i.e., surface pyrolysis law(s)] to define $h_{c,s}$ in terms of $\dot{m}''_{p,j}(t)$ and then Eq. (16) to define $\dot{q}''_s$. By requiring the mean microstate to be an accessible microstate $\dot{m}''_{p,j}$, etc. could then be defined.

The above is vague; it is difficult to be general here without being vague. An important point is that surface topography, $m''_{p,j}(t)$, and the mean state cannot all be arbitrarily specified if a consistent model is desired.

The discussion above has concentrated on the situation where fuel surface/oxidizer particle pairs are independent and the condensed phase preheat zone is much thicker than the largest oxidizer particle. Both assumptions are untrue to some degree. Does this invalidate the approach? No, it doesn't, but it does make it more complex because inter-particle interactions must be considered to relax these assumptions. Fortunately, on a deflagrating surface there is a finite "memory" because the combustion process literally "burns up" the "distant" past. Thus, interactions are limited to nearby particles. Interactions will occur through reactive zone interactions that modify q''_s, lateral energy transport in the condensed phase, and fluctuations in $T(y)$ from the mean. All aspects are related because they depend upon the probability of finding another particle with specific microstate within a certain distance from the particle being considered and the variation of the interaction with distance. Since phenomological laws are known for interactions and the number density of specific particles can be computed because the media is random, these interactions should be calculable.* This represents the current frontier of the theory.

Review of Current Models

To define the current technical position the status of steady-state combustion modeling must be surveyed. Current combustion models come in two forms: one-dimensional and statistical. One-dimensional models are inherently incapable of quantitative description of ballistic phenomena because heterogeneity is not included in an operational fashion. Since one-dimensional combustion models have been reviewed elsewhere[13 - 19], only statistical models will be reviewed herein.

Hermance Model[23] - Steady-state statistical combustion modeling was initiated by Hermance. His creative step was to combine a detailed physiochemical model for spherical oxidizer particle combustion with statistical concepts defining the mean microstate. Figure 2 illustrates the physiochemical model for a fuel surface/oxidizer particle pair. The unique feature is a crevice at the oxidizer/binder interface wherein heterogeneous reaction between gaseous oxidant and solid fuel occurs.

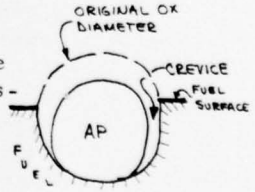

Fig. 2 Hermance Model (Ref 23)

Hermance employed the continuity equation

$$\bar{r}_{p_c} = \bar{m}''_f (S_f / S_p) + \bar{m}''_{ox} (S_{p,ox} / S_p) + \bar{m}''_{sr} (S_{p,sr} / S_p) \qquad (17)$$

*Miller, Donohue, and Peterson[21] have introduced interactions in an approximate way. This work is reviewed in the next section.

where the mass fluxes on the RHS were means for burning fuel surface/oxidizer particle pairs and the areas were for all pairs on the burning surface. It was subsequently assumed that the oxidizer regression rate was a step function

$$r_{ox} = 0 \qquad (0 \le t < t_{ign})$$
$$= r'_{ox} \qquad (t \ge t_{ign}) \tag{18}$$

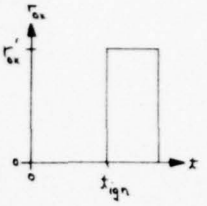

where t = o when the particle first penetrates the burning surface and t_{ign} is the ignition delay. Since the heterogeneous surface reaction requires oxidizer decomposition, $m''_{sr} = o$ for $o \le t < t_{ign}$. Therefore, for $o \le t < t_{ign}$ there is only fuel vapor flow from the surface of a fuel surface/oxidizer particle pair. Consequently, with an ignition delay $t_{ign} > o$, it is clear that the burning surface is populated with some fuel surface/oxidizer particle pairs possessing $m''_{ox} = m''_{sr} = o$. Applying Eq. (10) to the burning surface and noting that $m''_{ox} = m''_{sr} = o$ for some fuel surface/oxidizer particle pairs yields

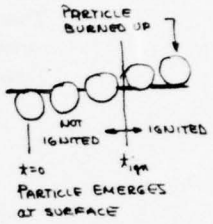

$$\bar{r}_{p_c} = \bar{\dot{m}}''_{p,f}(S_{p,f}/S_p) + \left[\bar{\dot{m}}''_{p,ox}(S_{p,ox}/S_p) + \bar{\dot{m}}''_{p,sr}(S_{p,sr}/S_p)\right]_{ign} \tag{19}$$

Contrasting Eqs. (17) and (19) shows that the former employs mean fluxes for ignited particles with surface areas for all particles. This is not consistent. Since $S_{p,ox,ign} < S_{p,ox}$ and $S_{p,sr,ign} < S_{p,sr}$, the rate predicted by Hermance's equation will be too large if all other things are equal. As the inconsistancy varies with t_{ign} and t_{ign} varies with pressure, pressure exponent will also be effected. However, when $t_{ign} \sim o$, this inconsistency vanishes. Therefore, Hermance's theory is limited to small ignition delays by this omission.

Hermance's analysis assumes the fuel surface is a plane. Therefore, the number of particles intersecting the surface S_p per unit of S_p is

$$dN/dS_p = D\, dN/dV \tag{20}$$

For the spherical particles assumed in this analysis the volume fraction of oxidizer is $\zeta_{ox} = (\pi D^3/6)\frac{dN}{dV}$, and the planform of each intersection of a particle with S_p is circular. Since the fraction of S_p occupied by oxidizer is ζ_{ox} $(dS_{p,ox}/dS_p = \zeta_{ox})$ and the mean diameter of intersections between S_p and the oxidizer particles is defined by $dS_{p,ox}/dS_p = (\pi \bar{D}^2/4)(dN/dS_p)$, algebraic manipulation gives

$$\bar{D} = \sqrt{2/3}\, D \tag{21}$$

This dimension, the mean for all particle intersections, was employed to define the characteristic dimension for the mean deflagrating state. However, since all particles are not burning, this assumption is inconsistent with physical reality unless $t_{ign} = o$. Note that this dimension defines characteristic latitudes on the spherical particle.

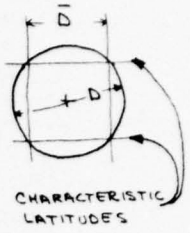

Assuming that the fuel regression rate is steady,

$$r_f = \bar{r} \tag{22}$$

Therefore, if L is the vertical distance from the north pole of an oxidizer particle to a characteristic latitude, the time required for the binder to regress to a characteristic latitude is

$$t_c = L / \bar{r} \tag{23}$$

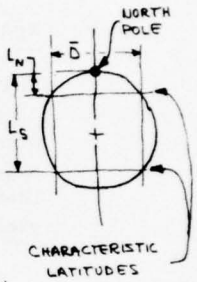

With the step function assumed for $r_{ox}(t)$ it is clear that, if $t_{ign} < t_{c,N}$ intersections with ignited particles can occur in both northern and southern characteristic latitudes. However, if $t_{c,N} < t_{ign} < t_{c,S}$ only the southern characteristic latitude is acceptable. Finally, if $t_{ign} > t_{c,S}$, neither characteristic latitude is acceptable! The latter situation means the model breaks down. The first situation implies the characteristic mean state is degenerate (northern and southern characteristic latitudes are both accessible). Hermance assumes intersections occur only at the southern characteristic latitude. This requires $t_{ign} > t_{c,N}$. However, aforementioned inconsistencies require $t_{ign} \sim 0$.* Hermance's model is, therefore, inconsistent under all conditions.

Hermance assumes the mean fissure width ϵ is given by

$$\epsilon = D - \bar{D} \tag{24}$$

Therefore, the mean heterogeneous reaction area per particle is

$$\Delta S_{sr} = \pi \bar{D} (D - \bar{D}) \tag{25}$$

and the total heterogeneous reaction area ratio is

$$S_{sr} / S_p = \pi \bar{D} (D - \bar{D}) \, dN/dS_p \tag{26}$$

The fuel surface is planar. Since $S_{p,ox} + S_f = S_p$ and $S_{p,ox} / S_p = f_{ox}$

$$S_f / S_p = 1 - f_{ox} \tag{27}$$

*This can be "cured" by accounting for the degeneracy of the mean state when $t_{ign} < t_{c,N}$.

Thus, all area ratio's in Eq. (17) are defined.

By assuming the temperature of oxidizer and binder are equal, oxidizer decomposition is an equilibrium process and the decomposition product is an ideal gas, and kinetic expressions for the heterogeneous reaction, the heterogeneous reaction mean mass flux was related to the surface temperature. By assuming a pyrolysis relation for the binder its mean mass flux was also related to surface temperature. For steady-state combustion binder and oxidizer mass flows must be in proportion to the ingredients. Therefore,

$$\overline{\dot{m}}''_{p,ox} = \overline{\dot{m}}'' \alpha_{ox} / \gamma_{ox} \qquad (28)$$

Consequently, the only unknown is the surface temperature.

The surface temperature was defined by solving a one-dimensional energy equation with heat release at the burning surface and at a gas phase flame. The latter's standoff distance was computed by assuming a second order reaction. Consequently, a complete set of equations relating mean rate to pressure and initial propellant temperature through roughly seventeen "parameters" was obtained.

Hermance also considered propellants with polydisperse spherical oxidizer. To extend the unimodal analysis to this situation it was implicitly assumed that fuel surface/oxidizer particle pairs with different size oxidizer particles possess the same deflagration rate.* Therefore, all have the same surface temperature so that the entire burning surface can be treated with the energy equation employed with the monodisperse propellant.

Hermance computed rate versus pressure for two monodisperse polysulfide/AP propellants and compared the results with data. Figure 3 shows that the model is capable of virtually duplicating rate/pressure characteristics for a specific propellant but that extrapolation (without parameter changes) to the same formulation with different particle size is definitely not quantitative. Since the model is not self-consistent, this behavior is not surprising.

Another major difficulty with Hermance's model is the dominant nature of the crevice. In the words of Reference 2, "This is unfortunate because in actuality the oxidizer does not regress as (Hermance) assumed; it does not maintain an overall spherical shape and there is little evidence of crevice formation.". Reference 2 notes further that SEM pictures tend to deny crevice existence and show that the oxidizer particles are recessed at high pressures and protrude at low pressure. Therefore, Ref. 2 concludes that "it seems very unlikely that the combustion mechanism could be dominated by a nonexistent cusp (crevice) and the associated reaction". This physical evidence led Beckstead, Derr, and Price[2,3] to discard Hermance's unit physiochemical model as physically unrealistic and develop a more realistic one.

*This will be termed the equal rate hypothesis.

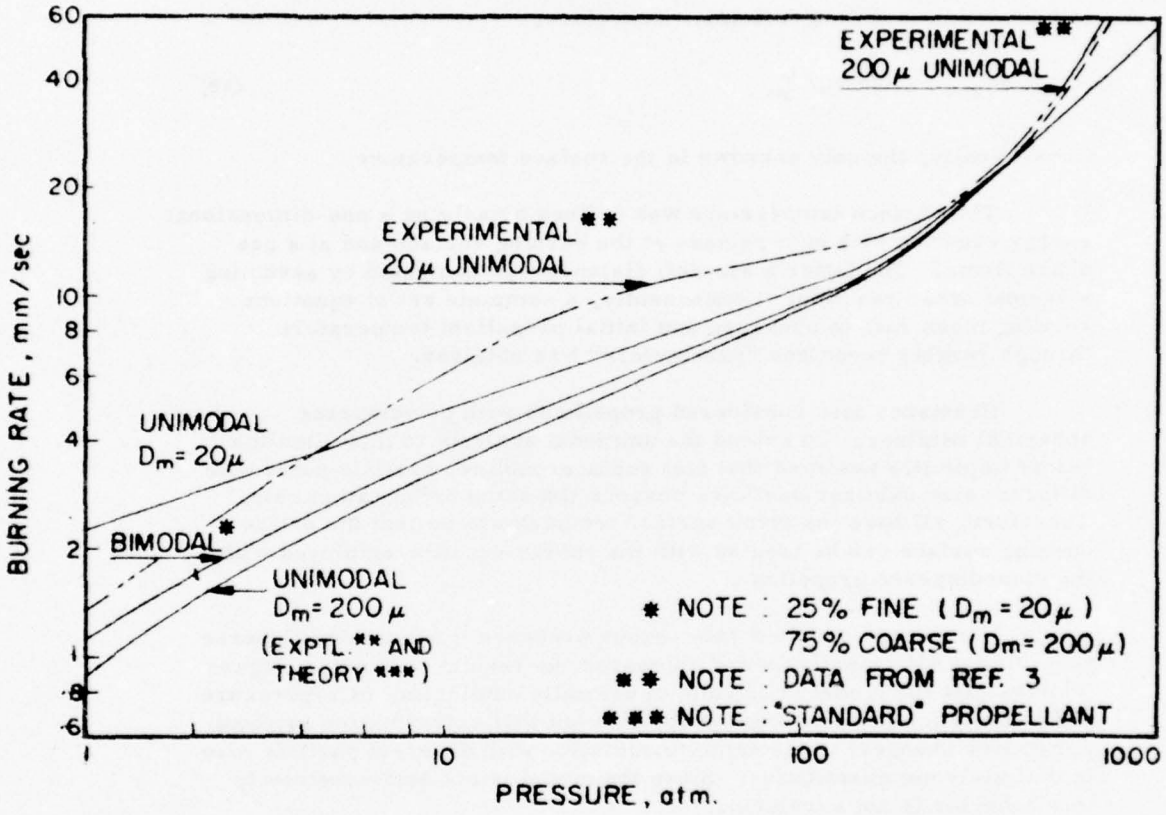

Figure 3 Comparison Theory and Experiment
Hermance's Model (Ref. 23)

Because the model is neither physically realistic nor self-consistent there seems to be little reason to pursue this model further.

Beckstead, Derr, Price Model[2,3] - Beckstead, Derr, and Price (BDP) basically embedded a realistic physiochemical model for fuel surface /oxidizer particle pair combustion in the statistical procedure developed by Hermance to upgrade that model. Figure 4 illustrates the physical model for a fuel surface/oxidizer particle pair. The unique features are a tri-flame structure (oxidizer decomposition flame, final diffusion flame, and primary flame) and geometric structure for the deflagrating oxidizer particle. The flame structure is a natural modification of the extended GDF flame structure developed by Summerfield and co-workers[24]. The latter is buttressed by considerable experimental data. The permissible oxidizer surface geometry also lies within bounds observed experimentally. Consequently, there are very good reasons to believe that the physiochemical model is realistic.

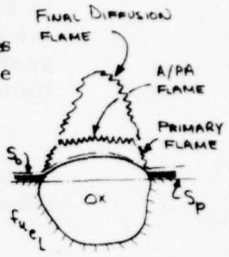

FIG. 4 BDP MODEL (REF 3)

Beckstead, Derr, and Price write the continuity equation as

$$\bar{r}_{p_c} = \bar{\dot{m}}'' = \bar{\dot{m}}''_f (S_f / S_o) + \bar{\dot{m}}''_{ox} (S_{ox} / S_o) \qquad (29)$$

where S_o is the total surface area of the burning surface. It is important to note that the means on the RHS are for deflagrating fuel surface/oxidizer particle pairs while the areas are for all pairs. It was subsequently assumed that oxidizer regression rate was a step function

$$\begin{aligned} r_{ox} &= 0 && (0 \le t < t_{ign}) \\ &= r'_{ox} && (t > t_{ign}) \end{aligned} \qquad (30)$$

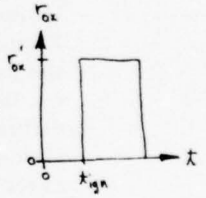

where t = o when the particle first penetrates the burning surface and t_{ign} is the ignition delay. Clearly, since an ignition delay $t_{ign} > 0$ is assumed, the burning surface will contain both ignited and non-ignited fuel surface/oxidizer particle pairs. Therefore, application of Eq. (3) yields

$$\bar{r}_{p_c} = \bar{\dot{m}}'' = \bar{\dot{m}}''_f (S_f / S_p) + \left[\bar{\dot{m}}''_{ox} (S_{ox} / S_p) \right]_{ign} \qquad (31)$$

Contrasting Eqs. (29) and (31) two differences are noted. First, if a mean mass flux for ignited oxidizer is to be employed, the associated area must also be limited to ignited oxidizer. Therefore, the BDP model is inconsistent in exactly the same fashion as Hermance's model. Consequently, the BDP model is limited to situations where $t_{ign} \sim 0$. However, note that in the BDP model that mean rate is referred to the total burning surface S_o rather than its planar projection S_p. Since strand and motor burning rates are based on a planar surface (because S_o isn't known), the burning rates computed by the BDP model cannot be compared directly with experimental data.* The latter inhibits utilization of the model.

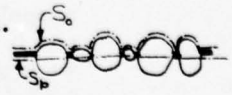

* Both of these defects are correctable.

Following Hermance[23] the dimension D was employed to define t_c and hence the mean microstate of a deflagrating fuel surface/oxidizer particle pair.* However, unlike Hermance the duality of the mean microstate when $t_{ign} < t_{c,N}$ was recognized. It is important to note that this recognition is clear in neither Ref. (2) nor Ref. (3); however, it is clear in the computer code. Unfortunately, $\bar{D}$ is a characteristic dimension for all particles on the burning surface and not for the deflagrating particles to which the dimension is applied. This inconsistency also limits the model to situations where $t_{ign} \sim o$.

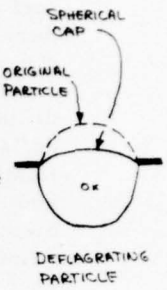

To define the oxidizer surface area it is assumed that the deflagrating surface of an oxidizer particle is a spherical "cap". Since the altitude of the cap at the mean microstate is

$$h = r_f t_c - r'_{ox} (t_c - t_{ign}) \qquad (32)$$

and it is further assumed that $r_f = \bar{r}$, h and subsequently S_{ox}/S_o can be expressed in terms of r'_{ox} and t_{ign}.

The flame structure was quantified by assuming that reactions were concentrated at flame standoff distances based on kinetic and diffusional considerations. Heat feedback to the burning surface was based on an area ratio weighted summation of the heat feedbacks from each flame. This implicitly assumes each flame in the triad acts independently. Unfortunately, this is not the case for it is clear from Figure 4 that the final diffusion flame cannot communicate directly with the burning surface; its effect is derived from modification of the oxidizer decomposition flame. That is, heat released in the final diffusion flame increases the temperature at the oxidizer decomposition flame which, since it is kinetically controlled, increases its reaction rate. This causes the oxidizer decomposition flame to move closer to the burning surface. It is this "thermal compression" of the oxidizer decomposition flame by the final diffusion flame that causes the heat feedback via the final diffusion + oxidizer decomposition flame path to exceed that from an independent oxidizer decomposition flame. It must be concluded that the analytical description of the flame structure is inconsistent with the physiochemical model. As with the other inconsistencies, these can also be "cured".

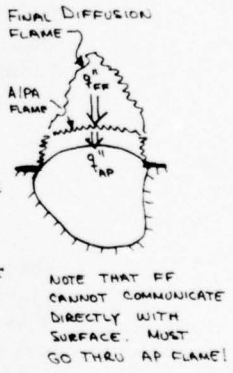

Beckstead, Derr, and Price have employed the model to compute ambient rate pressure characteristics for "unimodal" polysulfide/AP propellants (the same propellants employed by Hermance). Figure 5 presents a comparison of theory and experiment. Since the 20 μ propellant was selected as a baseline, the theory/experiment comparison is essentially exact. However, the theory is qualitative at best when extrapolated to the 200 μ propellant. Condon[25] has tested the models capability for predicting temperature sensitivity of the JANNAF standard propellant. Figure 6 illustrates the comparison between

*Another dimension, the mean width of the fuel surface surrounding the oxidizer particle is involved. This width was computed by assuming that the propellant has an ordered body centered cubic structure. As its structure is random, this dimension is also slightly in error.

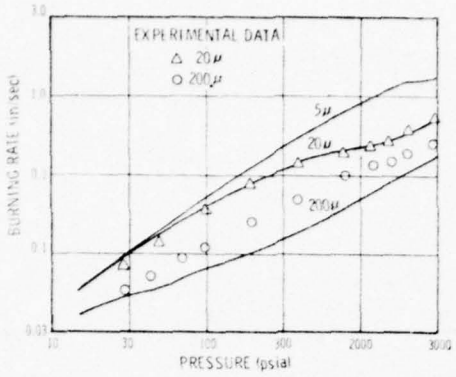

Figure 5 Comparison Theory and Equipment - BDP Model - Monodisperse AP/PS Propellant (Ref. 3)

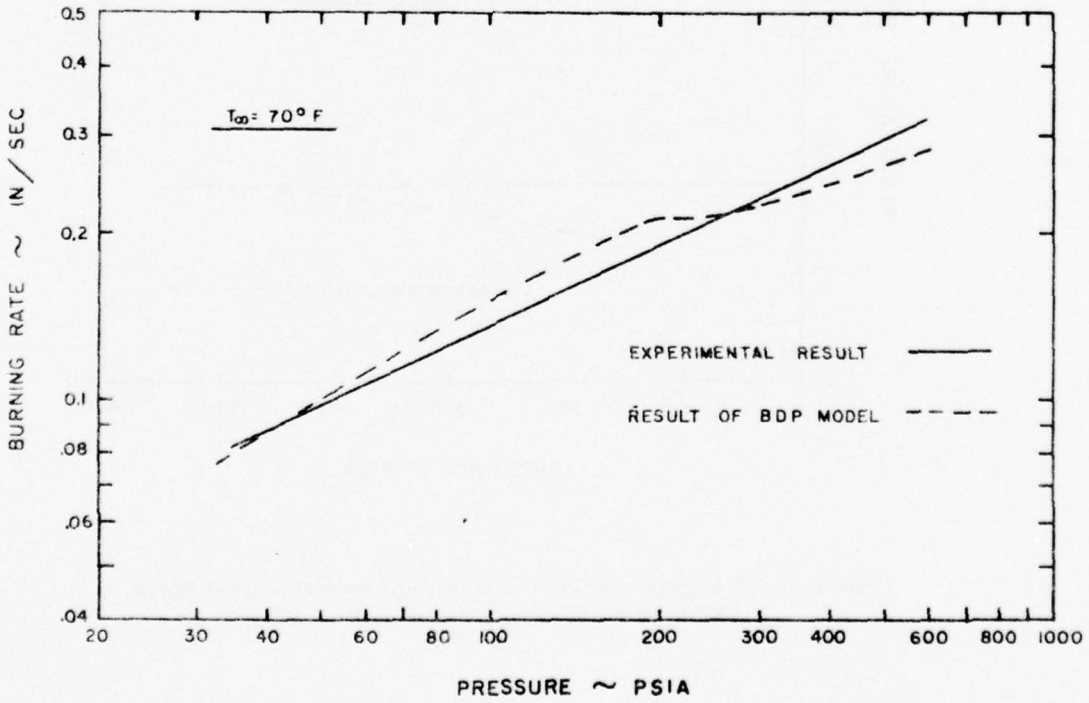

Figure 6a. Comparison Theory and Experiment - BDP Model - JANNAF Standard Propellant (Ref. 25)

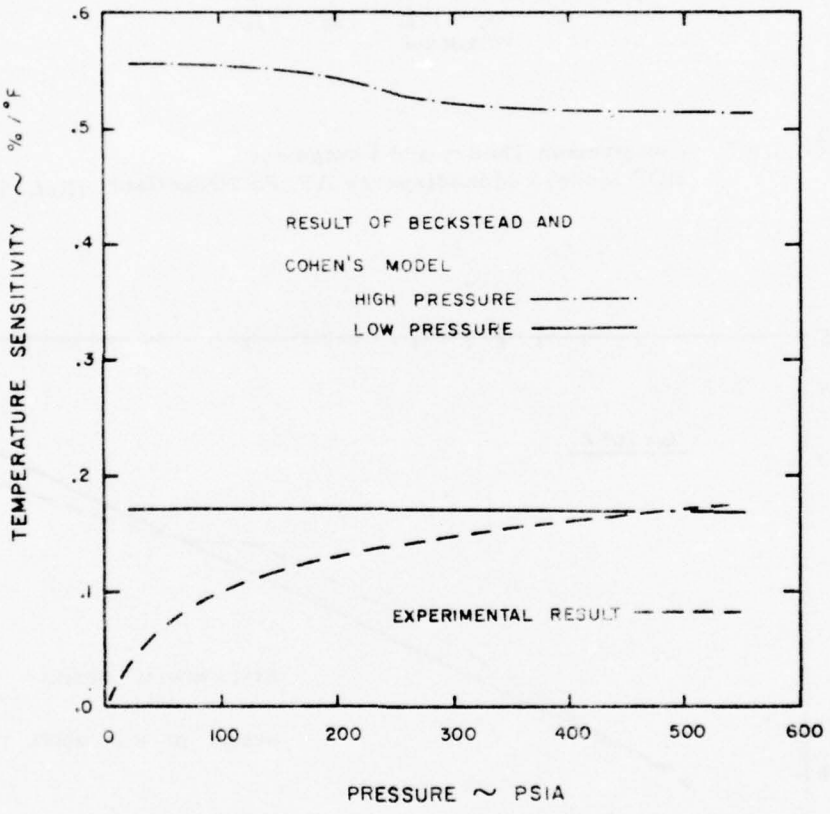

Figure 6b. Comparison Theory and Experiment - BDP Model - JANNAF Standard Propellant (Ref. 25)

theory and experiment for both σ_p and rate/pressure. Notice that while rate/pressure behavior is in reasonable agreement with experiment the theoretical σ_p differs substantially from experiment. These divergences between theory and experiment are not unexpected in view of the aforementioned inconsistencies in the model.

Contrasting the theory/experiment comparisons illustrated by Figs. 3 and 5 demonstrates that both the Hermance and BDP models fit the same data base equally well (remember Hermance adjusted parameters to the 200 micron data). This is a rather surprising result because Hermance's unit physiochemical model is physically unrealistic while BDP's isn't. Why did this occur? The only sensible explanation is that both theories have sufficient "adjustable" parameters available to provide an acceptable fit to virtually any limited data base. Since very few of these parameters are defined with precision, numerous parameters are available for curve fitting. This result demonstrates in a very concrete fashion that physical realism is not guaranteed by a model's ability to predict/correlate experimental data. In mathematicalese the ability to fit experimental data is a necessary but not sufficient condition for a model's physical validity.

Miller, Hartman, and Myers Model[20] - Miller, Hartman, and Myers (MHM) were also influenced by Hermance's innovative blending of combustion model and statistics. However, rather than following the path of a detailed combustion model plus statistics for monodisperse propellant they employed an existing qualitative combustion model and extended it to polydisperse situations. This approach was both innovative and practical. It was innovative because it embeds particle size explicitly in the resulting model in an operational fashion. It was practical because all real propellants are polydisperse. In addition, their approach is computationally undemanding.

Miller, Hartman, and Myers began their analysis for steady-state combustion with the continuity expression

$$\overline{\dot{m}} = \bar{r}\,\rho_c\,S_p = \overline{\dot{m}}_{AP} + \overline{\dot{m}}_f \tag{33}$$

In addition, application of continuity to fuel and oxidizer flows yields

$$\overline{\dot{m}}_f = \rho_f\,\overline{r_f\,S_f} = \rho_f\,\bar{r}_f\,S_{p,f} \tag{34}$$

$$\overline{\dot{m}}_{AP} = \rho_{AP}\,\overline{r_{AP}\,S_{AP}} = \rho_{AP}\,\bar{r}_{AP}\,S_{p,AP} \tag{35}$$

where the subscript p denotes a planar projection of the area. For steady-state deflagration the planar, areal mean regression rates are identical

$$\bar{r}_{AP} = \bar{r}_f = \bar{r} \tag{36}$$

Consequently,

$$\bar{r} = \frac{\overline{r_{AP} S_{AP}}}{S_{p,AP}} = \frac{\overline{r_f S_f}}{S_{p,f}} \tag{37}$$

Recognizing that the burning surface is composed of a polydispersion of particles, that the whole is the sum of its parts, and that in Reynold's rules of averaging the mean of a sum is the sum of the means( ), they form the mean as a sum over all particles on the burning surface. Thus, with the j index representing a particular size of particle

$$\bar{r} = \overline{r_{AP} S_{AP}} / S_{p,AP} = \sum_j \overline{r_{AP,j} S_{AP,j}} / S_{p,AP} \tag{38}$$

Comparison of Eqs. (38) and (10) shows that MHM invented the "petite ensemble" method. Since

$$\overline{r_{AP,j} S_{AP,j}} = \bar{r}_{AP,j} S_{p,AP,j} \tag{39}$$

Eq. (38) can be rewritten in terms of individual planar regression rates as

$$\bar{r} = \sum_j \bar{r}_{AP,j} S_{p,AP,j} / S_{p,AP} \tag{40}$$

Assuming that the burning surface is planar and the particles are spherical* the number of j particles per unit surface is

$$N_j / S_p = 6 \zeta_j / (\pi D_j^2) \tag{41}$$

However, volume fraction ζ_j and weight fraction w_j are related by

$$\zeta_j = w_j (\rho_c / \rho_{AP}) \tag{42}$$

Since the mean diameter of the intersected particles is

$$\bar{D}_j = \sqrt{2/3}\, D_j \tag{43}$$

and**

$$\bar{S}_{p,AP,j} = N_j \pi \bar{D}_j^2 / 4 \tag{44}$$

*See discussion preceding Eq. (21).

**Note that Eq. (10) in Ref. (20) is in error by the factor 2/3. As everything is later lumped into a constant, this makes no real difference.

MHM showed that

$$S_{p,AP,j} / S_p = \gamma_j = (\rho_c / \rho_{AP}) w_j \tag{45}$$

As

$$S_{p,AP} = \sum_j S_{p,AP,j} \tag{46}$$

Eq. (40) becomes

$$\bar{r} = \sum_j w_j \bar{r}_{AP,j} \Big/ \sum_j w_j \tag{47}$$

It appears that Eq. (47) applies only to spherical particles because that assumption was employed in the derivation. However, that is not the case because it can be shown that

$$S_{p,AP,j} / S_p = \gamma_j \tag{48}$$

irregardless of the shape of the particle.* Thus, the major restrictive assumption at this point is a planar burning surface.

To complete the analysis MHM chose the Summerfield GDF model[26] to relate $\bar{r}_j$ to D_j and environmental variables. However, since in that model

$$\bar{r}_{GDF} = \left[k_1' / p + k_2' D_j / p^{1/3} \right]^{-1} \tag{49}$$

it is clear that

$$\lim_{D_j \to \infty} \bar{r}_{GDF} = 0 \tag{50}$$

Miller, Hartman, and Myers noted that this limit was physically unattractive and, therefore, modified the GDF equation to

---

*Translate a plane S_p a distance ΔX in the propellant. The volume swept out is $S_p \Delta X$. The volume of j oxidizer in this volume is by definition $\gamma_j S_p \Delta X$. However, this volume of oxidizer is also given by $S_{p,ox,j} \Delta X$. Thus, $S_{p,ox,j} / S_p = \gamma_j$.

$$\bar{r}_j = r_o + \left[k_1/p + k_2 D_j / p^{1/3} \right]^{-1} \tag{51}$$

where $r_o \neq$ func (D_j). It is important to note that $\bar{r}_j$ is not dependent upon its neighbors. Therefore, the MHM theory neglects interactions.

To achieve their final burning rate expression they assumed that*

$$r_o = \alpha p^{1/3} \tag{52}$$

Substitution of Eqs. (51), (52), into Eq. (47), therefore, yields

$$\bar{r} = \alpha p^{1/3} + \sum_j w_j \left[k_1/p + k_2 D_j / p^{1/3} \right]^{-1} \Big/ \sum_j w_j \tag{53}$$

With this rate expression they noted that

$$\lim_{\max D_j \to 0} \bar{r} = \alpha p^{1/3} + p/k_1 \tag{54}$$

$$\lim_{\min D_j \to \infty} \bar{r} = \alpha p^{1/3} \tag{55}$$

Thus, they concluded there were definite bounds on the amount of rate control achievable with particle size manipulation. In addition, they concluded that both AP size and distribution are important. Therefore, rate cannot be correlated with a single weight mean diameter.

Equation (53) was employed to correlate strand rate/pressure data from sixteen different formulations (particle size distribution was the "variable"). Table 1 presents a tabulation of measured and calculated values. In most cases agreement is very good.

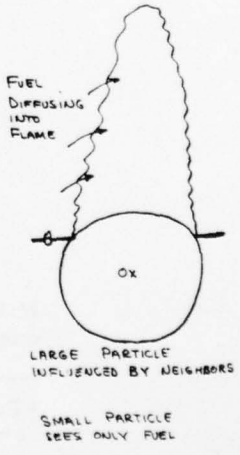

This work and Hermance's must be rated as the pioneering efforts in statistical combustion modeling. The defects of this model are those noted (planar burning surface, no interactions), those of the GDF model, and a total neglect of mixture ratio variations among the particles. The latter may be significant because small particles should be fuel rich relative to the norm. This occurs because such a small amount of fuel is required that competition with neighbors is slight. On the other hand, a large particle is probably fuel lean relative to the norm because it requires so much fuel that it must compete with its neighbors to such an extent that its appetite is never satiated. Since composite propellants are always fuel rich and as a rough rule rate degrades as one moves away from the stoichiometric condition, it can be expected that the larger particles will have higher rates and the smaller particles lower rates than predicted by the MHM theory.

*Glick[27] has noted that r_o should correspond to r_{AP} (p, T_∞) and that if it does Eq. (51) correlates exponent break data for AP composite propellants.

TABLE I

COMPARISON THEORY AND EXPERIMENT - MILLER'S MODEL - CTPB/AP/Fe_2O_3 POLYDISPERSE PROPELLANT (REF. 20)

Pressure (psia)	300		500		1500		2000	
	Burning Rate (in/sec)							
Propellant	exp.	calc.	exp.	calc.	exp.	calc.	exp.	calc.
TP-1	0.34	0.32	0.40	0.39	0.56	0.57	0.83	0.63
TP-2	0.32	0.34	0.38	0.42	0.75	0.64	1.50	0.71
TP-3	0.39	0.35	0.39	0.44	0.69	0.69	0.88	0.76
TP-4	0.39	0.35	0.43	0.45	0.76	0.69	0.87	0.77
TP-5	0.36	0.37	0.45	0.47	0.73	0.74	0.84	0.84
TP-6	0.41	0.39	0.45	0.50	0.84	0.81	0.99	0.91
TP-7	0.41	0.43	0.54	0.57	1.06	1.05	1.25	1.23
TP-8	0.46	0.43	0.62	0.61	1.23	1.22	1.46	1.48
TP-9	0.45	0.44	0.62	0.63	1.27	1.28	1.50	1.55
TP-10	0.54	0.50	0.72	0.70	1.33	1.41	1.55	1.69
TP-11	0.52	0.49	0.70	0.69	1.34	1.40	1.57	1.68
TP-12	0.40	0.45	0.60	0.61	1.23	1.18	1.49	1.39
TP-13	0.56	0.51	0.76	0.73	1.48	1.51	1.75	1.84
TP-14	0.52	0.51	0.73	0.71	1.44	1.46	1.65	1.77
TP-15	0.58	0.51	0.76	0.70	1.40	1.43	1.67	1.72
TP-16	0.54	0.51	0.72	0.71	1.38	1.42	1.62	1.72

On this basis it would be expected that propellants with wide distributions would be correlated worst. Propellants TP-7 to -9 and TP-11 to -16 have the widest distributions and tend to bear out the above suspicions.

Cohen, Derr, and Price Model[4] - The BDP model is limited to additive free, monodisperse propellants. However, all "real" propellants are polydisperse. Therefore, the BDP model has little relevance to practical propellants per se. Cohen, Derr, and Price partially "remedied" this situation by extending the model to bi-disperse propellants with an inert additive.

In the extension all basic assumptions of the BDP model are retained. The major new assumption is that all sizes of oxidizer particles have the same burning rate.* Therefore,

$$\overline{\dot{m}}''_{ox} = \overline{\dot{m}}''_{ox,j} = \overline{\dot{m}}''_{ox,k} \qquad (56)$$

where k, j are in the same set but $k \neq j$. With this assumption and the BDP model's ignition delay criteria the spherical cap height h_j can be computed for each oxidizer particle size [see Eq. (32)]. With the cap height known and

$$\bar{D}_j = \sqrt{2/3}\, D_j \qquad (57)$$

the geometry of the deflagrating oxidizer surface is known and, therefore, $(S_{ox}/S_{p,ox})_j$ computed for each particle size. Since $S_{p,ox,j}/S_p = \zeta_j$, the total oxidizer surface area is

$$S_{ox}/S_p = \sum_j (S_{ox}/S_{p,ox})_j\, \zeta_j$$

for the BDP model the ratio S_{ox}/S_b is desired. As

$$S_{ox} + S_f + S_i = S_o, \quad S_f = \zeta_f S_p, \quad S_i = \zeta_i S_p, \text{ and } S_{ox}/S_p =$$

is known, S_o/S_p and, subsequently, S_{ox}/S_o can be computed. Therefore, only $\dot{m}''_{ox}$ needs to be computed to define r with Eq. (29).

To compute $\dot{m}''_{ox}$ the energy balance employed by BDP with modifications to account for the presence of inert additives is employed. To compute heat feedback from the gas phase reaction zone the BDP methodology is employed. The only modification being that the characteristic fuel dimension is modified. It is computed on the assumption that all particles have the same annular thickness of fuel surrounding them.

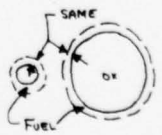

*Termed the equal rate hypothesis herein.

Computations derived from the model were presented. Figure 7 presents a comparison of theory and experiment for the ambient rate/pressure characteristics of a specific propellant. Note the excellent agreement.

This extension builds upon the BDP model without correcting any of its inconsistencies. Consequently, the "sins of the father are visited on the son". In addition, it is assumed that all particles possess the same rate irregardless of size. This assumption seems highly unlikely in view of the well known fact that particle size is a major factor in the rate control of AP composite propellants. The fact that agreement with experiment for a specific formulation was achieved should not be given too much weight. Recall that Hermance's invalid model and MHM's model, which assumed $m_j'' \neq m_k''$, both correlate data.

Note also that although the Cohen, Derr, Price model has inconsistencies and is limited to two particle sizes that these inconsistencies can be removed and the model extended to a true polydispersion by following the path indicated above.

Sammons Model[5] - The Sammons model extends the BDP model to propellants with polydisperse oxidizer and inert additives. The basic path followed is that blazed by Cohen, Derr, and Price. However, several unique features were added. First, the oxidizer is segregated into two classes: subcritical and supercritical. The former is assumed to undergo condensed phase reaction "at the burning surface" thereby modifying the surface heat release term heretofore assumed constant by both BDP and CDP. The supercritical oxidizer is assumed to burn as described by BDP. Second, the ignition delay is handled differently than by Cohen, Derr, and Price. Third, improvements in the computation of thermophysical properties and the short flame Burke-Shuman solution were introduced.

The surface geometry of the supercritical oxidizer is handled differently than by Cohen, Derr, and Price.* Instead of computing h_j, D_j, and $(S_{ox}/S_{os,p})_j$ for each particle size and then summing an average ignition delay is computed for the supercritical oxidizer as

$$\bar{t}_{ign} = \sum_i w_i t_{ign,i} \qquad (59)$$

where $t_{ign,\,i} = K_o D_i^n / p^m$ is the expression employed by BDP. Then the BDP expression for h/D is employed, i.e.

$$h/D = 0.5 \left(1 \pm 1/\sqrt{3}\right)\left(1 - r_{ox}/\bar{r}\right) + r_{ox}\bar{t}_{ign} \qquad (60)$$

*The description of what was actually done is very unclear.

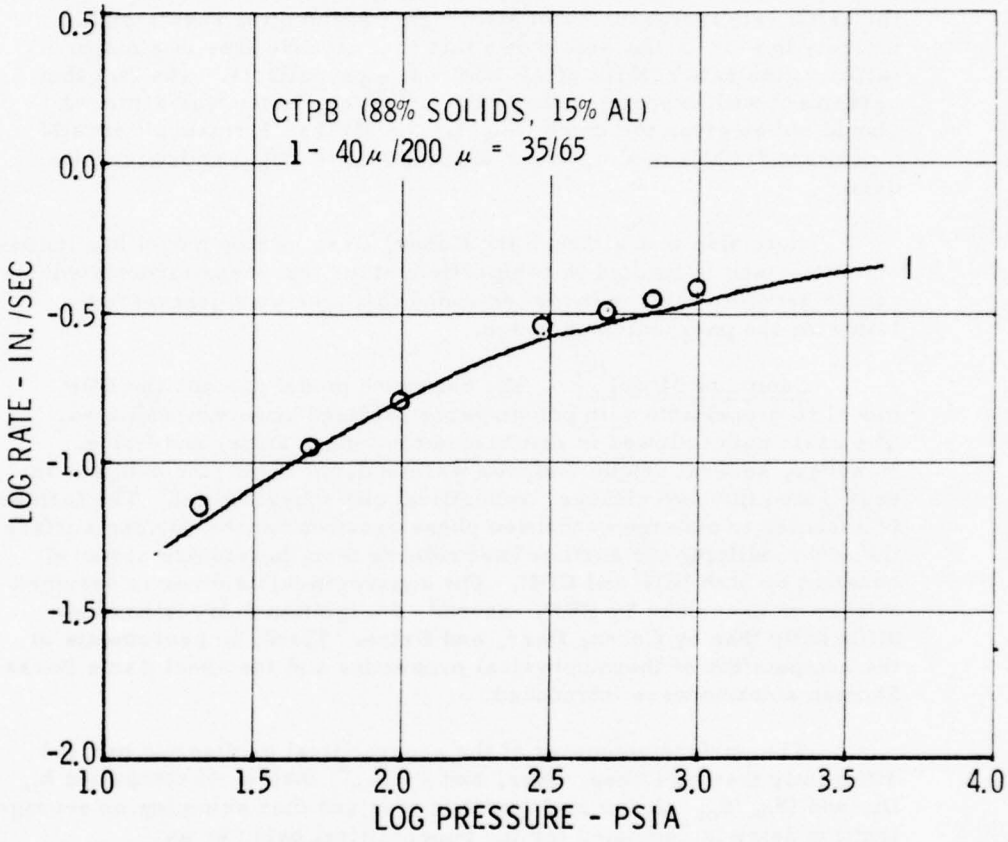

Figure 7. Comparison Theory and Experiment - Cohen, Derr, Price Model (Ref. 4)

With this h/D the value of S_{ox}/S_b is computed with the BDP expression.

$$S_{ox}/S_b = 3\left[(h/D)^+\right]^2+\left[(h/D)^-\right]^2+\frac{1}{3}\Big] \Big/ \left\{1+3\left[\left[(h/D)^+\right]^2+\left[(h/D)^-\right]^2\right]\right\} \qquad (61)$$

where the + and − superscripts denote the ± terms in Eq. (60).

Rate is basically obtained from the energy balance employed by BDP but modified to account for inerts and subcritical AP. The inerts are treated according to Cohen, Derr, and Price. However, details of the subcritical oxidizer treatment are unclear. The criteria specifying critical oxidizer particle size and the specific surface energy release associated with the subcritical oxidizer are not discussed.

Rate pressure characteristics were computed for several polydisperse propellants and compared with data. Results show that qualitative agreement exists.

This model suffers from the inconsistencies inherent in the BDP model. Moreover, it incorporates the equal rate hypothesis. Additionally, the method employed to obtain the average S_{ox}/S_b has no sound physical basis. Finally, the description of this model is very poor. To find out what is going on one must literally decode the computer program (an arduous task). In this writer's opinion this is not worthwhile.

Glick's "Grand Ensemble" Model[9, 10] - Glick noted that the burning surface of heterogeneous propellants was an ensemble of different microstates and criticized the BDP theory for (a) collapsing the microstates into a single mean microstate and (b) selecting the dimension characterizing the mean microstate from purely geometric arguments.* To circumvent this averaging process a statistical procedure was devised to satisfy continuity and thereby compute the mean rate in terms of microstate rates. In addition, Glick noted that, if the surface statistics were invariant in time, the mean nonsteady properties could be expressed in terms of nonsteady properties for single flames.

Two distribution functions F_{ox} and F_f were introduced such that the fraction of fuel surface/oxidizer pairs with $\epsilon_f \le \epsilon_f \le \epsilon_f + d\epsilon_f$ and $\epsilon_{ox} \le \epsilon_{ox} \le \epsilon_{ox} + d\epsilon_{ox}$ is

$$d^2N = (dN/dS_p)\, F_{ox}\, F_f\, d\epsilon_{ox}\, d\epsilon_f \qquad (62)$$

Assuming that the mass flux of oxidizer was given by the functional

*As shown, this criticism was well founded.

$$m''_{ox} = m''_{ox}\,(p,\ T_\infty,\ u,\ \epsilon_{ox},\ \epsilon_f,\ \cdots) \tag{63}$$

the mass flow of oxidizer from pairs with $\epsilon_{ox}, \epsilon_f$ is

$$d^2 m''_{ox} = m''_{ox}\,(dN/dS_p)\,F_{ox}\,F_f\,d\epsilon_{ox}\,d\epsilon_f \tag{64}$$

Therefore, the total oxidizer flow is given by integrating over all possible ϵ_{ox} and ϵ_f . For a monodisperse situation $0 \le \epsilon_{ox} \le \pi D^2/4$. For ϵ_f there is no reason for an upper bound; however, the fact that the particles cannot interpenetrate means that the smallest bit of fuel available is always non-zero. Therefore, $\epsilon'_f \le \epsilon_f \le \infty$. Consequently,

$$\bar{m}''_{ox} = \frac{dN}{dS_p} \int_0^{\pi D^2/4} F_{ox}\,\epsilon_{ox} \int_{\epsilon'_f}^{\infty} m''_{ox}\,F_f\,d\epsilon_f\,d\epsilon_{ox} \tag{65}$$

If mixture ratio is preserved (true in steady-state)

$$\bar{m}'' = \bar{r}\,\rho_c = \bar{m}''_{ox}/\alpha_{ox} \tag{66}$$

If changes in time are quasi-steady, mixture ratio is invariant in time. Therefore, if the surface statistics are also invariant in time, F_{ox} and F_f are time independent. Consequently.

$$d\bar{m}'' = \alpha_{ox}^{-1} \frac{dN}{dS_p} \int_0^{\pi D^2/4} F_{ox}\,\epsilon_{ox} \int_{\epsilon'_f}^{\infty} dm''_{ox}\,F_f\,d\epsilon_f\,d\epsilon_{ox} \tag{67}$$

Since the mean pressure coupled response function is defined as

$$\bar{R}_p = (d\bar{m}''/\bar{m}'')/(dp/p) \tag{68}$$

manipulation of Eqs. (67) and (68) gives

$$\bar{R}_p = \int_0^{\pi D^2/4} F_{ox}\,\epsilon_{ox} \int_{\epsilon'_f}^{\infty} m''_{ox}\,R_{p,ox}\,F_f\,d\epsilon_f\,d\epsilon_{ox} \Big/ \int_0^{\pi D^2/4} F_{ox}\,\epsilon_{ox} \int_{\epsilon'_f}^{\infty} m''_{ox}\,F_f\,d\epsilon_f\,d\epsilon_{ox} \tag{69}$$

It was noted that a similar expression held for the velocity coupled response function R_v and that one-dimensional functional forms for R_p (and R_v) could be employed.

To evaluate the integrals, F_{ox} (ϵ_{ox}), F_f (ϵ_t), and m''_{ox} need to be evaluated. To evaluate F_{ox} and F_f it was assumed that all accessible ϵ_t and ϵ_{ox} were equally probable and constraints on number and surface area applied. It was demonstrated that under these conditions the distribution functions possessed the functional form of the Boltzman factor. Therefore, F_{ox} and F_f were computed for propellants with monodisperse, spherical oxidizer. The distribution functions were extended to propellants with polydisperse, spherical oxidizer. The F_{ox} extension was rigorous; the F_f extension was approximate.

To demonstrate the method the GDF model[26] was employed for m''_{ox} and the rate/pressure characteristics of the resulting model for monodisperse propellants was tested against data[34]. The comparison showed that the "statistical" GDF and GDF models gave almost identical results.

This work represents an interesting line of attack. However, no attention was given to energy conservation and the fact that the microstates were themselves nonsteady. These considerations invalidate utilization of the GDF model in this statistical framework. Indeed, no existing model can be employed in this framework. Finally, the distribution function F_{ox} is incorrect because all ϵ_{ox} are not equally probable; all depths of intersection of the particle with S_p are .*

As noted in Fundamentals of Statistical Combustion Modeling the worst defect of this approach is the computational problem associated with tracking individual microstates through time. Because of this fact alone, this approach possesses little current interest.

Cohen's Nitramine Model[6 - 8] - Virtually all of the statistical combustion models apply to AP propellants. However, Cohen has adapted the BDP model to propellants with nitramine oxidizers. This development has (and still is) proceeded in several stages. In the first stage, the BDP model was modified to treat monodisperse nitramine propellants. In the second stage, the Cohen, Derr, Price methodology was employed to extend the monodisperse model to a bidisperse situation with mixed oxidizers. In the third stage, active binders were explored.

The initial nitramine propellant model developed by C ohen[6] was limited to monodisperse nitramine propellants and basically consisted of a nitramine unit physiochemical combustion model embedded in the BDP statistical framework. The unit physiochemical model was

*Suppose the particle is a rod with pointed ends. Obviously, the probability of $\epsilon_{ox} = 0$ is now much less than that for $\epsilon_{ox} = \pi D^2/4$.

based on ballistic cinephotographic and SEM (extinguished by rapid depressurization) investigations of nominal 195 micron and 5 micron additive free monodisperse HTPB/HMX propellants at the 75% total solids level over a wide pressure range. Consequently, the model incorporates the following features: no energy release in the sub-melt layer (supported by SEM results), existence of oxidizer and binder melts (supported by cinephotographic evidence), provision for termination of oxidizer melt (supported by cinephotographic evidence), and provision for deep "flame" penetration into the propellant via "deep penetration" HMX crystal deflagration (supported by cinephotographic evidence). Figure 8 illustrates the model for three situations: Nitramine melting, nitramine not melting, and nitramine not melting with deep penetration. When the nitramine melts it is assumed that the nitramine's burning surface is planar. However, when there is a binder melt, that melt may encroach upon the nitramine surface as shown. This possibility is embedded by a two parameter, purely empirical expression. When the nitramine does not melt, the nitramine surface geometry is determined via the same geometric relations (an ignition delay is utilized) employed by BDP with the exception that the recessed state is unbounded. That is, recession is allowed to extend beyond the boundaries of the deflagrating HMX particle to account for deep penetrations. In this extension boundedness is introduced through an empirical manufacturing parameter.

A question of prime importance to the model is "under what conditions does HMX melting cease?" This is answered on a thermal basis. Basically, an HMX particle is dropped into binder whose temperature time history simulates the thermal wave and removed after its transit time (thickness wave/burn rate). Obviously, if transit time is very short melting will not occur. Consequently, this procedure defines a critical burning rate; above it no melting; below it melting. By identifying exponent break point with HMX melt termination, Cohen shows that this procedure correlates break point/particle size data in the 40 - 300 micron size range; data in the < 40 micron range is not correlated (see Figure 9).

With particle geometry defined, the energy equation basically closes the problem by defining the mean surface temperature. The treatment here is also virtually identical to that employed by BDP with the exception that an endothermic term is included to account for nitramine melting (when melting occurs).

Execution of the model shows very good agreement with the rate/pressure characteristics of the experimental propellants. Figure 10 illustrates typical results. Table 2 presents a list of the standard parameters employed. As noted previously, these parameter values are not rigorously defined.* The exponent break

*The intention here is not to "put down" this analysis because all detailed models must utilize roughly the same amounts of "parameters". However, to disregard the ability of parameter adjustment to improve data correlation would be to lose contact with reality.

(a) SURFACE STRUCTURE FOR BULK MELTING; $h/D_o = 0$

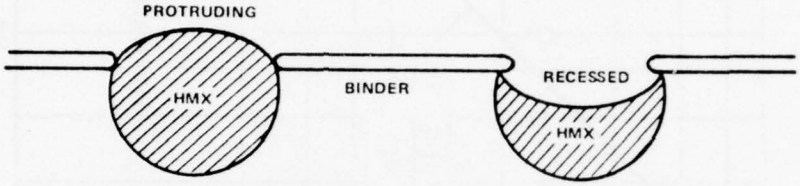

(b) SURFACE STRUCTURE OR FROZEN PARTICLES (ANALOGOUS TO THE AMMONIUM PERCHLORATE MODEL); $|h/D_o| < 1$

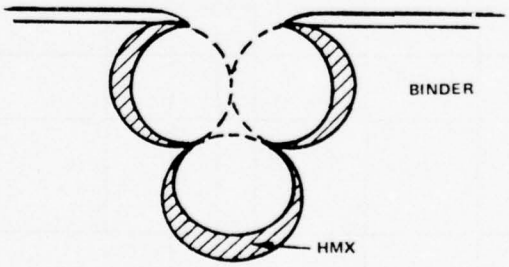

(c) SURFACE STRUCTURE FOR DEEP PENETRATION WITH N = 2; $-2 < h/D_o < -1$

Figure 8. Cohen's Nitramine Surface Geometry (Ref. 6)

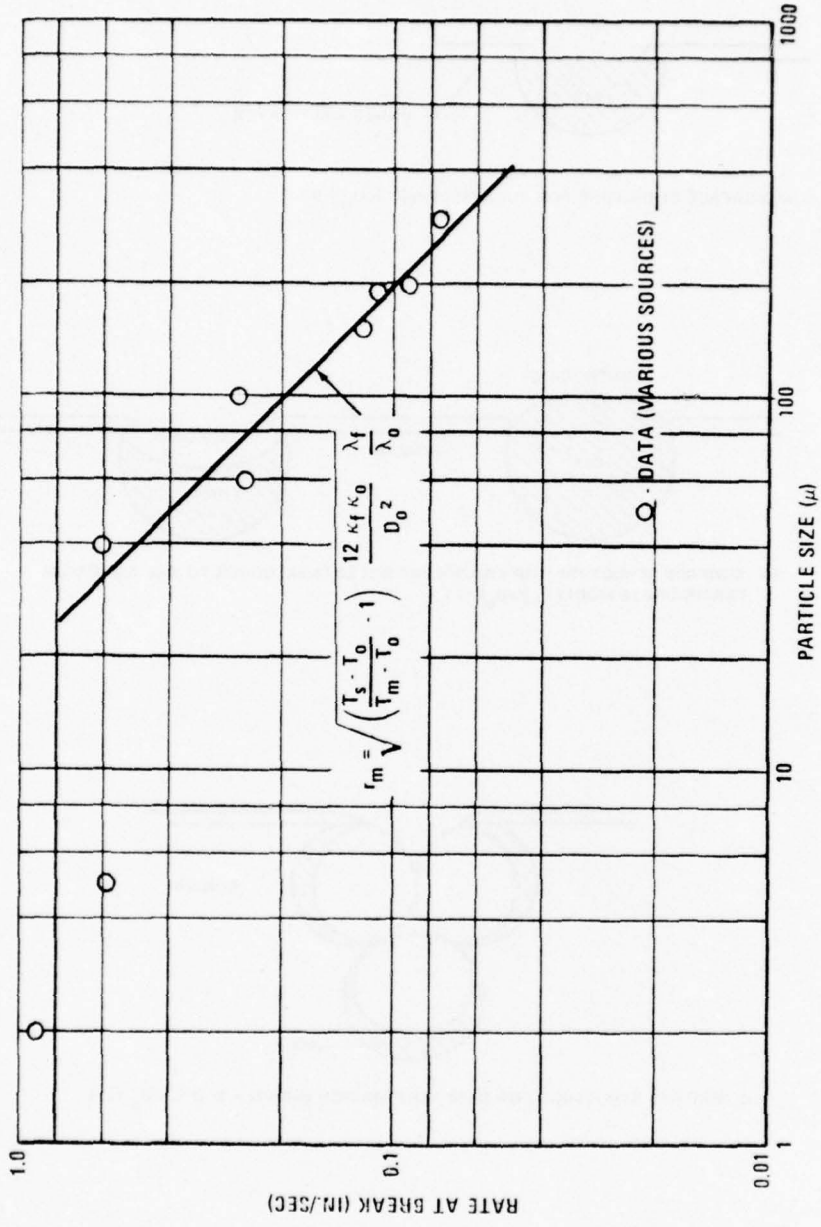

Figure 9 Relationship of Burning Rate and Particle Size at Break Points (Ref. 6)

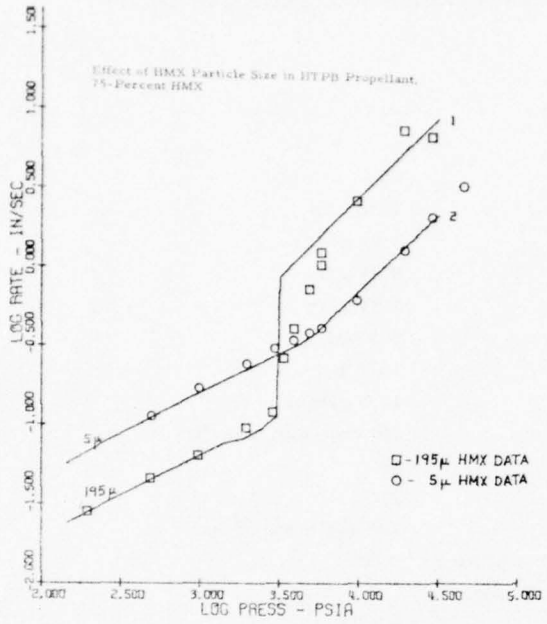

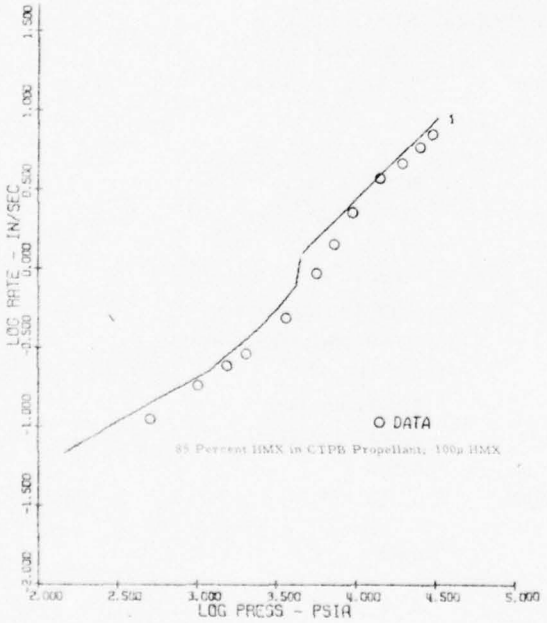

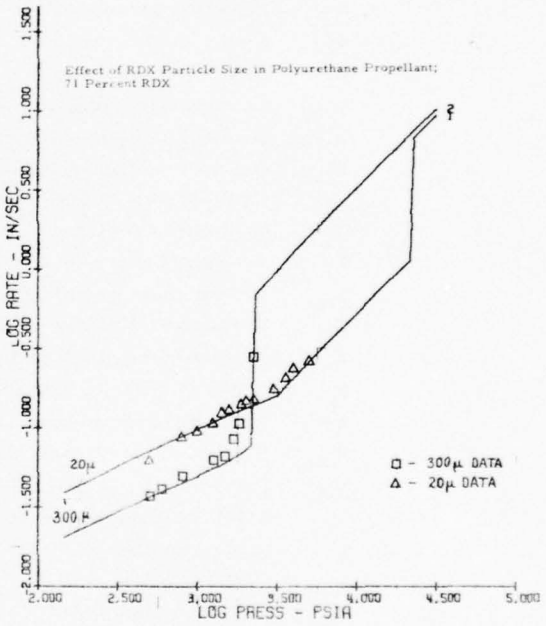

Figure 10. Comparison Theory and Experiment - Cohen Monodisperse Nitramine Model (Ref. 6)

TABLE 2

PARAMETERS EMPLOYED IN COHEN NITRAMINE MODEL (REF. 6)

α	Weight percent oxidizer	75.0
D_o	Mean diameter of oxidizer	195μ, 5μ
ρ	Propellant density	1.51 g/cc
ρ_f	Binder density	0.93 g/cc
ρ_{ox}	Oxidizer density	1.91 g/cc
Q_f	Binder heat of decomposition	569 cal/g
T_F	Propellant flame temperature	1675^{0}K
M	Gas molecular weight[1]	17.0 g/mol
Y	Diffusion parameter[1]	10^4 cm^2-atm/sec-^{0}K
Φ	Stoichiometric ratio[1]	53
C	Diffusion parameter[1]	17
Cign	Oxidizer ignition delay constant	190 sec-atm$^{0.72}$/cm$^{0.8}$
Pign	Oxidizer ignition delay pressure-dependence	0.72
Dign	Oxidizer ignition delay diameter-dependence	0.8
Q_L	Oxidizer heat of decomposition	-225 cal/g
Q_{LM}	Oxidizer heat of fusion	132 cal/g
E_f	Activation energy of binder decomposition	16.9 Kcal/mol
E_{ox}	Activation energy of oxidizer decomposition	50 Kcal/mol
A_f	Prefactor for binder decomposition	299 g/cm^2-sec
A_{ox}	Prefactor for oxidizer decomposition	5 x 10^9 g/cm^2-sec
δ	Order of diffusion flame reaction	2
δ	Order of oxidizer flame reaction	2
k_{PF}	Prefactor for diffusion flame reaction	30 g/cm^3-sec-atm^2
k_{ox}	Prefactor for oxidizer flame reaction	0.246 g/cm^3-sec-atm^2
T_{ox}	Oxidizer flame temperature	3275^{0}K
λ	Gas conductivity	0.0003 cal/cm-sec-^{0}K
λ_o	Oxidizer conductivity	0.00049 cal/cm-sec-^{0}K
λ_f	Binder conductivity	0.00044 cal/cm-sec-^{0}K
c_p	Heat capacity	0.3 cal/g-^{0}K
κ_o	Oxidizer diffusivity	0.0011 cm^2/sec
κ_f	Binder diffusivity	0.0011 cm^2/sec
T_m	Oxidizer melting point	278^{0}C
K	Coefficient for melt surface structure-diameter dependence	1.33$\mu^{-0.25}$
a	Melt surface structure diameter dependence	0.25
N	Manufacturing parameter	3, 1
n	Diffusion flame pressure-dependence	0.6
T_o	Initial propellant temperature	25^{0}C
P	Pressure range	10 - 2200 atm

associated with the nominal 195 micron propellant is associated with the termination of HMX melting and arises from the sudden elimination of the HMX heat of fusion from the energy equation (increases rate) and the removal of the melting geometric constraints. The latter lets S_{ox} suddenly increase thereby suddenly increasing rate.

In Ref. 7, Cohen extended the monodisperse model to handle a bidisperse mixture of two nitramine ingredients. That is, two particle sizes of nitramine A and two particle sizes if nitramine B were considered. This extension represents a melding of Cohen, Derr, and Price's extension of the BDP model from the monodisperse case to the bidisperse case", Cohen's unit nitramine physiochemical model[15], and a "relaxation" of the "equal burning rate hypothesis". The latter was necessitated by the mixed oxidizer situation. In essence Cohen, Derr, and Price's bidisperse procedure (and its concomittant equal rate hypothesis) was applied separately to each nitramine ingredient with Cohen's nitramine unit physiochemical model replacing the BDP unit physiochemical model and a separate energy equation for each nitramine specie. Mean rate was computed as a weighted sum of specie rates. Thus, this development represents a hybrid of "equal rate hypothesis" and unequal rate statistics. Figure 11 illustrates typical results.

In Ref. 8 Cohen extended the preceding model to include active binders and bidisperse two specie mixtures of nitramine/nitramine and nitramine/AP oxidizers. The inactive binder situation for bidisperse nitramine/AP oxidizers was a logical extension of the nitramine/nitramine situation and was achieved by simply embedding BDP's unit AP physiochemical model in the nitramine/nitramine framework. In other words, instead of computing the rates of bidisperse nitramine A and bidisperse nitramine B and then employing the weighted sum as the mean burning rate, bidisperse nitramine B was replaced by bidisperse AP! Three schemes were advanced for including an active binder. "First, it was assumed that the regression rate of the binder at any pressure was its intrinsic value (no oxidizer present). Second, the constraint of oxidizer-binder continuity was relaxed. Third, in the case of nitramine oxidizers it was assumed that there was no diffusion flame because the nitramine and binder are stoichiometrically balanced." No equations, etc. were produced to detail active binder inclusion in the model. The results of a sequence of calculations was presented for nitramine/nitramine with active and with inactive binders and mixed nitramine/AP with active and with inactive binders. Cohen noted that these results follow experimental trends.

Cohen's work to date represents a powerful, pioneering thrust toward realistic modeling of nitramine propellants. The only elements omitted are true polydisperse capabilities* and the ability to treat

*The question here is that of representing a bimodal mixture of polydisperse lots by two mean particle sizes. The results of Miller, Hartman, and Myers[20] suggest that one cannot. However, this was for AP composites. In any event, Cohen's model cannot handle true polydisperse blends.

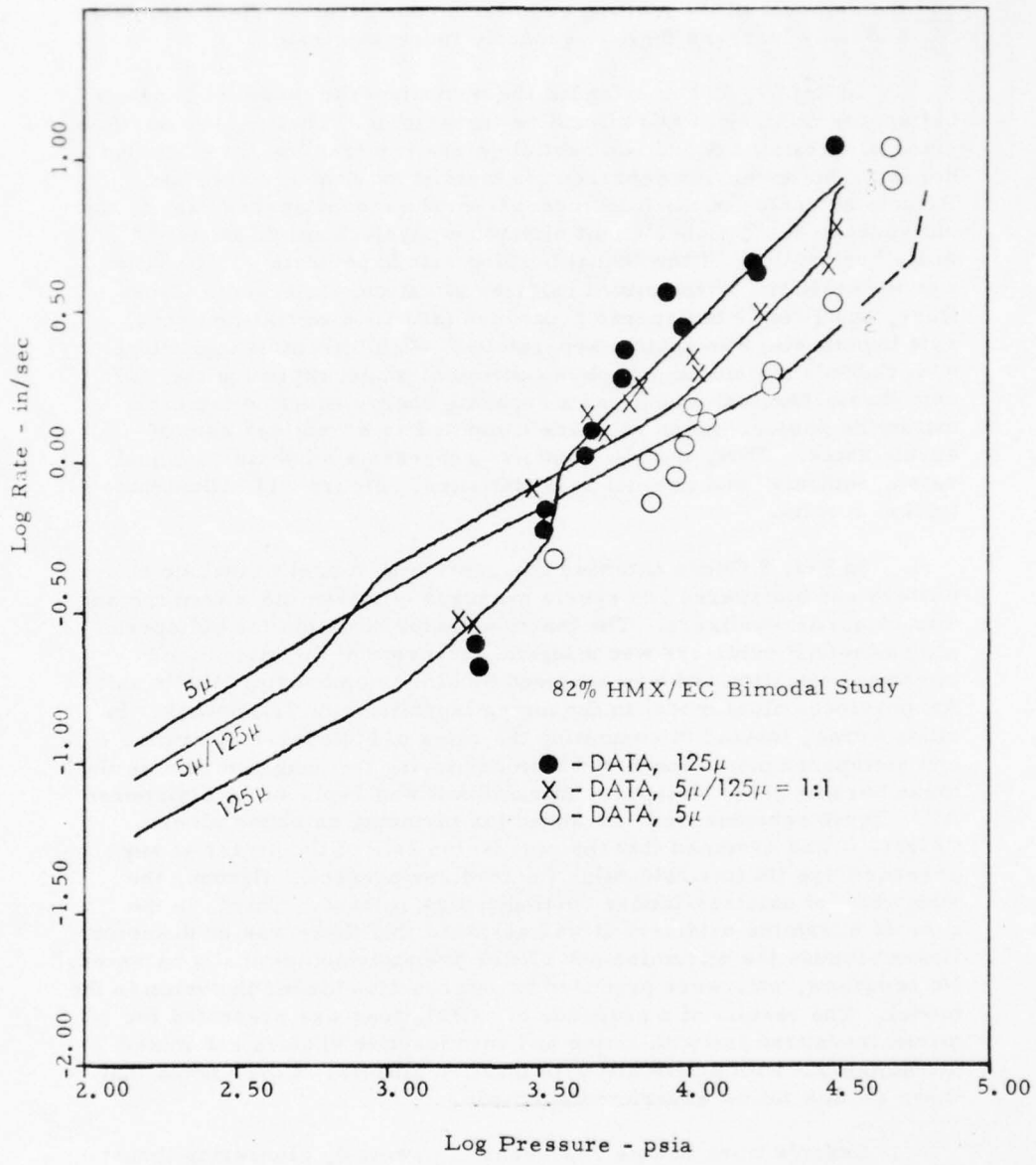

Figure 11. Comparison Theory and Experiment - Cohen's Multi Modal Nitramine Model (Ref. 7)

catalysts explicitly. However, the model, since it employs BDP methodology, possesses the noted inconsistencies associated with that model. Moreover, with deep penetrations the fuel surface is no longer planar. Consequently, the statistics of the surface are altered. These interactions were not treated by Cohen.

Miller, Donohue, and Peterson Model[21] - In this work the model of Miller, Hartman, and Myers is extended to include interaction effects. This extension was stimulated by the finding that the MHM theory did not correlate particle size effects well in uncatalyzed HTPB/AP propellants. In particular, it was found that emphasis was weighted to the coarse end of the distribution rather than the fine end of the distribution. As noted in the review of the MHM model, consideration of mixture ratio effects will tend to skew the weighting in the direction required.

Interactions among particles were assumed to occur from flame interactions. Specifically, it was assumed that the diffusion flame about an oxidizer particle was larger than the particle so that

$$D_{fl,j} = \epsilon D_j \tag{81}$$

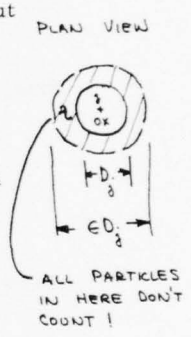

where $\epsilon \geq 1$. It was further assumed that all oxidizer particles lying in the j^{th} particles annular area

$$\Delta A_{x,j} = \pi (D_{fl,j}^2 - D_j^2)/4 = \pi(\epsilon^2-1) D_j^2/4 \tag{82}$$

would be "excluded".* If N_j'' is the number of j particles per unit planar surface, the total "exclusion area" of j^{th} particles is

$$A_{x,j} = N_j'' \Delta A_{x,j} = \pi N_j'' (\epsilon^2-1) D_j^2/4 \tag{83}$$

For an i^{th} particle to be excluded by a j^{th} particle it must fit in the j^{th} particle's annular "exclusion area". Thus,

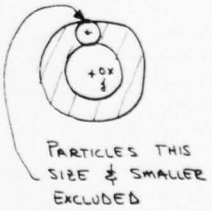

$$(D_{fl,j} - D_j)/2 = D_j(\epsilon-1)/2 \geq D_i \tag{84}$$

With D_j increasing with j this defines a critical $j = j_{c,i}$ such that only j^{th} particles with $j \geq j_{c,i}$ will exclude an i^{th} particle. Since the number of i^{th} particles per unit area is N_i'', the number of i^{th} particles excluded by a $j \geq j_{c,i}$ particle is

$$\Delta N_{i,x}'' = \pi N_i'' N_j'' (\epsilon^2-1) D_j^2/4 \tag{85}$$

*This means that the contribution of the excluded particles to the total flow of products is deleted. This is patent nonsense because mass is conserved.

The total number of i^{th} particles "excluded" is the sum over all j^{th} particles with $j \geq j_{c,i}$. Thus,

$$N''_{i,x} = \left[\pi N''_i (\epsilon^2-1)/4\right] \sum_{j_{c,i}} N''_j D_j^2 \qquad (86)$$

Consequently, the number of i^{th} particles that "contribute" is

$$N''_{i,A} = N''_i - N''_{i,x} = N''_i \left\{1-\left[\pi(\epsilon^2-1)/4\right] \sum_{j_{c,i}} N''_j D_j^2 \right\} \qquad (87)$$

It is clear that this postulated strategy "skews" effects to the larger particles because large particles "exclude" small particles and not vice versa.

As noted previously in the review of Ref. (9) $N''_i \propto w_i D_i^2$. Thus, employing the rate expression of Ref. (9)

$$\bar{r} = \sum_i \bar{r}_i w_i \left[1 - K(\epsilon^2-1) \sum_{j_{c,i}} w_j\right] / \sum_i w_i \qquad (88)$$

where K is a constant.

Miller, Donohue, and Peterson note that this is only a partial expression because particles hiding particles can be hidden. This leads to the expression

$$\bar{r} = K_0 \sum_i w_i \bar{r}_i - K_1 \left[\sum_i w_i \bar{r}_i \sum_{j_{c,i}} w_j\right]^{\eta} \qquad (89)$$

where $\eta < 1$ is an empirical constant. They have successfully employed this expression to correlate ambient rate/pressure/particle size distribution data for HTPB/AP propellants.

This approach represents a pioneering approach at pair/pair interactions and demonstrates how the statistics of the burning surface can be employed to deduce interactions within the framework of an assumed interaction model. For these concepts this work is valuable. However, "excluding" particles is nonsense because they are still there and their mass must go into gaseous products. In order words, the postulated interaction model is not physically plausible. As mentioned previously, there are sound physical reasons to assume that small particles are more fuel rich than large particles. Since the propellant as a whole is underoxidized and rate usually falls off as one moves away from the stoichiometric condition, rate will be skewed away from that predicted by the GDF model by mixture ratio effects. As Ebenezer,

Cole, and McAlevy[18] have formulated a mixture ratio sensitive GDF model, replacement of the GDF model in MHM's theory by this model would make more sense than physically implausible interaction mechanisms.

DEVELOPMENT OF POLYDISPERSE MODEL

General Comments - The work to be reported in this section was conducted over a two-year span. The goal of the first years work was primarily to embed the BDP model in a "correct statistical formulation" thereby effectively extending the model to additive free propellants with spherical oxidizer. The goal of the second years effort was basically to extend this model to aspherical particles and include binder melts. The first goal was accomplished by abandoning the original grand ensemble statistics and developing the petite ensemble method. However, in the operation of this code "problems" appeared.* In the process of exploring these "problems" further insites into the petite ensemble method were glimpsed and new methodology for selecting the mean state was developed. This impacted the aspherical particle work toughening that problem. During investigations of spherical problems (late in the program when petite ensemble methodology was thought to be surprise free) a further "glimmer" into the potential of the method was obtained. This "glimmer" showed that retention/explusion of partially consumed oxidizer particles and "deep penetrations" (see review of Cohen's Nitramine Model) should flow naturally from a proper combination of petite ensemble statistics and BDP model. These "enlightenments" have been stimulating but troublesome; they interfere with orderly progress and reporting. As for the reporting, the method is developed with generality as far as possible. After this point, main emphasis is placed on spherical particles. However, all partially completed work is included in appropriate appendices for future reference.

In retrospect there should have been no "surprises". However, it just wasn't that way. The spirit of the first "enlightenment" is included in the review of the BDP model. The second "enlightenment" consisted of realizing that under most conditions an oxidizer particle is either consumed before the fuel plane reaches its south pole or not. For latter situation, which occurs with large particles at low pressures, the partially consumed oxidizer particles are either "freed" or retained. The retention question is probably answered by response to the question "is there a surface melt"? If there is, the partially consumed particles probably stick to the surface. If not, they are probably freed. If they stick, there are more oxidizer particles on the burning surface than computed by planar statistics because planar statistics assumes particles vanish when the fuel plane reaches a particles south pole. The stuck particles are different than the original particles; they are smaller. Thus, a monodisperse propellant can become effectively bi-disperse under certain conditions. On the other hand, if partially

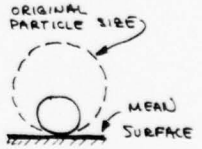

RESIDUAL PARTICLE SITUATION

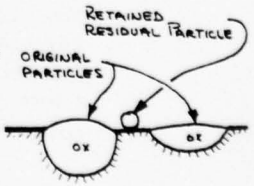

MONODISPERSE BECOMES BIDISPERSE

*See Ref. (28) for some details.

consumed solid particles are freed, oxidizer flows from the burning surface in both gaseous and solid (freed particles) forms. As the continuity expression employed counts only the gaseous form, that expression needs modification.

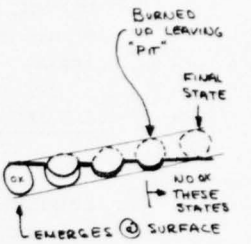

If the oxidizer particle is consumed before the fuel plane reaches its south pole, a fuel rich depression is left. Therefore, some of the microstates counted by the statistics are devoid of oxidizer! However, as the statistics are steady in time, the ergodic surmise applies so that some of these particle absent microstates persist for finite time. If there is no surface melt, continued pyrolysis of the binder at the particle absent sites can expose other particles which, if there is time, can ignite and burn. It is readily apparent that, if r_{ox} is large and t_{ign} very small, a multi-particle (deep) penetration is possible. On the other hand, suppose a mobile melt is present. The possibility now exists for melt to fill the empty site making it impossible for another particle to be uncovered. Response to the question "are particles uncovered at empty sites?" depends upon more than must the presence or absence of a surface melt. It must be a dynamic process because melt motion is required. It is important to note that if the empty sites do not fill, the burning surface is no longer quasi-planar. This is especially true if other particles are uncovered and ignited. Consequently, a rough surface must be allowed for.

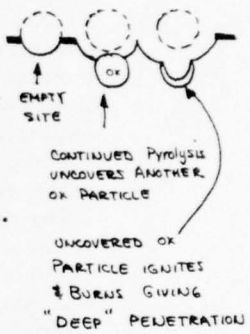

These questions are not simple; however, they are also not unanswerable. Indeed, the beauty of the petite ensemble method is that answers to these questions appear possible within its framework (a little bending may be necessary).

Statistical Framework - In Fundamentals of Statistical Combustion Modeling it has been shown that

$$\bar{m}_c'' = \bar{r}\rho_c = \sum_{j=1}^{Q_p} \bar{m}_{p,j}'' \, \Delta S_{p,j} / S_p \qquad (90)$$

where $\bar{m}_{p,j}''$ is the mean mass flux from and $S_{p,j}$ the portion of S_p occupied by the jth distinguishable particles. Particles on the burning surface are distinguishable because of specie, size, shape, and orientation. If the particles are spherical, their shape is defined and there are no distinguishable orientations. Therefore, only specie and size represent distinguishable features. However, for a general particle three parameters must be specified to define shape and size and three angles must be specified to define orientation. Consequently, a total of seven parameters is required to define a general distinguishable particle. Since

$$Q_p = \prod_{k=1}^{K} N_k \qquad (91)$$

where K is the total number of parameters and N_k is the number of steps in the k^{th} parameter required to adequately describe the variation with that parameter, it is seen that Q_p can be a very large number in propellant with mixed, polydisperse oxidizer having "general" particles. As noted previously, computation time is directly proportional to Q_p. Therefore, minimizing Q_p while retaining the essence of the problem is computationally important. Consequently, it shall be assumed that the particles are at most ellipsoids of revolution. This means that "orientableness" is retained but only one angle is required to distinguish that orientation and that asphericness is retained but only two dimensions are required to characterize size and shape. Therefore, particle characterization parameters are at most specie(s), size (D), aspect ratio (a), and orientation (ϕ). The size of the ellipsoid (D) is taken to be the maximum dimension normal to the axis of symmetry. The single sum in Eq. 90 is then replaced with the quadruple sum ($Q_p = N_s N_a N_d N_\phi$)

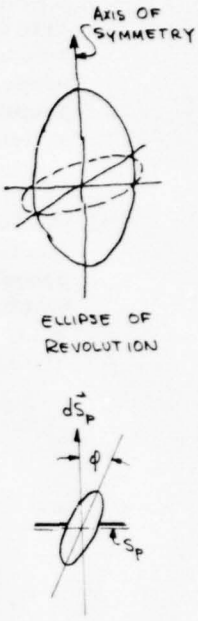

$$\bar{\dot{m}}''_c = \bar{r}\rho_c = \sum_{\lambda=1}^{N_\lambda}\sum_{a=1}^{N_a}\sum_{d=1}^{N_d}\sum_{\phi=1}^{N_\phi} \bar{\dot{m}}''_{p,\lambda,a,d,\phi}\,\Delta\bar{S}_{p,\lambda,a,d,\phi}/S_p \qquad (92)$$

If $N_{p,s,a,d,\phi}$ is the number of particles on S_p with $D \le D \le D+dD$, $a \le a \le a+da$, $\phi \le \phi \le \phi+d\phi$ and specie k per unit area of S_p, $d^3F_{p,\lambda,a,d,\phi}/da\,dD\,d\phi$ is a distribution function such that

$$\Delta^3 N_{p,\lambda,a,d,\phi} = N''_t\left(d^3F_{p,\lambda,a,d,\phi}/da\,dD\,d\phi\right)\Delta a\,\Delta D\,\Delta\phi \qquad (93)$$

and $\Delta\bar{S}_{p,\lambda,a,d,\phi}$ is the average planar surface for fuel surface/oxidizer particle pairs with s, a, D, ϕ parameters, Eq. 92 becomes

$$\bar{\dot{m}}''_c = \bar{r}\rho_c = N''_t\sum_{\lambda}^{N_\lambda}\sum_{a}^{N_a}\sum_{D}^{N_d}\sum_{\phi}^{N_\phi}\left(\bar{\dot{m}}''\Delta\bar{S}\right)_{p,\lambda,a,d,\phi}\left[d^3F_{p,\lambda,a,d,\phi}/da\,dD\,d\phi\right]\Delta a\,\Delta D\,\Delta\phi \qquad (94)$$

Passing to the limit as $N_a, N_d, N_\phi \to \infty$ and $\Delta a, \Delta D, \Delta\phi \to 0$ gives

$$\bar{\dot{m}}''_c = \bar{r}\rho_c = N''_t\sum_{\lambda=1}^{N_\lambda}\int\int\int\left(\bar{\dot{m}}''\Delta\bar{S}\right)_{p,\lambda,a,d,\phi}\left[d^3F_{p,\lambda,a,d,\phi}/da\,dD\,d\phi\right]da\,dD\,d\phi \qquad (95a)$$

For spherical particles $\bar{\dot{m}}''\Delta\bar{S}$ is independent of a and ϕ so that integration on these variables gives

$$\bar{\dot{m}}''_c = \bar{r}\rho_c = N''_t\sum_{\lambda=1}^{N_\lambda}\int\left(\bar{\dot{m}}''\Delta\bar{S}\right)_{p,\lambda,d}\left(dF_{p,\lambda,d}/dD\right)dD \qquad (95b)$$

Equation 95 is a statistical expression relating the mean burning rate of a propellant with mixed, polydisperse, aspheric oxidizer to the burning rate of monodisperse psuedo-propellants. If there are no interactions among fuel surface/oxidizer particle pairs, the monodisperse pseudo-propellant rates can be computed one at a time using any monodisperse propellant code. In what follows it is assumed that there are no interactions.

The next step is to investigate the statistical characteristics of the burning surface and thereby relate $\Delta\bar{S}_{p,\ell,a,d,\phi}$, the distribution function, and properties of the monodisperse psuedo-propellants to propellant formulation variables. From formulation variables the mass fraction of particles in the propellant with specie s, $a \le a \le a+da$, and $D \le D \le D+dD$ is, in principle, known from measurements.* Therefore, the volume fraction of these particles is

$$d\zeta_{\ell,a,d} = \rho_c \, dw_{\ell,a,d} / \rho_{ox,\ell} \tag{96}$$

and the number of these particles per unit volume of the propellant is

$$d^3N_{\ell,a,d}/dV = d^2\zeta_{\ell,a,d} / \Delta\bar{V}_{a,d} \tag{97}$$

where $\Delta\bar{V}_{a,d}$ is the volume of a particle with aspect ratio a and size D.

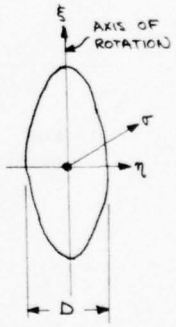

The size of the ellipsoid is taken to be the dimension normal to the axis of revolution as this represents the smallest dimension the particle will pass through. Therefore, in particle centered, cartesian coordinates η, σ, ξ the equation describing the particles surface is

$$\eta^2 + \sigma^2 + \xi^2/a^2 = (D/2)^2 \tag{98}$$

Consequently, the volume of a particle with a, D characteristics is

$$\Delta\bar{V}_{a,d} = 2\pi \int_0^{aD/2} \eta^2 d\xi = 2\pi \int_0^{aD/2} (D^2/4 - \xi^2/a^2)\, d\xi = \pi a D^3/6 \tag{99}$$

Thus,

$$d^3N_{\ell,a,d}/dV = 6\, d\zeta_{\ell,a,d} / (\pi a D^3) \tag{100}$$

*This information must be known for if we don't know what goes in we cannot expect to compute what comes out.

Assuming henceforth that the statistics of the particle arrangement in the condensed phase are homogeneous and isotropic, all orientations of aspheric particles are equally probable. Therefore, the number of particles per unit volume with s, a, D and $\varphi \le \varphi \le \varphi + d\varphi$ is*

$$d^4N_{s,a,d,\varphi}/dV = [d^3N_{s,a,d}/dV]\sin\varphi\, d\varphi/2 \qquad (101)$$

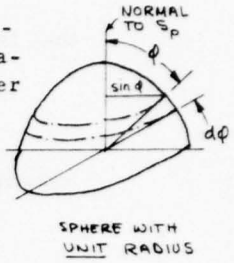

SPHERE WITH UNIT RADIUS

However, particles with $\varphi = \varphi$ and $\varphi = \pi - \varphi$ are indistinguishable because of the assumed particle symmetry. This double degeneracy is accounted for by doubling the probability and limiting φ to $0 \le \varphi \le \pi/2$. Thus, with Eq. 100

$$d^4N_{s,a,d,\varphi}/dV = 6\sin\varphi\, d\varphi\, d\zeta_{s,a,d}/(\pi a D^3) \qquad (102)$$

WHICH END OF SYMMETRIC PARTICLE IS UP? FOR THIS REASON CAN'T DISTINGUISH $\varphi = \varphi$ AND $\varphi = \pi - \varphi$

With number per unit volume known the next question is "what are the numbers/unit surface on the burning surface?" Assuming with BDP that the burning surface is a plane dotted with concave and/or convex particles, we need only consider the particles intersecting a plane S_p. Consider the relationship between a single particle and the plane S_p. Let φ denote the angle between the normal to S_p and the axis of revolution of the ellipsoid. Denote the location of the particle by the coordinates of its CG. Clearly, all particles with $y = \pm \bar{X}''_{a,d,\varphi}/2$ will intersect S_p. The volume containing s, a, d, φ particles that can intersect S_p is, therefore, $dV = \bar{X}''_{a,d,\varphi}\, dS_p$ so that

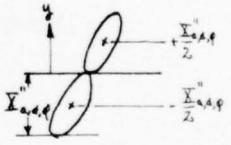

$$d^4N_{s,a,d,\varphi}/dS_p = 6\bar{X}''_{a,d,\varphi}\sin\varphi\, d\varphi\, d^2\zeta_{s,a,d}/(\pi a D^3) \qquad (103)$$

The next question is how many a, D, φ particles intersect S_p at a specific distance from the point of initial intersection with S_p. That is, how many particles intersect S_p with $X \le \bar{X} \le X + d\bar{X}$. To intersect S_p under these conditions the CG of the particle must lie in a volume $dV = S_p\, d\bar{X}$. Therefore, the number of a, D, φ particles that intersect S_p with $X \le \bar{X} \le X + d\bar{X}$ is

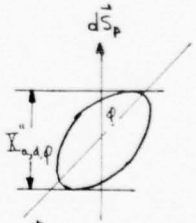

$$d^5N_{s,a,d,\varphi,\bar{X}}/dS_p = 6\sin\varphi\, d\varphi\, d\bar{X}\, d^2\varphi_{s,a,d}/(\pi a D^3) \qquad (104)$$

This shows that all $0 \le \bar{X} \le \bar{X}''_{a,d,\varphi}$ are equally probable.

The distance $X''_{a,d,\varphi}$ is the normal distance between two planes parallel to S_p and tangent to a particle with a and D. At the first quadrant tangency point (t) $d\xi/d\eta = -\tan\varphi$. Differentiating Eq. 98 with respect to η (set $\sigma = 0$)*, solving for $d\xi/d\eta$, setting that

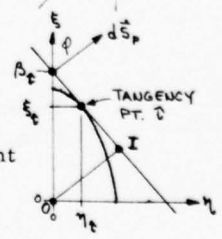

*Consider a sphere with unit radius and φ = being angle between radius vector and north polar axis. As orientations are equally probable, probability of orientation with angle φ is (area zone)/(area sphere) = $2\pi\sin\varphi\, d\varphi / 4\pi$.

**Since the particle is a body of revolution, there is no need to work in three dimension.

that result to $-\tan\varphi$, and solving for the first quadrant ξ_t yields

$$\xi_t = (a^2 D/2) \Big/ \sqrt{a^2 + \tan^2\varphi} \tag{105a}$$

Substituting this result in Eq. 98 ($\sigma = o$) gives

$$\eta_t = (D/2) \Big/ \sqrt{a^2 + \tan^2\varphi} \tag{105b}$$

The equation of the tangent plane through η_t, ξ_t is

$$\xi = -(\tan\varphi)\eta + \beta_t \tag{106a}$$

where

$$\beta_t = \xi_t + \eta_t \tan\varphi = (D/2)\sqrt{a^2 + \tan^2\varphi} \tag{106b}$$

From the geometry it is clear that $X''_{a,d,\varphi} = 2\,\overline{OI}$. Since $\overline{OI} = \beta_t \cos\varphi$

$$X''_{a,d,\varphi} = 2\beta_t \cos\varphi = D\cos\varphi\sqrt{a^2 + \tan^2\varphi} \tag{107}$$

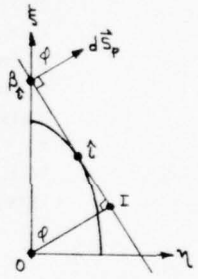

FIRST QUADRANT DETAILS - PLANE TANGENT TO PARTICLE.

Consequently,

$$d^4N_{s,a,d,\varphi} / dS_p = 6\sqrt{a^2 + \tan^2\varphi}\,\sin\varphi\cos\varphi\,d\varphi\,d^2\mathcal{V}_{s,a,d} / (\pi a D^2) \tag{108}$$

The mean planar intersection area between a particle with s, a, D, φ and S_p is defined by

$$d^4S_{p,s,a,d,\varphi} / dS_p = \Delta\bar{S}_{p,s,a,d,\varphi}\; d^4N_{s,a,d,\varphi} / dS_p \tag{109}$$

Translate the plane S_p a distance dy. The volume of particles with s, a, D, φ in this volume is

$$d^4V_{s,a,d,\varphi} = [d^4N_{s,a,d,\varphi} / dV]\; S_p\, dy\; \Delta\bar{V}_{a,d} \tag{110}$$

However, by continuity it is also

$$d^4V_{\lambda,a,d,\phi} = \left[d^4S_{p,\omega,a,d,\phi} / dS_p\right] S_p \, dy \qquad (111)$$

Therefore,

$$d^4S_{p,\omega,a,d,\phi} / dS_p = (d^4N_{\lambda,a,d,\phi} / dV)\, \Delta\bar{V}_{a,d} = \sin\phi \, d\phi \, d^2\gamma_{\lambda,a,d} \qquad (112)$$

so that from Eqs. 108, 104, and 112

$$\Delta\bar{S}_{p,\omega,a,d,\phi} = [\pi D^2/6]\left[a / \sqrt{a^2\cos^2\phi + \sin^2\phi}\right] \qquad (113)$$

Within the context of the BDP model this dimension alone would describe characteristic distances from the initial point of tangency of the particle with S_f that would, in turn, define the doubly degenerate mean state. However, as pointed out in the review of the BDP model this approach is correct only in the case of no ignition delay.

The mean statistical characteristics of the fuel surface in each monodisperse "cut" of fuel surface/oxidizer particle pairs cannot be determined exactly without detailed knowledge of the particle packing. Since this information is unavailable*, an approximation is introduced. Examination of the characteristics of regular geometric packings[29] suggests that the mean volume of "binder" associated with a specific particle should be roughly proportional to that particles surface area or $\Delta\bar{V}_b \propto \Delta\bar{S}_{ox,a,d}$. To allow for variability it is assumed that

$$\Delta\bar{V}_{b_{r,a,d}} = C\, \Delta\bar{S}^{n}_{ox,a,d} \qquad (114)$$

where n is an empirical parameter (to be defined by correlation with data) and C is the proportionality constant.

The surface area of an ellipsoid of revolution is

$$\Delta\bar{S}_{ox,a,d} = 4\pi \int_0^{D/2} \sqrt{1 + (d\xi/d\eta)^2}\; \eta \, d\eta \qquad (115)$$

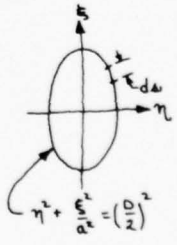

Differentiating Eq. 98 to find $d\xi/d\eta$ and employing $\nu^2 = (\frac{D}{2})^2 - \eta^2$ as a change of variable enables the resulting expression to be integrated in closed form yielding

$$\Delta\bar{S}_{ox,a,d} = \frac{\pi}{2} D^2 \left[1 + \frac{a^2}{\sqrt{1-a^2}} \ln \frac{1+\sqrt{1-a^2}}{a}\right] \qquad a < 1 \qquad (116a)$$

*There is no reason why it isn't except for inactivity.

$$\Delta \bar{S}_{ox,a,d} = \pi D^2 \qquad a = 1 \qquad (116b)$$

$$= \frac{\pi}{2} D^2 \left[1 + \frac{a^2}{\sqrt{a^2-1}} \sin \sqrt{\frac{a^2-1}{a^2}} \right] \qquad a > 1 \qquad (116c)$$

The volume fraction of binder is $\zeta_b = 1 - \zeta_{ox}$ (propellant assumed here to be solely binder and oxidizer). However, it is also

$$\zeta_b = \sum_{\omega=1}^{N_\omega} \iiint \Delta \bar{V}_{b,a,d} \left(d^4 N_{\omega,a,d,\phi} / dV \right) \qquad (117)$$

With Eqs. 102 and 114 this defines C as

$$C = \frac{\pi \zeta_b}{6} \Big/ \sum_{\omega=1}^{N_\omega} \iint \left[\Delta \bar{S}^{n}_{ox,a,d} / (a D^3) \right] d^2 \zeta_{\omega,a,d} \qquad (118)$$

With C and n known the mean volume of binder and oxidizer associated with monodisperse pseudo-propellants with s, a, d, characteristics are known. Therefore, the volume fraction of oxidizer in the pseudo-propellant is

$$\zeta^*_{ox,\omega,a,d,\phi} = \Delta V_{ox,a,d} \Big/ \left[\Delta V_{ox,a,d} + \Delta \bar{V}_{b,a,d} \right] \qquad (119a)$$

With Eqs. 99 and 114 this is

$$\zeta^*_{ox,\omega,a,d,\phi} = \left[1 + 6C \Delta \bar{S}^{n}_{ox,a,d} / (\pi a D^3) \right]^{-1} \qquad (119b)$$

Since pseudo-propellants are oxidizer and binder

$$\zeta^*_{b,\omega,a,d,\phi} = 1 - \zeta^*_{ox,\omega,a,d,\phi} \qquad (119c)$$

Translate a plane S_p in the propellant a distance Δy. The volume swept out is $S_p \Delta y$. The fraction of this swept out volume that is oxidizer is $\zeta_{ox} S_p \Delta y$. However, the fraction of this volume that is oxidizer is also $S_{p,ox} \Delta y$. Consequently,

$$\zeta_{ox} = S_{p,ox} / S_p \tag{120}$$

Therefore, in the pseudo-propellant (actually, this is a definition)

$$\zeta^*_{ox,\omega,a,d,\phi} = \Delta\bar{S}_{p,ox,\omega,a,d,\phi} / \Delta\bar{S}_{p,\omega,a,d,\phi} \tag{121}$$

where the bar-overs denotes means for fuel surface/oxidizer particle pairs. Therefore, with Eq. 113

$$\Delta\bar{S}_{p,\omega,a,d,\phi} = \left[\pi D^2/(6\zeta^*_{ox,\omega,a,d,\phi})\right]\left[a/\sqrt{a^2\cos^2\phi + \sin^2\phi}\right] \tag{122}$$

Attention in this program has been largely directed at additive free propellants. However, most practical propellants contain additives. Moreover, Cohen, Derr, Price[4] have demonstrated that rate, pressure characteristics of metallized propellants can be predicted by assuming the additive is chemically inert. Therefore, it appears that a useful approximation to real propellant behavior might be made by assuming that, insofar as rate defining processes go, additives are inert and are apportioned among the pseudo-propellants as a fixed fraction of binder. Subdividing binder into fuel, catalyst, and metal $dV_b = dV_f + dV_{cat} + dV_m$. Therefore, $dV_{cat}/dV_b = \varphi_{cat}/\zeta_b$, $dV_f/dV_b = \zeta_f/\zeta_b$, and $dV_m/dV_b = \zeta_m/\zeta_b$. Consequently, in any pseudo-propellant

$$\zeta^*_{f,\omega,a,d,\phi} = (\zeta_f/\zeta_b)\,\zeta^*_{b,\omega,a,d,\phi} \tag{123a}$$

$$\varphi^*_{cat,\omega,a,d,\phi} = (\varphi_{cat}/\zeta_b)\,\zeta^*_{b,\omega,a,d,\phi} \tag{123b}$$

$$\zeta^*_{m,\omega,a,d,\phi} = (\zeta_m/\zeta_b)\,\zeta^*_{b,\omega,a,d,\phi} \tag{123c}$$

The mass fraction of oxidizer in the pseudo propellant is

$$\alpha^*_{ox,\omega,a,d,\phi} = \Delta m_{ox,\omega,a,d} / \left[\Delta m_{ox,\omega,a,d} + \Delta m_{b,\omega,a,d}\right] \tag{124}$$

but $\Delta m = \rho \Delta V$ so that

$$\alpha^*_{ox,\omega,a,d,\phi} = \left[1 - \frac{\rho_{ox,\omega}}{\rho_b} \frac{\Delta \bar{V}_{b,\omega,a,d,\phi}}{\Delta \bar{V}_{ox,\omega,a,d,\phi}}\right]^{-1} = \left[1 - \frac{\rho_{ox,\omega}}{\rho_b} \frac{\zeta^*_{b,\omega,a,d,\phi}}{\zeta^*_{ox,\omega,a,d,\phi}}\right]^{-1} \quad (125)$$

Since $\alpha_{ox} = (\rho_{ox} / \rho_c)\, \zeta_{ox}$

$$\rho^*_{c,\omega,a,d,\phi} = \rho_{ox,\omega}\, \zeta^*_{ox,\omega,a,d,\phi} / \alpha^*_{ox,\omega,a,d,\phi} \quad (126)$$

With pseudo-propellant density known the mass fractions can be computed as

$$\alpha^*_{f,\omega,a,d,\phi} = (\rho_f / \rho^*_{c,\omega,a,d,\phi})\, \zeta^*_{f,\omega,a,d,\phi} \quad (127a)$$

$$\alpha^*_{m,\omega,a,d,\phi} = (\rho_m / \rho^*_{c,\omega,a,d,\phi})\, \zeta^*_{m,\omega,a,d,\phi} \quad (127b)$$

$$\alpha^*_{cat,\omega,a,d,\phi} = (\rho_{cat} / \rho^*_{c,\omega,a,d,\phi})\, \zeta^*_{cat,\omega,a,d,\phi} \quad (127c)$$

The specific heat of the condensed phase is

$$\kappa^*_{c,\omega,a,d,\phi} = \sum_i \alpha^*_{i,\omega,a,d,\phi}\, \kappa_i \qquad i = ox, f, cat, m \quad (128)$$

Treating additives as inert the flame temperature for any pseudo-propellant can be computed from a thermochemistry code. However, the number of such computations required to define flame temperature for all possible combinations of oxidizer, metal, fuel, catalyst and mixture ratio is excessive. Therefore, an approximate strategy, valid for small additive concentrations, is employed. Basically the adiabatic flame temperature of just fuel and oxidizer $T'_{flame} = f_{ume}(ox, f)$ is computed with the thermochemistry code and tabulated. This can be done once and for all for a specific fuel, ox combination. The inerts are then added as a diluent. Consequently,

$$T^*_{flame,\omega,a,d,\phi} = \frac{\kappa'_p T'_{flame} + \sum_j \alpha^*_{j,\omega,a,d,\phi} (\kappa_j T_\infty - Q_j)}{\kappa'_p + \sum_j \alpha^*_{j,\omega,a,d,\phi}\, \kappa_j} \qquad j = cat, m \quad (129)$$

where c_p' is the specific heat at constant pressure of the fuel and oxidizer and Q_j is the latent heat of fusion of the j^{th} inert material.

The volume fraction of oxidizer with s, a, d characteristics is

$$d^2\zeta_{s,a,d} = d^2V_{ox,s,a,d} / V_c \tag{130}$$

Since $d^2V_{ox,s,a,d} = dm_{ox,s,a,d} / \rho_{ox,s}$ and $V_c = m_c / \rho_c$

$$d^2\zeta_{s,a,d} = [d^2m_{ox,s,a,d} / m_c][\rho_c / \rho_{ox,s}] \tag{131}$$

Oxidizer particles in a propellant are the result of mixing several modes of oxidizer together. Each mode is characterized separately as to (a) the distribution of sizes (D) within that mode and (b) the specific surface in that mode. Therefore,

$$dm_{ox,s,d,k} / m_{ox,s,k} = F_{ox,s,k}\, dD \tag{133}$$

is known by measurement. The surface area in a mode is

$$S_{ox,s,k} = \int\int \Delta\bar{S}_{ox,s,a,d,k}\, d^2N_{ox,s,a,d,k} \tag{134}$$

where the surface area $\Delta\bar{S}_{ox,s,a,d}$ of a specific particle is given by Eq. 113. The mass of particles in the k^{th} mode with s, a, d characteristics is related to the number with that characteristic by

$$d^2N_{ox,s,a,d,k} = d^2m_{ox,s,a,d,k} / (\rho_{ox,s}\, \Delta\bar{V}_{a,d}) \tag{135}$$

or with Eq. 99

$$d^2N_{ox,s,a,d,k} = 6\, d^2m_{ox,s,a,d,k} / (\pi a\, D^3) \tag{136}$$

Thus, Eq. 134 becomes

$$S_{ox,s,k} = \frac{6}{\pi}\int\int\left[\Delta\bar{S}_{ox,a,d} / (a\,D^3)\right]\left[d^2m_{ox,s,a,d,k} / da\,dD\right] da\,dD \tag{137}$$

Therefore, to employ surface area measurements to define parameters in the modes distribution of size and shape the distribution of shape must be known because

$$\frac{dm_{ox,s,d,k}}{m_{ox,s,k}} = \int_a \frac{d^2 m_{ox,s,a,d,k}}{m_{ox,s,k}} \tag{138}$$

This information is just not available. Consequently, we are in a position where the theoretical model is more general than the available input information. Hence, to proceed further some assumption relative to the distribution of particle shape for specific size is required. Assume this distribution is log normal about some mean $\bar{a}_{s,k}$ with standard deviation $\sigma_{a,s,k}$. Then

$$\frac{d^2 m_{ox,s,a,d,k}}{dm_{ox,s,d,k}} = \frac{1}{\sqrt{2\pi}\,\sigma_{a,s,k}} \exp\left[-\frac{1}{2}\left(\frac{\ln a - \ln \bar{a}_{s,k}}{\sigma_{a,s,k}}\right)^2\right] d\ln a \tag{139}$$

and

$$d^2 m_{ox,s,a,d,k} = m_{ox,s,k} \frac{F_{ox,s,k}}{\sqrt{2\pi}\,\sigma_{a,s,k}} \exp\left[-\frac{1}{2}\left(\frac{\ln a - \ln \bar{a}_{s,k}}{\sigma_{a,s,k}}\right)^2\right] d\ln a\, dD \tag{140}$$

Consequently, the surface area/unit mass of oxidizer mode s,k is

$$\frac{dS_{ox,s,k}}{dm_{ox,s,k}} = \frac{6}{\pi\sqrt{2\pi}\,\sigma_{a,s,k}} \int_D \left\{ \int_a \frac{\Delta \bar{S}_{ox,s,d}}{a D^3} F_{ox,s,d,k} \exp\left[-\frac{1}{2}\left(\frac{\ln a - \ln a_{s,k}}{\sigma_{a,s,k}}\right)^2\right] d\ln a \right\} dD \tag{141}$$

This equation leaves one free parameter for each mode. This parameter can be determined by correlation to a data base.

With $a_{s,k}$ and $\sigma_{a,s,k}$ known in principle,

$$d^2 m_{ox,s,a,d} = \sum_{k=1}^{K_s} d^2 m_{ox,s,a,d,k} \tag{142}$$

where K_s is the number of oxidizer modes with species s. Therefore, combining Eqs. 132, 140, and 142 yields

$$d^2 f_{s,a,d} = \frac{\rho_c}{\rho_{ox,s}} \sum_{k=1}^{K_s} \frac{m_{ox,s,k}}{m_c} \frac{F_{ox,s,d,k}}{\sqrt{2\pi}\,\sigma_{a,s,k}} \exp\left[-\frac{1}{2}\left(\frac{\ln a - \ln \bar{a}_{s,k}}{\sigma_{a,s,k}}\right)^2\right] d\ln a\, dD \tag{143}$$

Since $\zeta_{ox} = V_{ox} / V_c$, $V_{ox} = \sum_{\omega=1}^{N_\omega} \sum_{k=1}^{K_\omega} V_{ox,\omega,k}$ and $V = m/\rho$

$$\zeta_{ox} = \rho_c \sum_{\omega=1}^{N_\omega} \sum_{k=1}^{K_\omega} \alpha_{ox,\omega,k} / \rho_{ox,\omega} \tag{144}$$

Moreover, since $\rho_c = (V_c / m_c)^{-1}$, $V_c = \sum_{\omega=1}^{N_\omega} \sum_{k=1}^{K_\omega} V_{ox,\omega,k} + V_f + V_{cat} + V_m$, and $V = m/\rho$

$$\rho_c = \left[\rho_f^{-1} + \alpha_{cat} \left(\rho_{cat}^{-1} - \rho_f^{-1} \right) + \alpha_m \left(\rho_m^{-1} - \rho_f^{-1} \right) + \sum_{\omega=1}^{N_\omega} \sum_{k=1}^{K_\omega} \alpha_{ox,\omega,k} \left(\rho_{ox,\omega}^{-1} - \rho_f^{-1} \right) \right]^{-1} \tag{145}$$

By definition $N_*'' \, d^3 F_{p,\omega,a,d,\varphi} = d^4 N_{\omega,a,d,\varphi} / dS_p$. Therefore, with Eq. 103

$$N_*'' \, d^3 F_{p,\omega,a,d,\varphi} = 6 \, \overline{X}_{a,d,\varphi}'' \sin\varphi \, d\varphi \, d^2\varphi_{\omega,a,d} / (\pi a D^3) \tag{146}$$

With Eqs. 107 and 143 this becomes

$$N_*'' \, d^3 F_{p,\omega,a,d,\varphi} = \frac{6\sqrt{a^2\cos^2\varphi + \sin^2\varphi}}{\pi D^2 a} \sin\varphi \, \frac{\rho_c}{\rho_{ox,\omega}} \sum_{k=1}^{K_\omega} \frac{m_{ox,\omega,k}}{m_c} \frac{F_{ox,\omega,d,k}}{\sqrt{2\pi}\,\sigma_{a,\omega,k}}$$

$$\exp\left[-\frac{1}{2} \left(\frac{\ln a - \ln \bar{a}_{\omega,k}}{\sigma_{a,\omega,k}} \right) \right] d\ln a \, dD \, d\varphi \tag{147}$$

Therefore, with Eq. 147, Eq. 95a becomes

$$\bar{r} = \frac{1}{\sqrt{2\pi}} \sum_{\omega=1}^{N_\omega} \rho_{ox,\omega}^{-1} \iiint \left(\bar{m}_{p,\omega,a,d,\varphi}''^{*} / \zeta_{ox,\omega,a,d}^{*} \right) \sum_{k=1}^{K_\omega} \frac{m_{ox,\omega,k}}{m_c} \frac{F_{ox,\omega,d,k}}{\sigma_{a,\omega,k}}$$

$$\exp\left[-\frac{1}{2} \left(\frac{d\ln a - d\ln \bar{a}_{\omega,k}}{\sigma_{a,\omega,k}} \right)^2 \right] d\ln a \, dD \sin\varphi \, d\varphi \tag{148a}$$

For spherical particles $\ln a = \ln \bar{a}$ and $m''^{*} \neq$ func (φ). Therefore, integration with respect to φ from $\varphi = 0$ to $\varphi = \pi/2$ gives

$$\bar{r}_{\text{spheres}} = \sum_{\omega=1}^{N_\omega} \rho_{ox,\omega}^{-1} \int_D \frac{\bar{m}_{p,\omega,a,d,\varphi}''^{*}}{\zeta_{ox,\omega,a,d}^{*}} \sum_{k=1}^{K_\omega} \frac{m_{ox,\omega,k}}{m_c} F_{ox,\omega,d,k} \, dD \tag{148b}$$

This is the result previously reported for spherical particles in Ref. 28.

Equation 148 relates the mean burning rate of composite propellant with mixed, polydisperse spheroidal oxidizer to the burning rate of a sequence of monodisperse psuedo-propellants. The properties of these monodisperse psuedo-propellants depend upon the specified propellant ingredients. The remaining theoretical problem is to compute the burning rate of a monodisperse psuedo-propellant. This will be handled herein with a modified BDP model.

MONODISPERSE COMBUSTION MODEL

The BDP model has been reviewed previously; several errors were noted. These are listed below:

1. mean burning rate based on wrong surface area,
2. characteristic dimension for oxidizers mean deflagrating state based on the ignited and unignited particles.
3. characteristic fuel dimension based on ordered particle arrangement when particles are really randomly ordered.
4. Final diffusion flames influence on the A/PA flame was neglected.

The discussion here deals solely with spherical particles. Portions dealing with ellipsoidal particles are found in Appendix II .

Surface Area Base - Applying conservation of mass to the control volume bounded by S_o and S_p yields

$$r_p S_p = r_o S_o \tag{149}$$

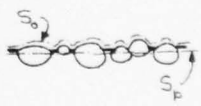

Since BDP compute r_o the correct rate is

$$r_p = r_o (S_o / S_p) \tag{150}$$

where S_o / S_p is available from their code.

Characteristic Dimension for Mean Deflagrating State - A central problem in statistical combustion modeling is to define a particles mean deflagrating state. It has been shown herein* that for a spherical particle the number of particles intersecting a planar surface is

$$dN / dS_p = 6 \zeta_{ox} / (\pi \bar{D}^2) \tag{151}$$

and that all depths of intersections are equally probable or

*For a monodisperse propellant $d^2 \mathcal{P}_{a,a,d} = \zeta_{ox}$. For spherical particles $a = 1$ and $\bar{X}''_{a,d,\phi} = D$. Therefore, integration of Eq. 143 from $\phi = o$ to $\phi = \pi/2$ gives the result shown.

$$d^2N / dS_p\, dx = (dN / dS_p)\, D^{-1} \qquad (152)$$

The BDP model assumes that binder regression rate (r_f) is stationary while oxidizer regression rate is a step function. Since, the ensemble of exposed particles contain samples of all states in a particles lifetime and statistics, rates, and initial particle geometry known, all micro-states are known because they are sequential. Therefore, mean states can be computed from sums over all states on the surface. This approach to definition of means is termed "petite ensemble averaging" and follows the spirit of integral methods.

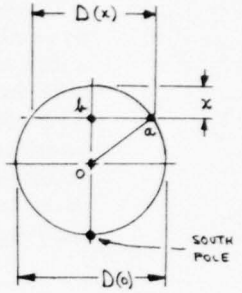

FIG. 12 PARTICLE GEOMETRY

The deflagrating surface of an oxidizer particle is assumed to be a spherical segment. Referring to Fig. 12 application of the Pathagorean theorem to triangle OabO yields

$$\left[D(x)/2\right]^2 = x\left[D(o) - x\right] \qquad (153)$$

and

$$x = \left[D(o)/2\right]\left[1 \pm \sqrt{1 - \left[D(x)/D(o)\right]^2}\right] \qquad (154)$$

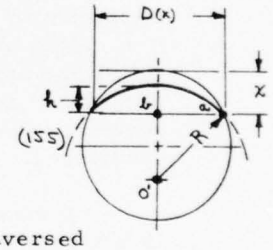

Application to triangle O'abO gives (with Eq. 153)

$$2Rh = h^2 + x\left[D(o) - x\right] \qquad (155)$$

The distance h is the difference between the distances traversed by binder and oxidizer. Therefore, during the ignited phase

$$h = r_f t - r_{ox}\left(t - t_{ign}\right) = x - r_{ox}\left(x - x_{ign}\right)/r_f \qquad (156)$$

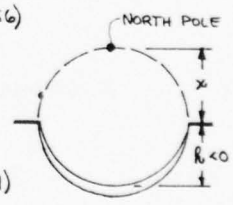

If h < o, the particle is consumed before x = D (o). Therefore,

$$o \le x \le D(o) + h(x) = x_{ign} + r_f D(o)/r_{ox} \qquad (157)$$

Consequently, for all $o \le x < x_{max}$ where

$$x_{max} = \min\left[D(o),\ x_{ign} + r_f D(o)/r_{ox}\right] \qquad (158)$$

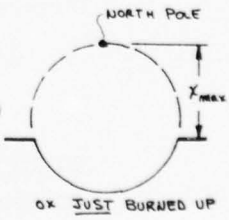

microstates will contain oxidizer while those with $\chi_{max} \le \chi \le D(o)$ will not. A microstate is empty for $\Delta t = [D(o) - \chi_{max}] / r_f$. During this time interval (a) continued pyrolysis may expose "new" oxidizer particles in the empty microstate or (b) the empty microstate may "fill up" with surface melt. Although either (a) or (b) are really dynamic phenomena*, clearly a surface melt is required for (b) and a dry surface guarantees (a). Since melt layer thickness decreases with increasing pressure, the probability of (a) occurring increases with increasing pressure. It should also increase with increasing particle size. These "trends" follow the behavior observed by Cohen in nitramine propellants.(6) Situation (a) means the burning surface is no longer quasi-planar (a basic assumption in this study). Therefore, only (b) will be considered herein.

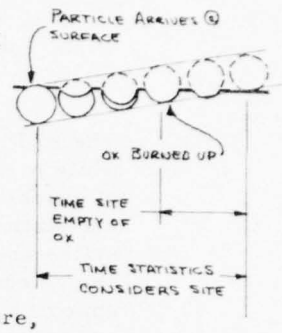

On the other hand, if

$$\chi_{ign} + r_f D(o) / r_{ox} > 1 \qquad (159)$$

the final microstate will possess oxidizer. The initial size of this residual oxidizer is

$$D_r(o) = \ell[D(o)] = D(o) - r_{ox}\left[D(o) - \chi_{ign_o}\right] / r_f \qquad (160)$$

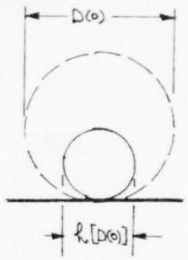

RESIDUAL PARTICLE SITUATION

These particles will be either (c) freed from the surface (blown away) or (d) retained on the surface. The choice of (c) or (d) also hinges on the pressure of a surface melt. If a melt is absent, (c) is probable. If a melt is present, (d) is probable. Since residual particles occur with large particles at lower pressures, a melt is probably present. Note that if residual particles are retained, the monodisperse propellant becomes effectively bidisperse. Both of these situations will be considered.

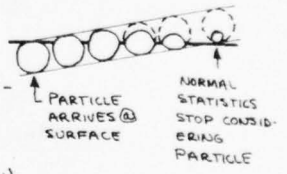

Considering now the normally accessible microstates, the surface area of a spherical segment is

$$\Delta \bar{S}_{ox} = 2\pi R \ell \qquad (161)$$

Combining Eqs. 155, 156, and 161 yields

$$\Delta S_{ox,ign} = \pi \left\{ \left[\left(1 - r_{ox}/r_f\right)^2 - 1 \right] \chi^2 + \left[2\chi_{ign} r_{ox}\left(1 - r_{ox}/r_f\right)/r_f + D(o) \right] \chi + \left(r_{ox} \chi_{ign} / r_f \right)^2 \right\} \qquad (162)$$

Therefore,

$$dS_{ox,ign} / dS_p = \int_{\chi_{ign}}^{\chi_{max}} \Delta S_{ox,ign} \frac{d^2 N}{dS_p\, d\chi}\, d\chi \qquad (163)$$

*The question here is how long does it take a melt to fill up the empty site. Clearly, the larger the site and the thinner the melt the longer it will take.

With Eqs. 151, 152, and 162 this gives

$$dS_{ox,ign}/dS_p = \zeta_{ox}\left\{2\left[\left(1-\frac{r_{ox}}{r_f}\right)^2-1\right]\left[\left(\frac{x_{max}}{D(0)}\right)^3-\left(\frac{x_{ign}}{D(0)}\right)^3\right]+\right.$$

$$3\left[2\,\frac{x_{ign}}{D(0)}\,\frac{r_{ox}}{r_f}\left(1-\frac{r_{ox}}{r_f}\right)+1\right]\left[\left(\frac{x_{max}}{D(0)}\right)^2-\left(\frac{x_{ign}}{D(0)}\right)^2\right]+ \qquad (164)$$

$$\left.6\left[\frac{r_{ox}}{r_f}\,\frac{x_{ign}}{D(0)}\right]^2\left[\frac{x_{max}}{D(0)}-\frac{x_{ign}}{D(0)}\right]\right.$$

The planar area of an oxidizer surface is

$$\Delta\bar{S}_{p,ox} = \pi\left[\frac{D(x)}{2}\right]^2 = \pi x\left[D(0)-x\right] \qquad (165)$$

Therefore, the fraction of planar area occupied by ignited particles is

$$dS_{p,ox,ign}/dS_p = \int_{x_{ign}}^{x_{max}} \Delta\bar{S}_{p,ox}\,\frac{d^2N}{dS_p\,dx}\,dx \qquad (166)$$

With Eqs. 151, 152 and 165 this becomes

$$dS_{p,ox,ign}/dS_p = \zeta_{ox}\left\{3\left[\left(\frac{x_{max}}{D(0)}\right)^2-\left(\frac{x_{ign}}{D(0)}\right)^2\right]-2\left[\left(\frac{x_{max}}{D(0)}\right)^3-\left(\frac{x_{ign}}{D(0)}\right)^3\right]\right. \qquad (167)$$

The number of ignited particles is

$$\frac{dN_{ign}}{dS_p} = \int_{x_{ign}}^{x_{max}} \frac{d^2N}{dS_p\,dx}\,dx = \frac{6\,\zeta_{ox}}{\pi\,D^2(0)}\left[\frac{x_{max}}{D(0)}-\frac{x_{ign}}{D(0)}\right] \qquad (168)$$

However,

$$\frac{dS_{p,ox,ign}}{dS_p} = \frac{\pi}{4}\,\bar{D}_{ign}^{\,2}\,\frac{dN}{dS_p} \qquad (169)$$

Therefore, the mean diameter of the ignited particles is

$$\bar{D}_{ign} = \sqrt{2/3}\;D(0)\left\{\frac{3\left[\left(\frac{x_{max}}{D(0)}\right)^2-\left(\frac{x_{ign}}{D(0)}\right)^2\right]-2\left[\left(\frac{x_{max}}{D(0)}\right)^3-\left(\frac{x_{ign}}{D(0)}\right)^3\right]}{\frac{x_{max}}{D(0)}-\frac{x_{ign}}{D(0)}}\right\}^{1/2} \qquad (170)$$

Note that the BDP value is not achieved if either $\chi_{iqn} > 0$ or $\chi_{max} < D(o)$. Figures 13 and 14 give $\bar{D}_{iqn}/D(o)$ and $dS_{ox,iqn}/dS_p$ as a function of $\chi_{iqn}/D(o)$ for several r_{ox}/r_f. Appropriate BDP values are indicated for comparison. Note that significant discrepancies can occur.

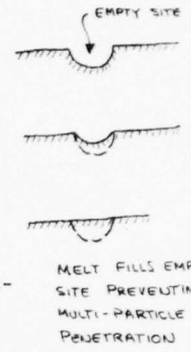

As mentioned previously, the situation where oxidizer depleted microstates occur is to be handled at present by assuming that melt fills the site.* The situation where residual oxidizer exists at the final microstate can be treated because the quasi-planar surface assumption is not violated.

If the burning surface is dry, the residual particle is "free" and will blow away. Thus, the oxidizer flowing away from the burning surface consists of both solid and gaseous phases. Application of mass conservation on both global and specie bases yields

$$\bar{m}''_c = \left[\int_{S_o} m''_{ox,g}\, dS + \dot{m}_{ox,r}\right]/(\alpha_{ox} S_p) \tag{171}$$

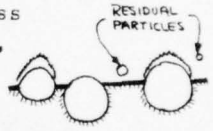

where $m''_{ox,g}$ is the mass flux of gaseous oxidizer and $m_{ox,r}$ is the mass flow rate of residual particles. Since only ignited particles evolve gas,

$$\int_{S_o} m''_{ox,g}\, dS = \int_{S_o} m''_{ox,iqn}\, dS \tag{172}$$

Combining Eqs. 171 and 172 and employing the mean value theorem for integrals yields

$$\bar{m}''_c = \left[\bar{m}_{ox,iqn}\, S_{ox,iqn} + \dot{m}_{ox,r}\right]/(\alpha_{ox} S_p) \tag{173}$$

The mass flow rate of residual particles is given by the product of their rate of creation and a residual particles initial mass. Since the BDP model assumes all deflagrating oxidizer surfaces are segments of a sphere

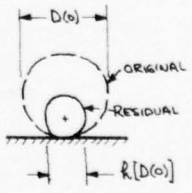

$$\Delta m_{ox,r} = \pi \rho_{ox} R^3[D(o)]/6 \tag{174}$$

Consider now a planar at t and t + dt. Since the distance traversed is rdt the propellant volume swept out is $dV = r\, S_p\, dt$. The number of attached oxidizer sites with their south poles in this volume is $dN = (dN_{ox}/dV)\, dV$ where $dN/dV = 6\chi_{ox}/[\pi D^3(o)]$. Therefore, the rate of creation of residual particles is

$$dN_r/S_p dt = 6\chi_{ox}\bar{r}/[\pi D^3(o)] \tag{175}$$

*This is a "crutch"; more work on this aspect is needed.

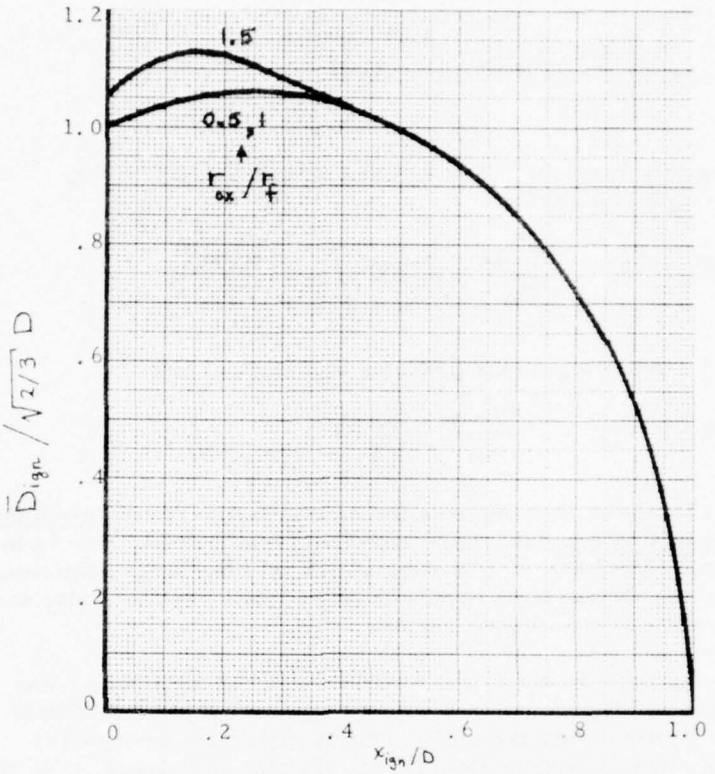

Figure 13 Mean Diameter of Ignited Particles

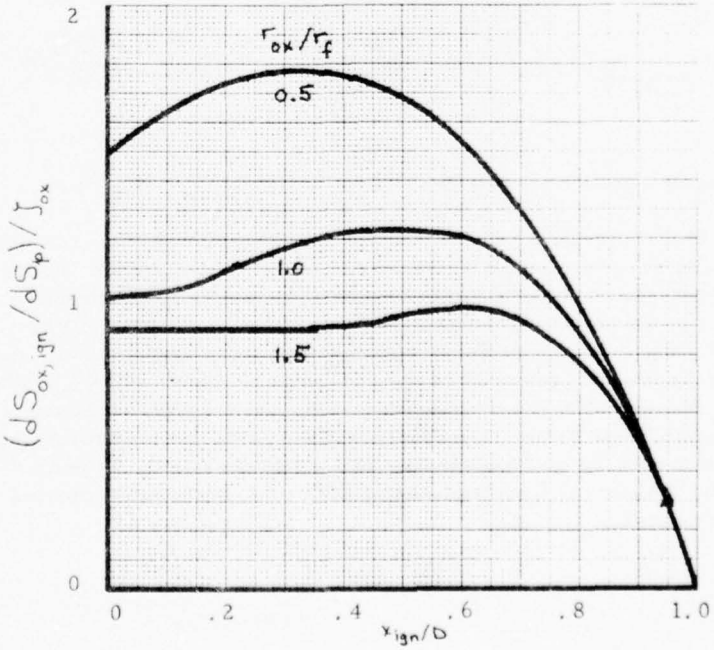

Figure 14 Surface Area of Ignited Particles

and

$$\dot{m}_{ox,r} = \bar{r}\,\gamma_{ox}\,\rho_{ox}\,S_p \left\{\frac{h[D(o)]}{D(o)}\right\}^3 \qquad (176)$$

Substituting this result into Eq. 173 and noting that $\bar{m}''_c = \bar{r}\rho_c$ and that $\alpha_{ox} = \gamma_{ox}\rho_{ox}/\rho_c$ yields

$$\bar{m}''_c = \bar{r}\rho_c = \frac{\bar{m}''_{ox,igm}}{\alpha_{ox}} \frac{S_{ox,igm}}{S_p} \Big/ \left\{1 - \left(\frac{h[D(o)]}{D(o)}\right)^3\right\} \qquad (177a)$$

If $h[D(o)] \leq o$ only gaseous products are evolved and

$$\bar{m}''_c = \bar{r}\rho_c = \frac{\bar{m}''_{ox,igm}}{\alpha_{ox}} \frac{S_{ox,igm}}{S_p} \qquad (177b)$$

Equation 177a shows that the creation of residual particles when the burning surface is dry causes the apparent mean burning rate to increase. Since $h[D(o)]/D(o) > 0$ is substantial only for large particles at low pressures, this modification will cause large particle rates to be increased in the low pressure region.

If $h[D(o)] > o$ and the residuals are not retained, some of the available oxidizer leaves unreacted. Therefore, the O/F ratio of the flames is effectively reduced. This is tatamount to reducing for the flame temperature calculations. Denote $\alpha_{ox,flame}$ as the proper value for flame temperature calculations. Therefore, since (a) $\gamma_{ox} = \alpha_{ox}\rho_c/\rho_{ox}$ and (b) $\alpha_{ox,flame} = [\alpha_{ox}\bar{m}''_c - \bar{m}''_{ox,r}]/\bar{m}''_c$

$$\alpha_{ox,flame} = \alpha_{ox}\left[1 - \left(\frac{h[D(o)]}{D(o)}\right)^3\right] \qquad \frac{h[D(o)]}{D(o)} > 0 \qquad (178)$$

For situations where $h[D(o)]/D(o) \leq o$ $\alpha_{ox,flame} = \alpha_{ox}$.

On the other hand, if the burning surface is wet, the residual particles will probably stick to the surface and be consumed thereon. This presents appreciable theoretical difficulties (not insurmountable) because these stuck residual particles alter the population of particles that exist on the burning surface. This means that distribution functions and pseudo-propellant properties are no longer defined solely by the propellant recipe. Environmental variables, since they influence the existence and characteristics of the residual particles, also influence distribution functions and pseudo-propellant properties. Appendix I presents the treatment (incomplete) of the stuck residual particles with a BDP like model.

Fuel Surface Considerations - The fraction of S_p that is fuel is $1-\zeta_{ox}$. Since there are $dN/dS_p = 6\zeta_{ox}/(\pi D^2)$ oxidizer sites on S_p, the mean fuel surface per site is

$$\Delta \bar{S}_f = \pi (1-\zeta_{ox}) D^2/(6\zeta_{ox}) \tag{179}$$

Arranging this fuel surface increment in an annulus about the mean ignited particle gives

$$\pi b^2 = \Delta \bar{S}_f + \pi \bar{D}_{ign}/4 \tag{180}$$

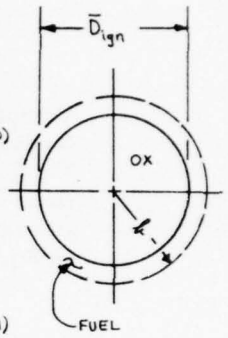

Employing Eqs. 170 and 179 and solving for b gives

$$b = (D/\sqrt{6})\sqrt{\frac{1-\zeta'_{ox}}{\zeta'_{ox}} + \frac{3\left[\left(\frac{x_{max}}{D(0)}\right)^2 - \left(\frac{x_{ign}}{D(0)}\right)^2\right] - 2\left[\left(\frac{x_{max}}{D(0)}\right)^3 - \left(\frac{x_{ign}}{D(0)}\right)^3\right]}{\frac{x_{max}}{D(0)} - \frac{x_{ign}}{D(0)}}} \tag{181}$$

The effective oxidizer volume fraction ζ'_{ox} has been introduced to account for the fact that the effective mixture ratio of the combustion reactions are altered when partially consumed oxidizer particles escape unreacted. Since $\zeta_{ox} = \alpha_{ox}\rho_c/\rho_{ox}$

$$\zeta'_{ox} = \alpha_{ox,\,flame}\,\rho_c/\rho_{ox} \tag{182}$$

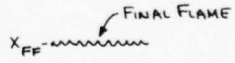

Flame Considerations - The gas phase temperature field for $0 \le x \le x_{FF}$ is divided into two parts. The final flame part $x_{AP} \le x \le x_{FF}$ and the AP part $0 \le x \le x_{AP}$. For the approximation employed by Ref. 2 energy release is concentrated at the flame locations. An energy balance at x_{FF} gives

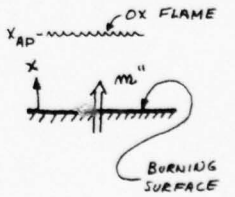

$$q''_{FF}(x^-_{FF}) = \dot{m}'' Q_{FF} \tag{183}$$

Since $T(x_{FF}) = T_{flame}$ integration of the energy equation from x_{FF} to x_{AP} gives ($\xi = \dot{m}'' c\, x/k$)

$$q''(x^+_{AP}) = \dot{m}'' Q_{FF} \exp\left[\xi_{AP} - \xi_{FF}\right] \tag{184}$$

$$T(x_{AP}) = T_{flame} + Q_{FF}\left\{\exp\left[\xi_{AP} - \xi_{FF}\right] - 1\right\}/c \tag{185}$$

An energy balance at X_{AP} gives

$$q''(x_{AP}^-) = m'' Q_{AP} + q''(x_{AP}^+) \tag{186}$$

Integration of the energy equation from X_{AP} to 0 gives

$$q''(0) = m''\left[Q_{AP} \exp(-\xi_{AP}) + Q_{FF} \exp(-\xi_{FF})\right] \tag{187}$$

$$T(0) = T(x_{AP}) + \left[Q_{AP} + Q_{FF} \exp(\xi_{AP} - \xi_{FF})\right]\left[\exp(-\xi_{AP}) - 1\right]/c \tag{188}$$

Comparison of Eq. (6) of Ref. 3 with Eq. (187) shows that the heat feedbacks from the AP+FF flame sequence is identical. Consequently, Eq. (6) of Ref. 3 does not need alteration. The only differences are that $T(x_{AP})$ is not the adiabatic flame temperature for AP and T(0) is available for comparison with T_s. The former means that in Eq. (18) of Ref. 3 should be

$$k_{AP} \exp\left\{E_{AP}/\left[RT(x_{AP})\right]\right\}$$

The latter means that a criteria for apportioning energy release between condensed phase and AP flame is available.

With the above modifications the AP flame is not adiabatic. Therefore, Eq. 20 of Ref. 3 becomes

$$Q_{AP} = c\left[T(x_{AP}) - T_\infty\right] + Q_L - q''(x_{AP}^+)/m'' \tag{189}$$

where, as discussed by Ref. 3, $0 \le Q_{AP} \le 810$ cal/gm and $Q_L = Q_{AP} - 330$

Results and Discussion

Numerical experiments were made using the BDP model to determine its ability to predict mixture ratio effects. Figure 15 presents results for both the original BDP model and a version modified to employ the fuel dimension based on random particle arrangement. These results clearly show that the BDP model exhibits singular behavior at high and low mixture ratios. The singular behavior was traced to the Burke-Schuman solution for diffusion flame height. Two fixes were instituted. First, the Burke-Schuman solution was replaced by a diffusion flame height based on dimensional arguments. This removed the aforementioned singularities and decreased run time. Second, J. A. Condon has found that the singular behavior can be overcome by employing more terms in the series solution present in the Burke-Schuman solution.* Near stoichiometric conditions the "single term solution" employed by BDP is adequate. However, at extreme rich or lean conditions as many as 100 terms may be required.

Table 3 shows the effects of some of the modifications described herein on BDP model predictions for $r(p)$ of the monodisperse PS/AP propellants indicated. In this table BDP(r_o) denotes the original BDP model, BDP(r_p) denotes the original model with rate based on S_p rather than S_o, BDP (b) denotes the BDP model with the b dimension based on random rather than ordered arrangement, BDP (B-S) denotes the BDP model with the multi-term (50) Burke-Schuman solution, and BDP (Geo.) denotes the BDP model with $\bar{D}_{ign}$ and $dS_{ox,ign}/dS_p$. Figure 15 compares results for BDP(r_o), BDP (B-S), and BDP (Geo.) graphically. These results show these corrections primarily impact high pressure behavior.

The BDP code was also modified to include residual particles that were not retained. Numerical results at high pressure indicated little effect (as expected). Numerical results at low pressure with large particles "blew up" because $\ell[D(o)]/D(o) \to 1$. This result was not expected. However, it merely illustrates what is known from experiment.--Namely, AP particles do not escape from the deflagrating surface unreacted. Consequently, theoretical determination of residual particle effects awaits the complete development and inclusion of retained residual particles.

The flame modifications noted in the text have not been added to the code yet.

A code for polydisperse, additive free propellants with spherical AP oxidizer was assembled and made operational. In this code it is assumed the particle size distributions in each oxidizer mode are log normal. That is, it is assumed that

*Sammons [5] employed this approach. However, Condon has found that Sammons employed incorrect values for the appropriate Bessel functions.

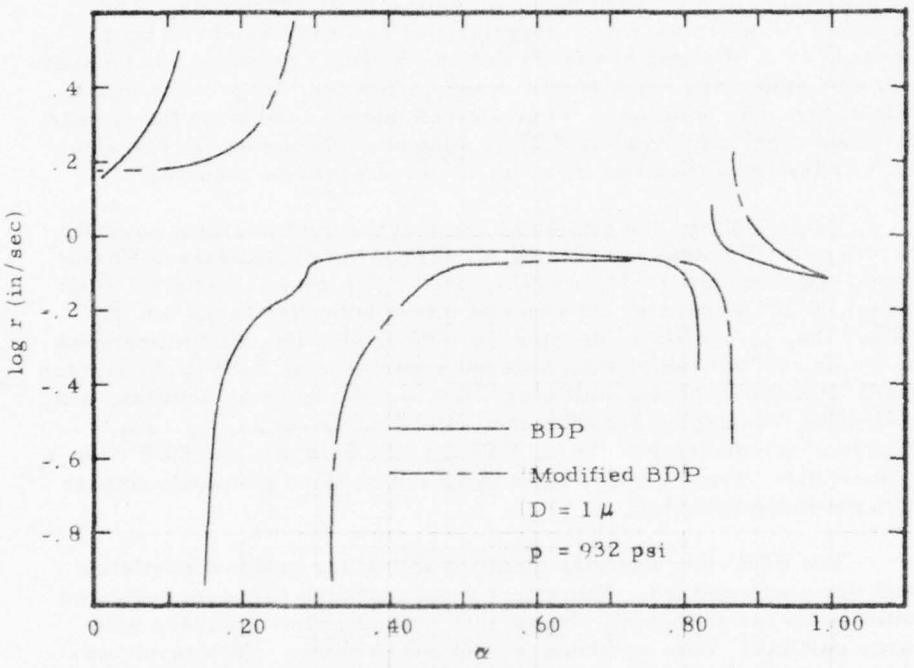

Figure 15. Burning Rate as a Fraction of Oxidizer Mass Fraction

TABLE 3

EFFECT OF BDP MODIFICATIONS ON $\bar{r}_{(p)}$
PS/AP MONODISPERSE PROPELLANT*

Pressure,	BDP (r_o)		BDP (r_p)		BDP (b)		BDP (B - S)		BDP (GEO.)	
psia	20 μ	200 μ	20 μ	200 μ	20 μ	200 μ	20 μ	200 μ	20 μ	200 μ
29.4	.0668	.0410	.0668	.0413	.0664	.0387	.0668	.0413	.0664	.0388
52.0	.1066	.0465	.1069	.0486	.1058	.0446	.1069	.0468	.1051	.0332
93.2	.1671	.0622	.1676	.0651	.1646	.0601	.1677	.0635	.1625	.0602
165.2	.2471	.0838	.2480	.0866	.2404	.0806	.2484	.0868	.2331	.0776
294.0	.3367	.1097	.3380	.1124	.3211	.1045	.3391	.1146	.3020	.0989
520.4	.4105	.1377	.4126	.1429	.3837	.1305	.4138	.1441	.3501	.1210
932.0	.4959	.1644	.5190	.1696	.4783	.1552	.5032	.1713	.3947	.1432
1652.0	.6763		.7263	.1965	.6526	.1797	.6994	.1968	.4923	.1627
2940.0	.9038		.9789	.2245	.8626	.2049	.9484	.2209	.6188	.1797

*Rates in in/sec.

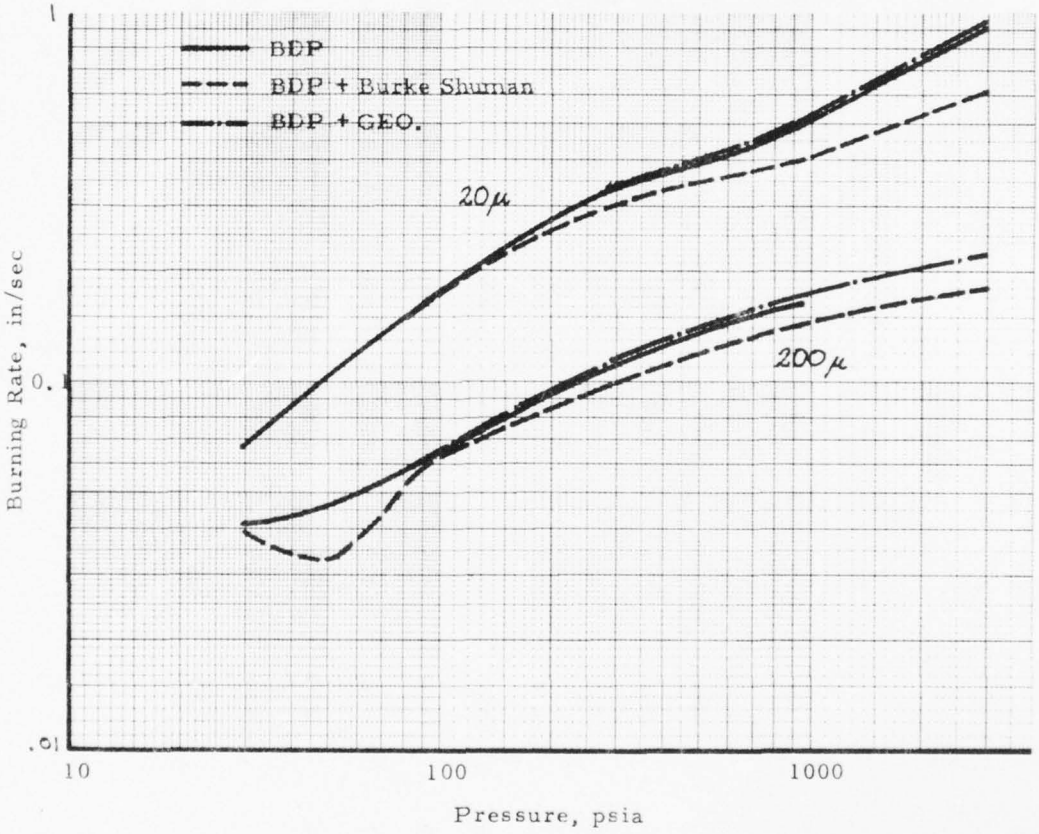

Figure 16 . Effect of BDP Modifications on $\bar{r}_{(p)}$ - PS/AP Monodisperse Propellant

$$F_{ox,a,k} = \frac{1}{\sqrt{2\pi}\,\sigma_{d,a,k}\,D}\ \exp\left[-\frac{1}{2}\left(\frac{\ln D - \ln \bar{D}_{a,k}}{\sigma_{d,a,k}}\right)^2\right]$$

Appendix III presents operating instructions, the FORTRAN IV listing, and a sample problem for the code.

T-BURNER VENT FLOW STUDY

Results in this study have been reported in the open literature (see Ref. 30 and 31). Therefore, it will not be redescribed in detail herein. However, certain comments are in order.

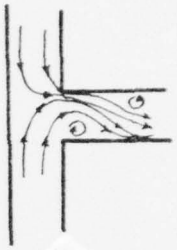

The hydraulic analogy studies demonstrate that flow in the vent region is a sequence of flow attachment and separation from alternate faces of the vent. This process creates a Karman vortex street downstream of the vent entrance. Therefore, the available acoustic energy (kinetic) at the vent entrance must be substantially transformed into the kinetic energy of the vortex system. Consequently, little, if any, amplification appears to occur at the vent.

The vent gain is the reverse of the flow turning loss. However, the flow turning loss is an irreversible process. Therefore, Culick's analysis "appears" to violate the second law of thermodynamics. However, recent results by Culick "appear" to refute the arguments of Ref. 31. Consequently, little, if any, amplification appears to occur at the vent.

FUTURE PLANS

This work has formulated a viable general approach to the combustion of composite propellants. However, specific application of the methodology (operational computer code) has been to polydisperse, additive free AP propellants with spherical oxidizer. Moreover, that code does account for neither retained residual oxidizer particles nor multiple particle penetrations. Consequently, the general direction of future efforts is reasonably clear.

- Implement retained residual particle methodology
- Implement flame modifications
- Develop methodology to treat multi-particle penetrations
- Extend modeling to nitramine "oxidizers"
- Implement metal and catalyst additive methodology
- Develop methodology to treat particle-particle interactions

PUBLICATIONS DERIVED FROM THIS PROGRAM

1. Hydraulic Analogy Study: T-Burner Vent Gain/Loss, CPIA Pub. No. 261, Vol. I, pp. 491 - 498, (1974).

2. On Reduction of Solid Rocket Data When the Pressure-Time History is Non-Neutral, J. Spacecraft and Rockets, Vol. 12, No. 6, pp. 383 - 384, (1975).

3. Comment on "The Stability of One-Dimensional Motions in a Rocket Motor," Combustion Science and Technology, Vol. 12, p. 197, (1976).

4. Comment on "A Modification of the Composite Propellant Erosive Burning Model of Lenoir and Robillard", accepted for publication by Combustion and Flame (1976).

5. Distribution Functions for Statistical Analysis of Monodisperse Composite Solid Propellant Combustion, accepted for publication by AIAA Journal (1976).

6. Statistical Analysis of Polydisperse, Heterogeneous Propellant Combustion: Steady-State, accepted for presentation at JANNAF Combustion Conference (1976).

ACKNOWLEDGEMENT

The principal investigator would like to acknowledge the substantial technical contributions of J. A. Condon to this work in both coding and theoretical developments.

NOMENCLATURE

LATIN SYMBOLS

a	aspect ratio of ellipsoidal particle (length/diameter)
b	$\bar{D} + \delta$
c	specific heat
C	constant defined by Eq. 118
D	diameter
e	specific internal energy
E	internal energy
F	distribution function
h	specific enthalpy or height of spherical cap of oxidizer particle
k	Thermal conductivity
K_s	number of oxidizer modes associated with s^{th} oxidizer specie
L	normal distance from plane S_p to plane S_o
m	mass
$\dot{m}$	mass flow rate
m''	mass flux
n	empirical exponent defined by Eq.
N	number of particles, number
p	pressure
q''	heat flux
Q	number of microstates or energy to gasify
r	burning rate
R	radius
S	surface area
t	time

T	temperature
u	velocity
V	volume
w	mass fraction
x	spatial coordinate as noted
X	spatial coordinate as noted
y	spatial coordinate as noted

GREEK SYMBOLS

α	mass fraction, mass/mass propellant
$\beta_{\uparrow}$	intercept defined by Eq. 106b
ζ	volume fraction, volume/volume propellant
δ	mean width of fuel around oxidizer particle
δ_{ℓ}	liquid layer thickness
Δ	denotes an increment
Δ_{r}	distance from solid/liquid interface to center of curvature of a retained residuals burning surface
ϵ	denotes an area element or ratio of outer diameter of excluded zone to particle diameter
η	parameter in Eq. 89
η, σ, ξ	orthogonal coordinates as noted
ρ	density

SPECIAL SYMBOLS

$\overline{(\ )}$	denotes a mean or value for a particle
$(\ )^{*}$	denotes a monodisperse, psuedo-propellant

SUBSCRIPTS

a	denotes particle aspect ratio or particles with
b	denotes binder

c	denotes condensed phase or characteristic
cat	denotes catalyst
d	denotes oxidizer particles with $D \leq D \leq D+dD$
f	denotes fuel
ign	denotes ignited particles
j	denotes j^{th} oxidizer particles
k	denotes k^{th} oxidizer model
m	denotes metal
N	denotes northern
o	denotes burning surface
ox	denotes oxidizer
p	denotes planar surface
r	denotes residual particles
sr	denotes heterogeneous reaction
S	denotes southern
φ	denotes particles with $\varphi \leq \varphi \leq \varphi + d\varphi$
∞	denotes initial propellant temperature
t	denotes point of tangency

REFERENCES

1. Culick, F. E. C., The Stability of One Dimensional Motions in a Rocket Motor, Combustion Science and Technology, 7, 4, 1973, p. 165.

2. Derr, R. L., Beckstead, M. W., and Cohen, N. S., "Combustion Tailoring Criteria for Solid Propellants," AFRPL-TR-69-190, Lockheed Propulsion Company, May 1969.

3. Beckstead, M. W., Derr, R. L., and Price, C. F., "A Model of Composite Solid-Propellant Combustion Based on Multiple Flames," AIAA J., 8, 12, 1970, pp. 2200 - 2207.

4. Cohen, N. S., Derr, R. L., and Price, C. F., "Extended Model of Solid Propellant Combustion Based on Multiple Flames," CPIA Publication 231, Vol. II, 1972, pp. 25 - 42.

5. Sammons, G. D., "Scientific Report: Multiple Flame Combustion Model Fortran IV Computer Program," Rocketdyne Division, Rockwell International, Report R-4827, March 1974.

6. Cohen, N. S., "Combustion of Nitramine Propellants," Final Scientific Report for Period 1 Jan. 1974 - 31 Dec. 1974, AFOSR Contract F44620-74-C-0031, Lockheed Propulsion Company, Jan. 1975.

7. Strand, L. D. and Cohen, N. S., "Nitramine Propellant Research," Quarterly Progress Report for Period 1 January 1975 to 31 March 1975, AFOSR Support Agreement No. AFOSR-ISSA-75-0005, JPL, May 1975.

8. Strand, L. D., and Cohen, N. S., "Nitramine Propellant Research", Quarterly Progress Report for Period 1 April 1975 to 30 June 1975, AFOSR Support Agreement No. AFOSR-ISSA-75-0005, JPL, August 1975.

9. Glick, R. L., "Statistical Analysis of Non-Metallized Composite Solid Propellant Combustion," CPIA Publication 243, Vol. I, 1973, pp. 157 - 184.

10. Glick, R. L., "On Statistical Analysis of Composite Solid Propellant Combustion," AIAA J., 12, 3, 1974, pp. 384 - 385.

11. Summerfield, M., et al, "Theory of Dynamic Extinguishment of Solid Propellants with Special Reference to Nonsteady Heat Feedback Law," J. Spacecraft and Rockets, 8, 3, 1971, pp. 251 - 258.

12. Novozhilov, B. V., "Non Stationary Combustion of Solid Rocket Fuels," FTD-MT-24-317-74, 1974.

13. Barrere, M., and Williams, F. A., "Analytical and Experimental Studies of the Steady-State Combustion Mechanism of Solid Propellants, ONERA T. P. No. 240, 1965.

14. Cohen, N. S., "Solid Propellant Combustion Literature Review," Lockheed Propulsion Company, Special Report 835-S-1, May 1968.

15. Culick, F. E. C., "A Review of Calculations for Unsteady Burning of a Solid Propellant," AIAA J., 6, 12, 1968, pp. 2241 - 2254.

16. Williams, F. A., Barrere, M., and Huang, N. C., Fundamental Aspects of Solid Propellant Rockets, AGARDograph 116, 1969.

17. Derr, R. L., Ewing, D., and Baker, D., "Combustion Theories for Solid Propellants," Combustion Laboratory, Thermal Sciences and Propulsion Center, School of Mechanical Engineering, Purdue University, June 1973.

18. Ebenezer, J. S., Cole, R. B., and McAlevy, R. F., "An Investigation of the Steady-State Burning of Ammonium Perchlorate Composite Solid Propellants," Department of Mechanical Engineering, Stevens Institute of Technology, Report ME-RT 73004, June 1973.

19. Kuo, K. K. and Razdan, M. K., "Review of Erosive Burning of Solid Propellants," CPIA Publication 273, Vol. II, 1975, pp. 323 - 338.

20. Miller, R. R., Hartman, K. O., and Myers, R. B., "Prediction of Ammonium Perchlorate Particle Size Effect on Composite Propellant Burning Rate," CPIA Publication 196, 1970, pp. 567 - 591.

21. Miller, R. R., Donohue, M. T., and Peterson, J. P., "Ammonium Perchlorate Size Effects on Burn Rate-Possible Modification by Binder Type," CPIA Publication 273, Vol. II, 1975, pp. 371 - 387.

22. Van Wylen, G. J. and Sonntag, R. E., Fundamentals of Classical Thermodynamics, (John Wiley and Sons, New York, 1967), pp. 93 - 105.

23. Hermance, C. E., "A Model of Composite Propellant Combustion Including Surface Heterogeneity and Heat Generation," AIAA J., 4, 9, 1966, pp. 1629 - 1637.

24. Steinz, J. A., Stang, P. L., and Summerfield, M., "The Burning Mechanism of Ammonium Perchlorate-Based Composite Solid Propellants," Aerospace and Mechanical Sciences Report No. 830, Department of Aerospace and Mechanical Sciences, Princeton University, N. J., 1969.

25. Condon, J. A., "Investigation of the Burning Rate Temperature Sensitivity of the JANNAF Standard Composite Solid Propellant," Interim Technical Report, Thermal Sciences and Propulsion Center, School of Mechanical Engineering, Purdue University, 1975.

26. Summerfield, M., et. al., "Burning Mechanism of Ammonium Perchlorate Propellants," Solid Propellant Rocket Research, Progress in Astronautics and Rocketry, Vol. I, (Academic Press, New York, 1960) pp. 141 - 182.

27. Glick, R. L., "On Exponent Breaks in Composite Solid Propellants," J. Spacecraft and Rockets, 12, 3, 1975, pp. 185 - 187.

28. Glick, R. L., "Steady-State Combustion of Nonmetallized Composite Solid Propellant," Thiokol Corporation, Interim Report, Contract F44620-74-C-0080 (1975).

29. Dallavalle, J. M., Micromeritics, (Pitman Publishing Co., New York, 1948), pp. 123 - 143.

30. Glick, R. L., "Hydraulic Analogy Study: T-Burner Vent Gain/Loss," CPIA Pub. No. 261, Vol. I, pp. 491 - 498, (1974).

31. Glick, R. L., Comment on "The Stability of One-Dimensional Motions in a Rocket Motor," Combustion Science and Technology, Vol. 12, p. 197 (1976).

APPENDIX I

RESIDUAL PARTICLES

When residual particles are retained, something holds them to the burning surface. The most likely candidate is a surface melt. That is, the oxidizer particles are stuck in a surface melt. If this is correct, the evolutionary trend in the combustion of the stuck residual will be something like that sketched in the margin. Note that if an interfacial phalanx flame "frees" the particle it will simply float away. Indeed, it would not have become stuck in the first place. This suggests that interfacial flames may not be important.

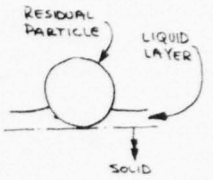

Consider now a specific evolutionary state in some detail. The equation of the original residual particle is*

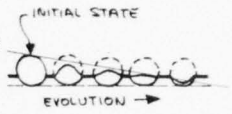

$$\eta^2 + \left\{\xi - h[D(o)]/2\right\}^2 = \left\{h[D(o)]/2\right\}^2 \qquad \text{I-1}$$

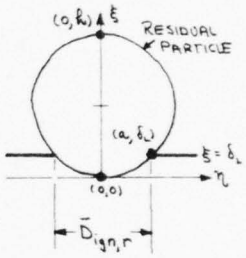

The point of intersection (a, δ_L) between the particle and the liquid layer must lie on this surface so that

$$a^2 = \delta_L\, h[D(o)] - \delta_L^2 \qquad \text{I-2}$$

Therefore, a and hence the mean intersection diameter $\bar{D}_{ign,\,r} = 2a$ are known and

$$\bar{D}_{ign,r} = 2\sqrt{\delta_L\left\{h[D(o)] - \delta_L\right\}} \qquad \text{I-3}$$

Note that in this situation <u>all</u> residual particles are ignited.

Following BDP the deflagrating surface is assumed to be always a segment of a sphere. Therefore, (see marginal sketch)

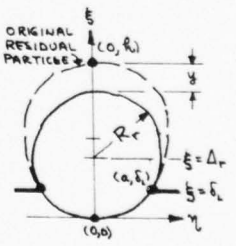

$$\eta^2 + (\xi - \Delta_r)^2 = R_r^2 \qquad \text{I-4}$$

where R_r is the radius of burning surface of the residual particle and (o, Δ_r) are the coordinates of the center of that spherical segment. This surface must pass through (O, h [D (o)] - y) and (a, δ_L). This gives two equations for Δ_r and R_r. Solving gives

$$\Delta_r = \frac{\delta_L h[D(o)] - \left\{h[D(o)] - y\right\}^2}{2\left(\delta_L - \left\{h[D(o)] - y\right\}\right)} \qquad \text{I-5}$$

* Only two dimensions need be considered because the particle is a body of revolution.

$$R_r = \left\{ h[D(o)] - y \right\} - \Delta_r \qquad \text{I-6}$$

The area of a spherical cap is

$$\Delta S_{ox,r} = 2\pi R_r \left(\left\{ h[D(o)] - y \right\} - \delta_L \right) \qquad \text{I-7}$$

Substituting Eqs. I-5 and I-6 this becomes*

$$\Delta S_{ox,r} = 2\pi \left\{ \delta_L \left\{ y - h[D(o)]/2 \right\} + \left\{ h[D(o)] - y \right\}^2/2 \right\} \qquad \text{I-8}$$

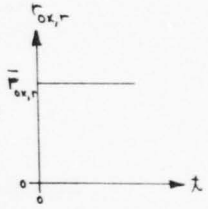

Assuming, as in the BDP model, that instantaneous oxidizer regression rate is constant in time for a specific particle, all microstates are equally probable. Therefore,

$$\frac{d^2N_r}{dS_p\,dy} = h^{-1}[D(o)]\,\frac{dN_r}{dS_p} \qquad \text{I-9}$$

Consequently,

$$\frac{dS_{ox,r}}{dS_p} = \int_o^{h[D(o)]} \Delta S_{ox,r}\,\frac{d^2N_r}{dS_p\,dy}\,dy \qquad \text{I-10}$$

Employing Eqs. I-8 and I-9 and integrating

$$\frac{dS_{ox,r}}{dS_p} = \frac{\pi}{3}\,h^2[D(o)]\,\frac{dN_r}{dS_p} \qquad \text{I-11}$$

From Eq. 174 the creation rate of residuals is

$$\frac{d^2N_r}{dS_p\,dt} = \frac{6\bar{r}\,\dot{y}_{ox}}{\pi D_{ox}^3} = \bar{r}\,\frac{dN_d}{dV} \qquad \text{I-12}$$

Since $m_{ox,r}(o) = \pi \rho_{ox}\, h^3[D(o)]/6$ the mass flux of <u>solid</u> residual oxidizer being created at the burning surface is

$$(\dot{m}''_{ox,r})_{created} = \frac{\pi \bar{r}\,\rho_{ox}\,h^3[D(o)]}{6}\,\frac{dN}{dV} \qquad \text{I-13}$$

*Checks at y = o and h [D (o)]; $\Delta S_{ox,r} > o$ for $y \gg o$.

The rate at which residual oxidizer is being gasified is

$$\left(\dot{m}''_{ox,r}\right)_{gasified} = \bar{r}_{ox,r}\,\rho_{ox}\,\frac{dS_{ox,r}}{dS_p} = \pi\,\bar{r}_{ox,r}\,\rho_{ox}\,\frac{k[D(o)]^2}{3}\,\frac{dN_r}{dS_p} \qquad \text{I-14}$$

At steady-state these rates are equivalent so that

$$\frac{dN_r}{dS_p} = \frac{k[D(o)]}{2}\,\frac{\bar{r}}{\bar{r}_{ox,r}}\,\frac{dN}{d\bar{V}} \qquad \text{I-15}$$

Therefore, $[D_{ox} = D(o)]$

$$\frac{dS_{ox,r}}{dS_p} = f_{ox}\left\{\frac{k[D(o)]}{D(o)}\right\}^3\frac{\bar{r}}{\bar{r}_{ox,r}} \qquad \text{I-16}$$

Equations I-3 and I-16 define the geometry of the residual particles for a residual BDP model.

The existence of retained residual particles means there are more particles on the burning surface than one computes from the propellant ingredients. In the petite ensemble approach each distinguishable particle is recognized in the statistical framework and a monodisperse psuedo-propellant is generated for that distinguishable particle. Therefore, retained residual particles mean that the statistics of the burning surface are altered. Although this aspect of the problem has not been explored at this time, no great "theoretical" difficulty is forseen (just time). However, as the distribution function is now dependent upon the combustion model, the present model becomes the interior of an iteration loop involving the distribution function. Consequently, "exact" treatment of retained residuals will probably triple or quadruple run time.

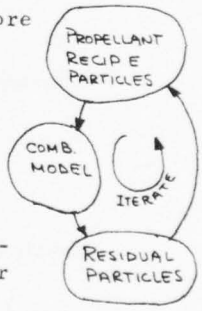

APPENDIX II

ELLIPTICAL PARTICLES

A central difficulty with aspherical particles is finding an expression for the deflagrating surface of the particle that satisfies the following criteria: deflagrating surface possess same intersection with Sp as ellipsoidal oxidizer particle, deflagrating surface lies within ellipsoidal particle, and deflagrating surface possess a tangent point within ellipsoidal particle to Sp. This "exercise" in Analytical Geometry appears reasonably simple. However, it has proven to be difficult.

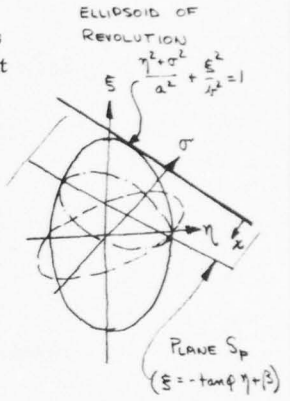

The equation for an ellipsoid of revolution is

$$(\eta^2+\sigma^2)/a^2 + \xi^2/b^2 = 1 \qquad \text{II-1}$$

In an η = constant plane assume that deflagrating surface has the form

$$\sigma^2 = A + B\xi^2 \qquad \text{II-2}$$

This guarantees a fit to the original ellipsoid. Conditions defining A and B are

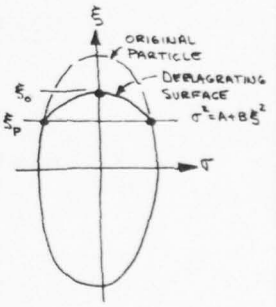

$$A + B\xi_o^2 = 0 \qquad \text{II-3a}$$

$$\sigma_p^2 = A + B\xi_p^2 \qquad \text{II-3b}$$

where ξ_o denotes the value of ξ at $\sigma = 0$ and ξ_p denotes the value of ξ at the intersection of S_p and the particle. Solving for A and B gives

$$A = \sigma_p^2 \xi_o^2 / (\xi_o^2 - \xi_p^2) \qquad \text{II-4a}$$

$$B = -\sigma_p^2 / (\xi_o^2 - \xi_p^2) \qquad \text{II-4b}$$

The curve in the $\sigma = 0$ plane must approach an ellipse as $\chi \to 0$. Thus, the simplest possible curve must approach a segment of an ellipse. Assuming that this ellipse is translated and stretched but axis of symmetry is always parallel to the particles

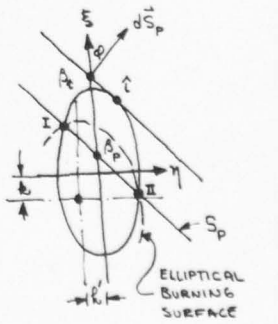

$$\frac{(\eta-h')^2}{a_1^2} + \frac{(\xi-k)^2}{a_2^2} = 1 \qquad \text{II-5}$$

Then $h' = s\sin\phi$ and $k = s\cos\phi$ so that

$$[(\eta - s\sin\phi)/a_1]^2 + [(\xi - s\cos\phi)/a_2]^2 = 1 \qquad \text{II-6}$$

This curve must pass through the intersection of S_p with the particle at $\sigma = 0$ $(\eta_I, \xi_I ; \eta_{II}, \xi_{II})$. Thus, $(A_1 = a_1^{-2}; A_2 = a_2^{-2})$

$$A_1 (\eta_I - s \sin\phi)^2 + A_2 (\xi_I - s \cos\phi)^2 = 1 \qquad \text{II-7a}$$

$$A_1 (\eta_{II} - s \sin\phi) + A_2 (\xi_{II} - s \cos\phi)^2 = 1 \qquad \text{II-7b}$$

Solving for A_1 and A_2 yields

$$A_1 = \frac{1 - A_2 (\xi_I - s \cos\phi)^2}{(\eta_I - s \cos\phi)^2} \qquad \text{II-8a}$$

$$A_2 = \frac{1 - \dfrac{(\eta_{II} - s \sin\phi)^2}{(\eta_I - s \sin\phi)^2}}{(\xi_{II} - s \cos\phi)^2 - (\xi_I - s \cos\phi)^2 \dfrac{(\eta_{II} - s \sin\phi)^2}{(\eta_I - s \sin\phi)^2}} \qquad \text{II-8b}$$

Differentiating Eq. II-6 with respect to η and setting that result to $-\tan\phi$ gives

$$A_1 (\eta - s \sin\phi) = A_2 (\xi - s \cos\phi) \tan\phi \qquad \text{II-9}$$

The locus of points a distance h from S_p is

$$\xi = -\tan\phi \; \eta + \beta_h \qquad \text{II-10}$$

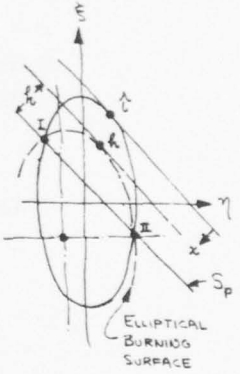

Therefore, since the point where $d\xi/d\eta = -\tan\phi$ must lie on this line the coordinates of the tangency point are

$$\eta_h = \frac{s \sin\phi (A_1 - A_2) + A_2 \beta_h \tan\phi}{A_1 + A_2 \tan^2\phi} \qquad \text{II-11a}$$

$$\xi_h = -\tan\phi \; \eta_h + \beta_h \qquad \text{II-11b}$$

Since η_h, ξ_h must also be on the ellipse

$$A_1 (\eta_h - s \sin\phi)^2 + A_2 (\xi_h - s \cos\phi)^2 = 1 \qquad \text{II-12}$$

Solving for s gives

$$s = \frac{A_1 \eta_h \sin\phi + A_2 \xi_h \cos\phi \pm \sqrt{(A_1 \eta_h \sin\phi + A_2 \xi_h \cos\phi)^2 - (A_1 \sin^2\phi + A_2 \cos^2\phi)(A_1 \eta_h^2 + A_2 \xi_h^2 - 1)}}{A_1 \sin^2\phi + A_2 \cos^2\phi} \qquad \text{II-13}$$

Since $\xi_p = -\tan\phi \; \eta_p + \beta_p$

$$\xi_p^2 = (\beta_p - \eta_p \tan\phi)^2 \qquad \text{II-14}$$

As σ_p lies on the particles surface

$$\frac{\sigma_p^2}{a^2} = 1 - \frac{\xi_p^2}{b^2} - \frac{\eta_p^2}{a^2} \qquad \text{II-15}$$

so that

$$\sigma_p^2 = a^2 - \eta^2 - \left(\frac{a}{b}\right)^2 \left(\beta_p - \eta \tan\varphi\right)^2 \qquad \text{II-16}$$

The $\sigma = 0$ curve is given by Eq. II-6 so that

$$\xi = \omega\cos\varphi \pm \sqrt{(\omega\cos\varphi)^2 - \left[A_1(\eta - \omega\cos\varphi)^2 + A_2(\omega^2\cos\varphi) - 1\right]/A_2} \qquad \text{II-17}$$

Since $\xi(\sigma = 0) = \xi_0$ and $\xi_0^2(\eta)$ is known, the equation for the deflagrating surface is known.

APPENDIX III

COMPUTER CODE

Input Instructions

CARD 1: Data Card

NUMBER REQUIRED: One per run

FUNCTION: Specify number of oxidizer types, pressure range, print parameter, accuracy parameter in Bessel series expansion and limit on number of terms in Bessel series.

FORMAT: (I5, 2F10.5, 2I5, F10.5)

Columns 1-5: NOX, number of oxidizer species

Columns 6-15: PSTART, pressure to start incremental calculations, atm

Columns 16-25: PSTOP, pressure to stop incremental calculations, atm

Columns 26-30: IPRINT, = 0 suppresses OUTPUT of rate v. s. D., IPRINT = 1 prints v vs. Do

Columns 31-35: LIMBES, Limit on number of terms on Bessel series solution

Columns 36-45: ERRBES, minimum error allowed in Bessel series solution

CARD 2: Data Card

NUMBER REQUIRED: One per run

FUNCTION: Specify integration parameters

FORMAT: (2I5, 3F10.0)

Columns 1-5: NCOUNT, number of intervals in the numerical integration of total propellant mass flux. Typically 30

Columns 6-10: NXCOUN, number of intervals in the numerical integration for the proportionality constant C in the equation for the volume of fuel associated with a particle in a polydisperse packing. Typically 300

Columns 11-20: XN, diameter exponent in the equation for the volume of fuel associated with a particle in a polydisperse packing. ($\sim$ 2.0)

Columns 21-30: DSTART, Particle diameter to start integration

Columns 31-40: DSTOP, Particle diameter to stop integration

CARD 3: Data Card

NUMBER REQUIRED: One card per run

FUNCTION: Specify fuel type

FORMAT: (I5)

Columns 1-5: IFUEL, IFUEL = 1 if HTPB, IFUEL = 2 if PBAN

CARD 4: Data Card

NUMBER REQUIRED: One card per run

FUNCTION: Specify propellant parameters

FORMAT: (6E12.6)

Columns 1-12: TZERO, initial propellant temperature, deg K

Columns 13-24: XALFA, Oxidizer mass fraction

Columns 25-36: QFUEL, heat of pyrolysis of the fuel binder, cal/g

Columns 37-48: RHOF, density of fuel binder, g/cm^3

Columns 49-60: AF, arrhenius frequency factor of fuel binder, g/cm^2-sec

Columns 61-72: EF, activation energy of the fuel binder, cal/mole

CARD 5: Data Card

NUMBER REQUIRED: One per run

FUNCTION: Specify propellant parameters

FORMAT: (6E12.6)

Columns 1-12: BETA, mass fraction of metal

Columns 13-24: RHOM, density of metal, g/cm^3

Columns 25-36: QM, heat release of metal combustion, cal/g

Columns 37-48: PCSUBP, specific heat of propellant, cal/g °K

Columns 49-60: PLAMB, thermal conductivity of propellant, cal/cm-sec-°K

Columns 61-72: XK, proportionality constant for responce function peak

CARD 6: Data Card

NUMBER REQUIRED: One per run

FUNCTION: Specify oxidizer type

FORMAT: (I5)

Columns 1-5: IOXID, IOXID = 1 if AP, 2 if KP, and 3 if HMX

CARD 7: Data Card

NUMBER REQUIRED: One card per oxidizer type

FUNCTION: Specify propellant parameters

FORMAT: (6E12.6)

Columns 1-12: Not Used

Columns 13-24: GMWD, Molecular weight of final flame products

Columns 25-36: XNOID, Proportionality constant for final diffusion flame

Columns 37-48: XNUPD, proportionality constant for primary diffusion flame

Columns 49-60: PMWD, molecular weight of primary flame products

Columns 61-72: Not used

CARD 8: Data Card

NUMBER REQUIRED: One card per oxidizer type

FUNCTION: Specify propellant parameters

FORMAT: (6E12.6)

Columns 1-12: QLD, latent heat of vaporization of the oxidizer, cal/g

Columns 13-24: RHOXD, density of the oxidizer, g/cm^3

Columns 25-36: AOXD, arrhenius frequency factor of the oxidizer g/cm^2-sec

Columns 37-48: EOXD, activation energy of the oxidizer cal/mole

Columns 49-60: TAPD, temperature of the AP flame, deg K

Columns 61-72: Not used

CARD 9: Data Card

NUMBER REQUIRED: One card per oxidizer type

FUNCTION: Specify propellant parameters

FORMAT: (6E12.6)

Columns 1-12: CIGND, oxidizer ignition delay parameter, $sec(atm)^m\ cm^{-n+1}$ where m=POWIGN and n= POWD

Columns 13-24: POWIGD, pressure exponent in oxidizer particle ignition delay term

Columns 25-36: POWDD, diameter exponent in oxidizer particle ignition delay term

Columns 37-48: CONFD, CONF = 0 if parabolic flame assumed, CONF = 1 if conical flame assumed

Columns 49-72: Not used

CARD 10: Data Card

NUMBER REQUIRED: One card per oxidizer type

FUNCTION: Specify propellant parameters

FORMAT: (6E12.6)

Columns 1-12: KPFD, rate constant of primary flame, g/cm^3-sec-atm)

Columns 13-24: KAP1D, rate constant of AP flame at low pressure, $g/(cm^3\text{-sec-atm})$

Columns 25-36: KAP2D, rate constant of AP flame at high pressure, $g/cm^3\text{-sec-atm}$)

Columns 37-48: XN1D, reaction order of primary flame

Columns 49-60: XN2D, reaction order of AP flame at low pressure

Columns 61-72: XN3D, reaction order of AP flame at high pressure

CARD 11: Data Card

NUMBER REQUIRED: One care per oxidizer type

FUNCTION: Specify propellant parameters

FORMAT: (6E12.6)

Columns 1-12: CSUBPD, average heat capacity of solids and gases, cal/g-°K

Columns 13-24: XLAMBD, average thermal conductivity of the combustion gases, cal/cm-sec-°K

Columns 25-36: GAMMAD, diffusion parameter, cm^2/sec

Columns 37-48: AFHD, flame height factor

Columns 49-60: EPSD, exponent for diffusion pressure dependence

Columns 61-72: YD proportionality constant for short diffusion flame (not used)

CARD 12: Data Card

NUMBER REQUIRED: One card per oxidizer type

FUNCTION: Specify number of particle size distribution modes

FORMAT: (I5)

Columns 1-5: MODES, number of particle size distribution modes

CARDS 13 $\longrightarrow$ 12 + MODES: Data Card

NUMBER REQUIRED: One card per mode per oxidizer type

FUNCTION: Specify oxidizer size distribution parameters

FORMAT: (3F10.0)

Columns 1-10: SIGMA, standard deviation of oxidizer size distribution for a particular mode

Columns 11-20: DBAR, mean oxidizer crystal size for a particular mode, microns

Columns 21-30: ALFAI, mass fraction of oxidizer in a particular mode relative to propellant mass

CARD 13 + MODES: Control Card

NUMBER REQUIRED: One card per case

FUNCTION: Program terminator

FORMAT: (I5)

Columns 1-5: NSTOP, If (NSTOP .LT. 1) START NEXT CASE, if (NSTOP .GE. 1) STOP EXECUTION.

```
                EXTERNAL ORGANI
000002          REAL KAP1,KAP2,KPF,MOX,MT,KAP1D,KAP2D,KPFD
000002          COMMON    A1,       A2,       AF,       AFH,      ALFAST,   AOX,
                1         BETAF,    BSQR,     CIGN,     CON1,     CSUBP,    CSP,
                2         C4P,      DELDI,    DZERO,    EF,       EOX,      EPS,
                3         GAMMA,    GMW,      HDN,      HUP,      KAP1,     KAP2,
                4         KPF,      PMW,      POWD,     POWIGN,   PSTART,   PSTOP,
                5         QAP,      QFF,      QFUEL,    QL,       QPF,      R,
                6         RAP,      RF,       RHOF,     RHOSP,    RHOX,     RUN
000002          COMMON    SOX,      TAP,      TAV,      TF,       TZERO,    XALFA,
                1         XLAMB,    XN1,      XN2,      XNUP,     XNUST,    XNU1,
                2         XSTPF,    XSTPD,    XSTARD,   XSTAP
000002          COMMON/DOUBLE/      MOX,      MT,       TS
000002          COMMON/ALL/         P
000002          COMMON/OPTIM/       N,        DELS,     DLMIN,    ITLIM,    IPI
000002          COMMON/XINI/        K
000002          COMMON/OXN/         NOX
000002          COMMON /RWN/        BETA,     RHOM,     GM
000002          COMMON /INPTR/      PCSUBP,   PLAMB,    XK,       IPRINT
000002          COMMON/BLP1/ TFD(3), GMWD(3), XNU1D(3), XNUPD(3),
                1 PMWD(3), QLD(3), RHOXD(3), AOXD(3), EOXD(3), TAPD(3),
                2 CIGND(3), POWIGD(3), POWDD(3), CONFD(3), TAVD(3),
                3 KPFD(3), KAP1D(3), KAP2D(3), XN1D(3), XN2D(3), XN3D(3),
                4 CSUBPD(3), XLAMBD(3), GAMMAD(3), AFHD(3), EPSD(3), YD(3)
000002          COMMON/R1/ FSKP(100,3), XMT(100), D(100), PR(20), RR(20), NSAMP
                1 , NCOUNT
000002          DIMENSION X(25), TSV(100), XI(100), FD(100)
000002          CALL INPUT(JJ,0,D,FSKP,NCOUNT,DDO,IOX)
000011          CALL CONCAL(0)
000013          JAK = 0
000014          RBAR = 0.0
000014          KP = 1
000015          PX = 14.7*P
000020          WRITE(6,5002) PX, IOX
000027          WRITE(6,5001)
000033          K = 1
000034          GO TO 9
000035     25   CONTINUE
000035          WRITE(6,5002) PX, IOX
000045          IF(KP.EQ.0) GO TO 50
000046          WRITE(6,5001)
000052     50   CONTINUE
000052          JAK = 0
000053     22   CALL INPUT(JJ,2,D,FSKP,NCOUNT,DDO,IOX)
000062          IF(KP.EQ.0) TS = TSV(JJ)
000065      9   CALL BDP(IOX,JAK)
000067          TSV(JJ) = TS
000071          IF(KP.EQ.0) GO TO 51
000072          XSTPDD = XSTPD*10000.
000074          XSTPFD = XSTPF*10000.
000075          XSTAPD = XSTAP*10000.
000077          XSTAR = XSTARD*10000.
000101          WRITE(6,5000) DZERO, K, TS, XNUST, ALFAST, RHOSP, TF, BETAF, XSTPD
                1D, XSTPFD, XSTAPD, XSTAR
000134     51   CONTINUE
000134          JAK = 1
000135          CALL XSTOR(JJ,XMT,XNUST,MT)
```

```
000140          IF(NCOUNT - JJ) 23,22,22
000143       23 CALL INTEG(IOX,XMT,D,FSKP,DDO,NCOUNT,XVAL)
000152          WRITE(6,400) XVAL
000160          XR = (1.0/RHOXD(IOX))*XVAL
000163          RBAR = XR + RBAR
000165          IF(NOX - IOX) 30,30,29
000170       29 IOX = IOX + 1
000172          JJ = 1
000173          GO TO 25
000175       30 JJ = 1
000174          R = RBAR
000175          RBAR = 0.0
000176          CALL OUTPUT(1,IOX)
000200          IF(P-PSTOP) 31,32,32
000203       31 CALL CONCAL(1)
000205          IOX = 1
000206          RP = IPRINT
000207          PX = 14.7*P
000212          GO TO 25
000212       32 CALL OUTPUT(2,IOX)
000214          READ(5,103) NSTOP
000222          STOP
000224      103 FORMAT(I5)
000224      400 FORMAT(10X,24HVALUE OF RATE INTEGRAL =,F8.5//)
000224     1001 FORMAT(2F10.0)
000224     1002 FORMAT(3I5)
000224     5000 FORMAT(F12.2,F11.4,F9.0,3F10.4,F9.0,F10.4,4F10.2)
000224     5001 FORMAT(8X,5HDZERO,5X,6H RATE ,4X,4H IS ,4X,6H XNUST,4X,6HALFAST,4X
            1,6H RHOSP,4X,4H TF ,4X,6H BETAF,5X,5HXSTPD,5X,5HXSTPF,5X,5HXSTAP,5
            1X,5H XSTD//)
000224     5002 FORMAT(12H PRESSURE IS,F7.1,10X,33H THE OXIDIZER BEING CONSIDERED
            1IS,I3//)
000224          END
        C       ******                          INPUT                          ******

PROGRAM LENGTH INCLUDING I/O BUFFERS    4146
UNUSED COMPILER SPACE                   2700


                SUBROUTINE INPUT(JJ,M,D,FSKP,NCOUNT,DDO,IOX)
000011          REAL KAP1,KAP2,KPF,MOX,MT,KAP1D,KAP2D,KPFD
000011          COMMON   A1,        A2,        AF,        AFH,       ALFAST,    AOX,
                1        BETAF,     BSGR,      CIGN,      CON1,      CSUBP,     CSP,
                2        CVP,       DELDI,     DZERO,     EF,        EOX,       EPS,
                3        GAMMA,     GMW,       HDN,       HDP,       KAP1,      KAP2,
                4        KPF,       PMW,       POWD,      POWIGN,    PSTART,    PSTOP,
                5        QAP,       QPF,       QFUEL,     QL,        QPF,       R,
                6        RAP,       RF,        RHOF,      RHOSP,     RHOX,      RON
000011          COMMON   SOX,       TAP,       TAV,       TF,        TZERO,     XALFA,
                1        XLAMB,     XN1,       XN2,       XNUP,      XNUST,     XNU1,
                2        XSTPF,     XSTPD,     XSTART,    XSTAP
000011          COMMON/DOUBLE/      MOX,       MT,        TS
000011          COMMON/ALL/         P
000011          COMMON /XPUT/       NXCOUN
000011          COMMON/OXN/         NOX
000011          COMMON /RWN/        BETA,      RHOM,      QM
000011          COMMON /INPTR/      PCSUBP,    PLAMB,     XR,        IPRINT
000011          COMMON /BESFAC/     LIMBES,    ERRBES
```

```
000011          COMMON/BDP1/ TFD(3), GMWD(3), XN01D(3), XNUPD(3),
               1 PMWD(3), WLD(3), RHOXD(3), AOXD(3), EOXD(3), TAPD(3),
               2 CIGND(3), POWIGD(3), POWDD(3), CONFD(3), TAVD(3),
               3 KPFD(3), KAP1D(3), KAP2D(3), XN1D(3), XN2D(3), XN3D(3),
               4 CSUBPD(3), XLAMBD(3), GAMMAD(3), AFHD(3), EPSD(3), YD(3)
000011          COMMON/FLAM/IOXN(3), IFUEL
000011          COMMON/DD1/ ALFAI(5,3), SIGMAI(5,3), DBARI(5,3), MODES
000011          COMMON/E/ ESTART, ETAO, ETAL, JAZO, JAZL, B, ZST, ETAP, ETAF,
               1 IFLAG
000011          DIMENSION XD(800), D(100), NMODES(3), FSKP(100,3), FDP(800),
               1 XFSKP(800,3)
000011          IF(M - 1) 1, 1, 15
000013   199    FORMAT(15,2F10.5,215,F10.5)
000013     1    READ(5,199) NOX, PSTART, PSTOP, IPRINT, LIMBES, ERRBES
000033          READ(5,100) NCOUNT, NXCOUN, XN, DSTART, DSTOP, ESTART
000064          XNCOUN = NCOUNT
000065          XNXCOU = NXCOUN
000066          DDO = (DSTOP/DSTART)**(1./XNCOUN)
000074          XDDO = (DSTOP/DSTART)**(1./XNXCOU)
000101          READ(5,200) IFUEL
               C      IFUEL = 1 / HIPB /, 2 /PBAN /
000107          READ(5,802) IZERO, XALFA, GFUEL, RHOF, AF, EF
000132          READ(5,802) BETA, RHOM, GM, PCSUBP, PLAMB, XK
000155          CALL OUTPUT(4,IOX)
000160          DO 80 IOX=1,NOX
000165          READ(5,200) IOXID
               C 200 FORMAT (A4)
000173    200   FORMAT(15)
               C      IF(IOXID.EQ.IAP) GO TO 40
               C      IF(IOXID.EQ.IKP) GO TO 43
               C      IF(IOXID.EQ.IHMX) GO TO 46
000177          IF(IOXID.EQ.1) GO TO 40
000201          IF(IOXID.EQ.2) GO TO 43
000202          IF(IOXID.EQ.3) GO TO 46
000204    40    IOXN(IOX) = 1
000207          GO TO 50
000207    43    IOXN(IOX) = 2
000212          GO TO 50
000212    46    IOXN(IOX) = 3
000215    50    CONTINUE
000215          READ(5,802) TFD(IOX), GMWD(IOX), XN01D(IOX), XNUPD(IOX)
               1 , PMWD(IOX)
000240          READ(5,802) WLD(IOX), RHOXD(IOX), AOXD(IOX), EOXD(IOX),TAPD(IOX)
000266          READ(5,802) CIGND(IOX), POWIGD(IOX), POWDD(IOX), CONFD(IOX)
000311          READ(5,802) KPFD(IOX), KAP1D(IOX), KAP2D(IOX), XN1D(IOX),
               1 XN2D(IOX), XN3D(IOX)
000342          READ(5,802) CSUBPD(IOX), XLAMBD(IOX), GAMMAD(IOX), AFHD(IOX),
               1 EPSD(IOX), YD(IOX)
000377     3    TAVD(IOX) = (TAPD(IOX) + TFD(IOX))/2.000
000416          READ(5,199) MODES
000424          NMODES(IOX) = MODES
000427          DO 10 II = 1,MODES
000434          READ(5,101) SIGMAI(II,IOX), DBARI(II,IOX), ALFAI(II,IOX)
000457    10    CONTINUE
000461          MODES = NMODES(IOX)
000464          CALL OUTPUT(3,IOX)
000472     80   CONTINUE
000475          JJ = 1
```

```
000475          SUM = 0.0
000476          FSUM = 0.0
000477          SUM2 = 0.0
000477          DI = 0.0
000500          DO 5 IOX1 =1,NOX
000502          MODES = NMODES(IOX1)
000504          DO 4 IJ = 1,MODES
000521          XSUM = ((1.0/RHOXD(IOX1))-(1.0/RHOF))*ALFAI(IJ,IOX1)
000522          SUM = SUM + XSUM
000523        4 CONTINUE
000524          SUM2 = SUM2 + SUM
000526          SUM = 0.0
000532        5 CONTINUE
000535          RHOT = 1.0/((1.0/RHOF) + SUM2)
000540          WRITE(6,300) RHOT
000546      300 FORMAT(1H1,10X,20HPROPELLANT DENSITY =,F7.4/)
000552          SUM = 0.0
000552          SUM2 = 0.0
000553          DO 7 IOX2 = 1,NOX
000555          MODES = NMODES(IOX2)
000557          DO 6 IJJ=1,MODES
000573          XSUM = (ALFAI(IJJ,IOX2)/RHOXD(IOX2))
000574          SUM = SUM + XSUM
000575        6 CONTINUE
000576          SUM2 = SUM2 + SUM
000600          SUM = 0.0
000604        7 CONTINUE
000607          XNU = RHOT*SUM2
000611          WRITE(6,301) XNU
000616      301 FORMAT(10X,21HVOLUME FRAC OF OXID =,F7.4/)
000622          FSUMKP = 0.0
000622          SUM3 = 0.0
000623          DI = DSTAR1*XDDO
000625          DO 13 III=1,NXCOUN
000627          DO 12 IOX3 = 1,NOX
000630          MODES = NMODES(IOX3)
000632          DO 11 JJJ =1,MODES
000634          CALL DISTF (DI, JJJ,III,IOX3,YVECR,DBAR1,SIGMA1)
000645          XFSUM = ALFAI(JJJ,IOX3)/YVECR
000646          FSUMKP = FSUMKP + XFSUM
000654       11 CONTINUE
000661          XFSKP(III,IOX3) = FSUMKP
000662          FSUMKP = 0.0
000663          XSUM3 = (RHOT/RHOXD(IOX3))*XFSKP(III,IOX3)
000666          SUM3 = SUM3 + XSUM3
000673       12 CONTINUE
000676          FDP(III) = SUM3
000676          SUM3 = 0.0
000700          XD(III) = DI
000701          DI = DI*XDDO
000704       13 CONTINUE
000706          CALL CCAL(FDP,XD,XN,XNU,XDDO,C)
000712          WRITE(6,302) C
000725      302 FORMAT(10X,25HC FROM VF = C*DZERO**N IS,F8.5/)
000727          DI = DSTAR1*DDO
000730          DO 23 IZZ =1,NCOUNT
000732          DO 22 IOX4=1,NOX
000733          FSUMKP = 0.0
```

```
000735          MODES = NMODES(IOX4)
000736          DO 21 JZZ=1,MODES
000740          CALL DISTF(DI,JZZ,IZZ,IOX4,YVECR,UBARI,SIGMAI)
000751          XFSUM = ALFAI(JZZ,IOX4)/YVECR
000752          FSUMKP = FSUMKP + XFSUM
000760       21 CONTINUE
000762          FSKP(IZZ,IOX4) = FSUMKP
000767       22 CONTINUE
000771          U(IZZ) = DI
000772          DI = DI*UOO
000774       23 CONTINUE
000776          IOX = 1
000777       15 CONTINUE
001005          DZERO = D(JJ)
001007          XNUST = 1.0/(1.0 + 6.0*C*DZERO**(XN-3.0)/3.141592654)
001015          ALFAST = 1.0/(1.0 + 6.0*C*RHOP*DZERO**(XN-3.0)/(3.141592654*RHOXD(
                1IOX)))
001027          RHOSP = RHOXD(IOX)*XNUST/ALFAST
001031       38 CONTINUE
001031          RETURN
001032      100 FORMAT(2I5,5F10.5)
001032      101 FORMAT(3F10.5)
001032      802 FORMAT (6E12.6)                                                  469 0221
001032          END
          C     ********                      CCAL                      ********

SUBPROGRAM LENGTH                       11043
UNUSED COMPILER SPACE                   400


                SUBROUTINE CCAL(FDP,XD,XN,XNU,XMUL,C)
000010          COMMON /XPUT/       NXCOUN
000010          DIMENSION FDP(800), XD(800)
000010          A = 0.0
000010          B1 = 3.141592654*(1.0 - XNU)/6.0
000014          JZ = 1
000017        2 XL1 = FDP(JZ)*XD(JZ)**(XN - 4.0)
000025          XL2 = FDP(JZ + 1)*XD(JZ + 1)**(XN - 4.0)
000031          XDDD = XD(JZ+1) - XD(JZ)
000035          APART = (XL1 + XL2)*XDDD/2.0
000040          JZ = JZ + 1
000041          A = A + APART
000043          IF (JZ - NXCOUN) 2, 4, 4
000045        4 C = B1/A
000047          RETURN
000047          END
          C     ********                      DISTF                     ********

SUBPROGRAM LENGTH                       102
UNUSED COMPILER SPACE                   4300


                SUBROUTINE DISTF(DI,JJJ,III,IOX,YVECR,UBARI,SIGMAI)
000011          DIMENSION UBARI(5,3), SIGMAI(5,3)
000011          X = ALOG(DI)
000012          XM = ALOG(UBARI(JJJ,IOX))
000027          SIG = ALOG(SIGMAI(JJJ,IOX))
000034          ZIP = .5*((X-XM)/SIG)**2
```

```
000040          IF(ZIP.GT.150.) ZIP = 150.
000050          YVECR = SIG*2.506628275D0*EXP(ZIP)
000060          RETURN
000060          END
          C     ******                    CONCAL                          ******

SUBPROGRAM LENGTH                  134
UNUSED COMPILER SPACE              4300


                SUBROUTINE CONCAL (J)                                                469 0040
          C     THIS SUBROUTINE INCREMENTS THE PRESSURE                              469 0041
000002          DIMENSION FAC(10)                                                    469 0042
000002          REAL KAP1, KAP2, KPF, MOX, MT
000002          COMMON    A1,       A2,       AF,       AFH,      ALFAST,   AOX,
                1         BETAF,    BSQR,     CIGN,     CONI,     CSUBP,    CSP,
                2         C4P,      DELDI,    DZERO,    EF,       EOX,      EPS,
                3         GAMMA,    GMW,      HON,      HOP,      KAP1,     KAP2,
                4         KPF,      PMW,      POWD,     POWIGN,   PSTART,   PSTOP,
                5         QAP,      QFF,      QFUEL,    QL,       QPF,      R,
                6         RAP,      RF,       RHOF,     RHOSP,    RHOX,     RON
000002          COMMON    SOX,      TAF,      TAV,      TF,       TZERO,    XALFA,
                1         XLAMB,    XN1,      XN2,      XNOP,     XNOST,    XNU1,
                2         XSTPF,    XSTPO,    XSTARO,   XSTAP
000002          COMMON/DOUBLE/      MOX,      MT,       TS
000002          COMMON/ALL/         P
000002     1    IF (J) 2, 2, 15                                                      469 0057
000004     2    FAC(1)=1.0
000005          FAC(2)=1.11
000007          FAC(3)=3.17
000010          FAC(4)=5.62
000012          FAC(5)=10.0
000015          JJ = 0                                                               469 0068
000014          I = 1                                                                469 0069
000015    15    IF (JJ - I) 16, 20, 20                                               469 0070
000020    16    XMULT = PSTART                                                       469 0071
000021          JJ = 1                                                               469 0072
000022          I = 1                                                                469 0073
000023    20    IF (I-6) 50,21,21
000026    21    XMULT = XMULT*10.                                                    469 0075
000030          I = 2                                                                469 0076
000031    50    P = XMULT*FAC(I)                                                     469 0077
000035          I = I + 1                                                            469 0078
000035          RETURN                                                               469 0079
000035          END                                                                  469 0080
          C     ********                    BOP                           ********

SUBPROGRAM LENGTH                  66
UNUSED COMPILER SPACE              4200


                SUBROUTINE BOP(IOX,JAK)
000004          REAL KAP1,KAP2,KPF,MOX,MT,KAP1O,KAP2O,KPFO
000004          COMMON    A1,       A2,       AF,       AFH,      ALFAST,   AOX,
                1         BETAF,    BSQR,     CIGN,     CONI,     CSUBP,    CSP,
                2         C4P,      DELDI,    DZERO,    EF,       EOX,      EPS,
                3         GAMMA,    GMW,      HON,      HOP,      KAP1,     KAP2,
                4         KPF,      PMW,      POWD,     POWIGN,   PSTART,   PSTOP,
```

```
                5           GAP,        QFF,        GFUEL,      GL,         GPF,        K,
                6           KAP,        KF,         RHOF,       RHOSP,      RHOX,       RUN
000004          COMMON      SOX,        TAP,        TAV,        TF,         TZERO,      XALFA,
                1           XLAMB,      XN1,        XN2,        XNUP,       XNUST,      XNU1,
                2           XSTPF,      XSTPD,      XSTARD,     XSTAP
000004          COMMON/DOUBLE/          MOX,        MT,         TS
000004          COMMON/ALL/             P
000004          COMMON /XPUT/           NXCOUN
000004          COMMON /RUN/            BETA,       RHOM,       QM
000004          COMMON/BUFI/ TFD(3), GMWD(3), XNU1D(3), XNUPD(3),
                1 PMWD(3), GLD(3), RHOXD(3), AOXD(3), EOXD(3), TAPD(3),
                2 CIGND(3), POWIGD(3), POWDD(3), CONFD(3), TAVD(3),
                3 KPFD(3), KAP1D(3), KAP2D(3), XN1D(3), XN2D(3), XN3D(3),
                4 CSUBPD(3), XLAMBD(3), GAMMAD(3), AFHD(3), EPSD(3), YD(3)
000004          IF(JAK) 1,1,2
000005        1 TS = 900.
000006          A1 = .5*(1.0 + 1.0/SQRT(3.0))
000013          A2 = 0.5*(1.0 - 1.0/SQRT(3.0))
000020          R = .06*SQRT(P)
000026          SOX = XNUST
000027          GMW = GMWD(IOX)
000030          XNU1 = XNU1D(IOX)
000032          XNUP = XNUPD(IOX)
000033          PMW = PMWD(IOX)
000035          QL = QLD(IOX)
000036          RHOX = RHOXD(IOX)
000040          AOX = AOXD(IOX)
000041          EOX = EOXD(IOX)
000043          TAP = TAPD(IOX)
000044          CIGN = CIGND(IOX)
000046          POWIGN = POWIGD(IOX)
000047          POWD = POWDD(IOX)
000051          CONF = CONFD(IOX)
000052          KPF = KPFD(IOX)
000054          KAP1 = KAP1D(IOX)
000055          KAP2 = KAP2D(IOX)
000057          XN1 = XN1D(IOX)
000060          XN2 = XN2D(IOX)
000062          XN3 = XN3D(IOX)
000063          CSUBP = CSUBPD(IOX)
000065          XLAMB = XLAMBD(IOX)
000066          GAMMA = GAMMAD(IOX)
000070          AFH = AFHD(IOX)
000071          EPS = EPSD(IOX)
000073        2 CONTINUE
              C   CALL FLAME1(ALFAST,IOX,TF)
000073          TF = TFD(IOX)
000074          TAV = (TF + TAP)/2.0
000077          CALL STEMP
000100          RETURN
000101          END
              C   ******                  STEMP                          ******

SUBPROGRAM LENGTH                   133
UNUSED COMPILER SPACE               3600

          SUBROUTINE STEMP                                          469 0001
```

AD-A031 006 THIOKOL CORP HUNTSVILLE ALA HUNTSVILLE DIV F/G 21/9.2
MEAN FLOW/ACOUSTIC INTERACTIONS AND STATISTICAL ANALYSIS OF STE--ETC(U)
JUN 76 R L CLICK F44620-74-C-0080
UNCLASSIFIED U-76-18 AFOSR-TR-76-1099 NL

2 OF 2
ADA031006

END

DATE
FILMED
11 - 76

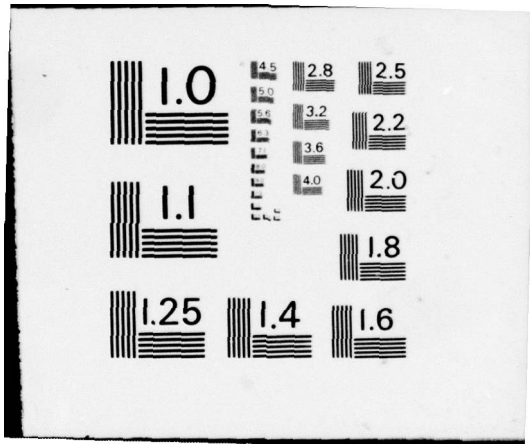
1.0
1.1
1.25
1.4
1.6
1.8
2.0
2.2
2.5
2.8
3.2
3.6
4.0
4.5
5.0
5.6
6.3
7.1
8.0
9.0
10.0
11.2
12.5
14.0
16.0
18.0
20.0
22.4

```
000001          REAL KAP1, KAP2, KPF, MOX, MT
000001          COMMON    A1,         A2,         AF,         AFH,        ALFAST,     AOX,
               1          BETAP,      BSQR,       CIGN,       CON1,       CSUBP,      CSP,
               2          CVP,        DELD1,      DZERO,      EF,         EOX,        EPS,
               3          GAMMA,      GMW,        HON,        HOP,        KAP1,       KAP2,
               4          KPF,        PMW,        POWD,       POWIGN,     PSTART,     PSTOP,
               5          QAP,        QFF,        QFUEL,      QL,         QPF,        R,
               6          RAP,        RF,         RHOF,       RHOSP,      RHOX,       RON
000001          COMMON    SOX,        TAP,        TAV,        TF,         TZERO,      XALFA,
               1          ALAMB,      XN1,        XN2,        XNOP,       XNUST,      XNU1,
               2          ASTPF,      XSTPD,      XSTARD,     XSTAP
000001          COMMON/DOUBLE/        MOX,        MT,         TS
000001          COMMON/ALL/           P
000001          COMMON/ES/ RF, RP, ETAP, ETAP
000001          DIMENSION ARGLST(20),AN(5)                                          469 0097
000007          ALFA = ALFAST
000010          XNU = XNUST
000011          RHOP = RHOSP
000013          RF = 0
000013          RP = 0
000014          QFF = CSUBP*((TF - TZERO) - ALFA*(TAP - TZERO) + (1.0 - ALFA)/
               1 CSUBP*QFUEL)/ALFA
000025          QPF = CSUBP*((TF - TZERO) + ALFA*QL/CSUBP + (1.0 - ALFA)*QFUEL/
               1 CSUBP)
000035          QAP = CSUBP*(TAP - TZERO) + QL
000035          XNC = XN2
000036          RATC = KAP1                                                         469 0102
000040          MT = RHOP*R                                                         469 0103
000042          XMT = 0.0
          C     BEGINNING OF COMPETING FLAME CALCULATION                            469 0105
000042          ARGLST(1) = TS                                                      469 0106
000044          ARGLST(2) = RATC
000045          ARGLST(3) = XNC
000047          ITTER = 0
          C     CONVERGENCE CALCULATION ON TS FOLLOWS                               469 0113
000047          T1 = TS
000051          E1 = DON(ARGLST)
000053          T2 = TS - E1
000055          T2 = AMAX1(T2,TZERO)
000060          T2 = AMIN1(T2,TAP)
000063          ARGLST(1) = T2
000064          E2 = DON(ARGLST)
000067       40 TS = (E1*T2 - E2*T1)/(E1 - E2)
000074          TS = AMAX1(TS,TZERO)
000077          TS = AMIN1(TS,TAP)
000102          ARGLST(1) = TS
000103          E3 = DON(ARGLST)
000104          IF(ABS(1. - (E3+TS)/TS) - .001) 60,60,61
000112       61 IF(ABS(E2).LT.ABS(E1)) GO TO 70
000116          E2 = E3
000117          T2 = TS
000120          ITTER = ITTER + 1
000122          IF(ITTER.GT.50) GO TO 80
000125          GO TO 40
000125       70 E1 = E3
000126          T1 = TS
000130          ITTER = ITTER + 1
000132          IF(ITTER.GT.50) GO TO 80
```

```
000135          GO TO 40
000135       80 WRITE(6,998)
000141      998 FORMAT(5X,'ITTERATION LIMIT EXCEEDED')
000141      999 FORMAT(3E16.8,F10.2)
000141       60 CONTINUE
000141          R = MT/RHOP
000143          RETURN                                                    469 0151
000144          END                                                       469 0152
              C ******                        DON                              ******

SUBPROGRAM LENGTH                  265
UNUSED COMPILER SPACE             3600


                FUNCTION DON (ARGLST)
              C CALCULATE IS FOR COMPETING FLAMES                         469 0224
000002          REAL KAP1, KAP2, KPF, MOX, MT
000002          COMMON   A1,       A2,       AF,       AFH,      ALFAST,   AUX,
                1        BETAF,    BSWR,     CIGN,     CON1,     CSUBP,    CSP,
                2        CVP,      DELDI,    DZERO,    EF,       EOX,      EPS,
                3        GAMMA,    GMW,      HDN,      HDP,      KAP1,     KAP2,
                4        KPF,      PMW,      POWD,     POWIGN,   PSTART,   PSTOP,
                5        QAP,      QFF,      QFUEL,    QL,       QPF,      R,
                6        RAP,      RF,       RHOF,     RHOSP,    RHOX,     RON
000002          COMMON   SOX,      TAP,      TAV,      TF,       TZERO,    XALFA,
                1        XLAMB,    XN1,      XN2,      XNUP,     XNUST,    XNU1,
                2        XSTPF,    XSTPD,    XSTARD,   XSTAP
000002          COMMON/DOUBLE/     MOX,      MT,       IS
000002          COMMON/ALL/        P
000002          COMMON /RWN/       BETA,     RHOM,     WM
000002          COMMON/E/ ESTART, ETAU, ETAL, UAZU, UAZL, B, ZSI
000002          COMMON/ES/ KF, KP, ETAF, ETAP
000002          DIMENSION ARGLST(20)                                      469 0241
000002          IS = ARGLST(1)                                            469 0242
000003          RATC = ARGLST(2)
000004          XNC = ARGLST(3)
000006          RHOP = RHOSP
000007          ALFA = ALFAST
000011          XNU = XNUST
000013          MOX = AUX*EXP(-EOX/(1.987*TS))
000021          CALL SOXCAL(TS,XNU,SOX)
000023          MT = MOX*SOX/ALFA
000025          IF(KP.EQ.0) ETAP = ESTART
000031          XSTPD = ETACAL(XNU,1,ETAP)*B/ZSI*AFH
000040          KP = 1
000040          XSTPF = MT/(KPF*P**XN1)
000045          XSTAP = MOX/(RATC*P**XNC)
000052          IF(KF.EQ.0) ETAF = ESTART
000056          XSTARD = B*ETACAL(XNU,0,ETAF)*AFH/ZSI
000065          KF = 1
000065          BETAF =(XSTAP - XSTPF)*AFH/XSTPD
000070          IF(BETAF.GE.1.0) BETAF = 1.0
000075          IF(BETAF.LE.0.0) BETAF = 0.0
000100          ZAP = CSUBP*MOX*XSTAP/XLAMB
000103          ZAT = CSUBP*MT*(XSTAP + XSTARD)/XLAMB
000106          IF(BETAF-1.0) 97,96,90
000111       90 ZPF = CSUBP*MT/XLAMB*(XSTPF + XSTPD)
000116          GO TO 98
```

```
000116      97  ZPF = CSUBP*MT/XLAMB*(XSTAP*AFH + XSTPF)
000124      98  IF(ZAT.LT.-100.) ZAT = -100.
000127          IF(ZAP.LT.-100.) ZAP = -100.
000132          IF(ZPF.LT.-100.) ZPF = -100.
000135          IF(ZAT.GT.100.) ZAT = 100.
000140          IF(ZAP.GT.100.) ZAP = 100.
000143          IF(ZPF.GT.100.) ZPF = 100.
000146          XTS = TZERO - ALFA*GL/CSUBP - (1. - ALFA - BETA)*GFUEL/CSUBP
               1 - BETA*GM/CSUBP + (1. - BETAF)*(ALFA*GAP/CSUBP*EXP(-ZAP) + GPF/
               2 CSUBP*EXP(-ZAT)*ALFA) + BETAF*GPF/CSUBP*EXP(-ZPF)
000210          XTS = AMAX1 (XTS, TZERO)
000213          DON = ARGLST(1) - XTS                                          469 0296
000214          GO TO 100
000215      99  DON = ARGLST(1)
000216     100  RETURN                                                         469 0297
000220          END                                                            469 0298
          C     ******                    SOXCAL                      ******

SUBPROGRAM LENGTH                  272
UNUSED COMPILER SPACE              5400


               SUBROUTINE SOXCAL(TS1,XNO,SOX1)
000005          REAL KAP1, KAP2, KPF, MOX, MT
000005          COMMON    A1,       A2,       AF,       AFH,      ALFAST,   AOX,
                1         BETAF,    BSQK,     CIGN,     CON1,     CSUBP,    CSP,
                2         CAP,      DELDI,    DZERO,    EF,       EOX,      EPS,
                3         GAMMA,    GMW,      HDN,      HOP,      KAP1,     KAP2,
                4         KPF,      PMW,      POWD,     POWIGN,   PSTART,   PSTOP,
                5         WAP,      WPF,      WFUEL,    WL,       WPF,      R,
                6         RAP,      RF,       RHOF,     RHOSP,    RHOX,     RON
000005          COMMON    SOX,      TAP,      TAV,      TF,       TZERO,    XALFA,
                1         ALAMB,    XN1,      XN2,      XNUP,     XNUST,    XNU1,
                2         ASTPF,    XSTPO,    XSTART,   XSTAP
000005          COMMON/DOUBLE/      MOX,      MT,       TS
000005          COMMON/ALL/         P
000005          RF = AF*EXP(-EF/(1.987*TS1))/RHOF
000020          RAP = MOX/RHOX
000022          TIGN = CIGN*(DZERO*0.0001)**(POWD+1.)/P**POWIGN
000035          XDO = RF*TIGN/(DZERO*0.0001)
000035          VDO = XDO + RF/RAP
000037          DDO = AMIN1(1.0,VDO)
000043          RAPORF = RAP/RF
000045          SOX1 = 6.0*XNO*(((1.0-RAPORF)**2-1.0)*(DDO**3-XDO**3)/3.0 +
               1  (2.0*XDO*RAPORF*(1.0-RAPORF)+1.0)*(DDO*DDO-XDO*XDO)/2.0 +
               2  (RAPORF*XDO)**2*(DDO-XDO))
000070          IF(SOX1.LT.0.0) SOX1 = .5
000072          RETURN
000073          END

SUBPROGRAM LENGTH                  157
UNUSED COMPILER SPACE              4000
```

```
      **********                        FLAMET                        **********
            SUBROUTINE FLAMET(ALFAST,IOX,TF)
000005      COMMON/FLAM/IOXN(3), IFUEL
000005      DIMENSION TFA(2,3,21), HTPBAP(21), PBANAP(21)
000005      IF = IFUEL
000006      I=IOXN(IOX)
000010      DATA( HTPBAP(J),J=1,21)/959.0, 1025.0, 1088.0, 1148.0, 1205.0,
           1  1258.0, 1308.0, 1355.0, 1399.0, 1440.0, 1477.0, 1511.0, 1542.0,
           2  1575.0, 1660.0, 1825.0, 2300.0, 2832.0, 3210.0, 2550.0, 1400.0/,
           3  ( PBANAP(JJ),JJ=1,21)/1039.0, 1069.0, 1101.0, 1130.0, 1157.0,
           4  1183.0, 1208.0, 1232.0, 1256.0, 1280.0, 1304.0, 1330.0, 1357.0,
           5  1388.0, 1569.0, 2020.0, 2511.0, 2959.0, 2990.0, 2405.0, 1320.0/
000010      DO 10 J=1,21
000020      TFA(1,1,J) = HTPBAP(J)
000021      TFA(2,1,J) = PBANAP(J)
000022   10 CONTINUE
000030      XKK = (ALFAST + .05)*20.0
000032      KK = XKK + 1
000035      JJ = (KK-1)*5
000037      XJJ = JJ/100.0
000041      TF = TFA(IFUEL,1,KK) - 20.0*(XJJ-ALFAST)*(TFA(IFUEL,I,KK) -
           1  TFA(IFUEL,1,KK-1))
000052      RETURN
000052      END
      C     ********                    XSTOR                     ********

SUBPROGRAM LENGTH                       556
UNUSED COMPILER SPACE                   4100


            SUBROUTINE XSTOR(JJ,XMT,XNUST,MT)
000006      REAL MT
000006      DIMENSION XMT(100)
000006      XMT(JJ) = MT/XNUST
000010      JJ = JJ + 1
000011      RETURN
000011      END
      C     ********                    INTEG                     ********

SUBPROGRAM LENGTH                       20
UNUSED COMPILER SPACE                   4500


            SUBROUTINE INTEG(IOX,XMT,D,FSKP,DDD,NCOUNT,XVAL)
000011      DIMENSION B(3),C(3,3),V(3),XMT(100),FSKP(1000,3),D(100)
000011      A = 0.0
000012      DO 1 LL=1,3
000027      B(LL) = XMT(NCOUNT+LL-3)*FSKP(NCOUNT+LL-3,IOX)/D(NCOUNT+LL-3)
000032      C(LL,1) = 1.0
000035      C(LL,2) = D(NCOUNT+LL-3)
000036      C(LL,3) = D(NCOUNT+LL-3)**2
000037    1 CONTINUE
000046      CALL QUAD(B,C,V)
000050      APART3 = D(NCOUNT-1)*(V(1)+V(2)*D(NCOUNT-1)/2.+V(3)*D(NCOUNT-1)**2
           1 /3.) - D(NCOUNT)*(V(1)+V(2)*D(NCOUNT)/2.+V(3)*D(NCOUNT)**2/3.)
000076      DO 2 LL=1,3
000106      B(LL) = XMT(LL)*FSKP(LL,IOX)/D(LL)
000110      C(LL,1) = 1.0
```

```
000114          C(LL,2) = D(LL)
000115          C(LL,3) = D(LL)**2
000116          CALL QUAD(B,C,V)
000120        2 CONTINUE
000125          APART1 = D(2)*(V(1)+V(2)*D(2)/2.+V(3)*D(2)**2/3.) -
                1          D(1)*(V(1)+V(2)*D(1)/2.+V(3)*D(1)**2/3.)
000142          LLL = 1
000143        3 CONTINUE
000145          APART = (D(LLL+2)*(V(1)+V(2)*D(LLL+2)/2.+V(3)*D(LLL+2)**2/3.)
              1 - D(LLL)*(V(1)+V(2)*D(LLL)/2.+V(3)*D(LLL)**2/3.))/2.
000165          A = A + APART
000167          IF(LLL.GE.NCOUNT-2) GO TO 7
000172          LLL = LLL + 1
000173          DO 4 I=1,2
000175          B(I) = B(I+1)
000177          DO 4 J=1,3
000206          C(I,J) = C(I+1,J)
000207        4 CONTINUE
000222          B(3) = XMT(LLL+2)*FSKP(LLL+2,IOX)/D(LLL+2)
000224          C(3,1)=1.0
000226          C(3,2) = D(LLL+2)
000227          C(3,3) = D(LLL+2)**2
000230          CALL QUAD(B,C,V)
000232          GO TO 3
000236        7 XVAL = APART1/2.0 + APART3/2.0 + A
000243          RETURN
000243          END

SUBPROGRAM LENGTH                    322
UNUSED COMPILER SPACE                3560
```

```
**********                    QUAD                    **********
      SUBROUTINE QUAD(B,C,V)
000005      DIMENSION B(3), C(3,3), V(3)
000010      V(3) = ((C(1,2)-C(3,2))*(B(1)-B(2))-(C(1,2)-C(2,2))*(B(1)-B(3)))/
     1 ((C(1,3)-C(2,3))*(C(1,2)-C(3,2))-(C(1,3)-C(3,3))*(C(1,2)-C(2,2)))
000031      V(2) = ((C(1,3)-C(3,3))*(B(1)-B(2))-(C(1,3)-C(2,3))*(B(1)-B(3)))/
     1 ((C(1,2)-C(2,2))*(C(1,3)-C(3,3))-(C(1,2)-C(3,2))*(C(1,3)-C(2,3)))
000051      V(1) = B(1) - V(2)*C(1,2) - V(3)*C(1,3)
000055      RETURN
000056      END

SUBPROGRAM LENGTH                  150
UNUSED COMPILER SPACE              4300


      FUNCTION ETACAL(XNU,IPD,ETA1)
000005      COMMON   A1,       A2,       AF,       AFH,      ALFAST,   AUX,
     1           BETAP,    BSWR,     CIGN,     CON1,     CSUBP,    CSP,
     2           C4P,      DELOI,    DZERO,    EF,       EOX,      EPS,
     3           GAMMA,    GMW,      HON,      HOP,      KAP1,     KAP2,
     4           KPF,      PRW,      POWD,     POWIGN,   PSTART,   PSTOP,
     5           QAP,      QFF,      QFUEL,    QL,       QPF,      R,
     6           RAP,      RF,       RHOF,     RHOSP,    RHOX,     RUN
000005      COMMON   SUX,      TAP,      TAV,      TF,       TZERO,    XALFA,
     1           ALAMB,    XN1,      XN2,      XNUP,     XNUST,    XNU1,
     2           XSTPF,    XSTPO,    XSTRO,    XSTAP
000005      COMMON/DOUBLE/    MUX,      MT,       TS
000005      COMMON/ALL/       P
000005      COMMON/E/ ESTART, ETAO, ETAL, JAZO, JAZL, B, ZSI, ETAP, ETAF,
     1 IFLAG
000005      IF(XNU.LT.0.1.OR.XNU.GT.0.99) GO TO 1
000015      ESTART = ETA1
000016      CALL ETACON(XNU,IPD,ETA1)
000017      ETACAL = ETA1
000022      RETURN
000023    1 IF(XNU.LT.0.1) GO TO 10
000026      IF(JAZO.EQ.0) ESTART = ETA1
000030      XNUO = 0.99
000032      CALL ETACON(XNUO,IPD,ETAO)
000034      ESTART = ETAO
000035      XNUL = 0.90
000037      CALL ETACON(XNUL,IPD,ETAL)
000043      AZ = ALOG(ETAO/ETAL)/ALOG((1.-XNUO)/(1.-XNUL))
000061      BZ = ETAO*(1./(1.-XNUO))**AZ
000066      ETA1 = BZ*(1.-XNU)**AZ
000073      ETACAL = ETA1
000074      JAZO = 1
000075      RETURN
000077   10 XNUO = .2
000100      IF(JAZL.EQ.0) ESTART = ETA1
000103      CALL ETACON(XNUO,IPD,ETAO)
000107      JAZL = 1
000110      ETA1 = XNU*ETAO/XNUO
000113      ETACAL = ETA1
000114      RETURN
000115      END

SUBPROGRAM LENGTH                  157
```

```
UNUSED COMPILER SPACE                    4100

                SUBROUTINE ETACON(XNU,IPD,ETA1)
000005          REAL MT
000005          COMMON    A1,         A2,         AF,         AFM,        ALFAST,     AUX,
                1         BETAP,      BSQR,       CIGN,       CON1,       CSUBP,      CSP,
                2         CVP,        DELD1,      DZERO,      EF,         EOX,        EPS,
                3         GAMMA,      GMW,        HDM,        HUP,        KAP1,       KAP2,
                4         KPF,        PMW,        POWD,       POWIGN,     PSTART,     PSTOP,
                5         WAP,        WPF,        WPUEL,      WL,         WP,         R,
                6         RAP,        RF,         RHOF,       RHOSP,      RHOX,       RUN
000005          COMMON    SOX,        TAP,        TAV,        TF,         TZERO,      XALFA,
                1         ALAMB,      XN1,        XN2,        XNUP,       XNUST,      XNU1,
                2         XSTPF,      XSTPD,      XSTART,     XSTAP
000005          COMMON/DOUBLE/        MOX,        MT,         TS
000005          COMMON/ALL/           P
000005          COMMON/E/ ESTART, ETAU, ETAL, JAZU, JAZL, B, ZSI, ETAP, ETAF,
                1 IFLAG
000005          COMMON /BESFAC/       LIMBES,     ERRBES
000005          DIMENSION ANS(4)
000005          IF(IPD) 5,5,10
000006      5   GMW1 = GMW
000007          XNUX = XNU1
000011          TA = TAP
000012          TGB = TF
000014          GO TO 11
000015      10  GMW1 = PMW
000016          XNUX = XNUP
000020          TA = TS
000021          TGB = TAP
000023      11  ITLIM2 = 50
000024          JX = 2
000025          JZ = -1
000026          K = 0
000027          FULL = 0.0
000027          TEST = XNUX/(XNUX + 1.)
000032          IF(XNU.GT.TEST) GO TO 30
000035          GO TO 31
000035      30  JX = 1
000036          JZ = 1
000037      31  TGP = (TGB+TA)/2.0
000042          RHOGP = P*GMW1/(82.055*TGP)
000045          UGP = MT/RHOGP
000046          B = BCAL(ANU)
000047          ZSI = GAMMA*TGP**1.75/(P*UGP*B)
000057          C = SQRT(ANU)
000065          C1 = SQRT(1.0 + 58.72708256*ZSI*ZSI)
000071          C2 = 2.0*C*(XNUX+1.)/(XNUX-C*C*(XNUX+1.))
000076          ARG = 3.8317059*C
000100          CALL BESSEL(0.0,ARG,ANS)
000105          Z = C2*ANS(2)/(3.8317059*((-.402759957)**JX))
000111          IF(Z.LT.1.0) GO TO 50
000115          ESTART = 2.*ZSI*ZSI/(C1 - 1.0)*ALOG(Z)
000126      50  CONTINUE
000126          ETA1 = ESTART
000127          N = 1
000130          ITER = 0
```

```
000131      59  J = 0
000132      60  J = J + 1
000134          IF(ETA1.LT.0.) ETA1 = ETAOLD*.5**J2
000142          ARG1 = BROOT(J)
000144          C1 = SQRT(1.0 + 4.0*(ARG1*ARG1*ZS1*ZS1))
000152          ARG2 = ARG1*C
000155          CALL BESSEL(ARG1,ARG2,ANS)
000161          C3 = ANS(2)/(ARG1*ANS(1)**JX)
000166          C4 = (1.-C1)*ETA1/(2.*ZS1*ZS1)
000173          PART1 = C3*EXP(C4)
000201          PART2 = PART1*C4/ETA1
000202          FULL1 = FULL1 + PART1
000204          FULL2 = FULL2 + PART2
000206          IF(ABS(PART1).GT.ERRBES.AND.J.LT.LIMBES) GO TO 60
000216          ETAOLD = ETA1
000216          ETA1 = ETA1 - (FULL1 - (XNUX/C - C*(XNUX+1.))/(2.*(XNUX+1.)))/
               1 FULL2
000226          FULL1 = 0.0
000226          FULL2 = 0.0
000227          ITTER = ITTER + 1
000231          IF(ITTER.GT.ITLIM2) GO TO 73
000234          GO TO 74
000234      73  WRITE(6,994) ETA1, ETAOLD
000244     994  FORMAT(5X,'ITTERATION LIMIT EXCEEDED.',5X,'ETA1 =',E16.8,5X,
               1 'ETAOLD =',E16.8,/)
000246          GO TO 70
000247      74  IF(ABS(1.-ETA1/ETAOLD).LT.1.E-6) GO TO 75
000254          GO TO 59
000255      75  ESTART = ETA1
000256      70  RETURN
000257          END

SUBPROGRAM LENGTH                    403
UNUSED COMPILER SPACE                5100


                FUNCTION BCAL(XNU)
000002          REAL MUX, MT
000002          COMMON   A1,       A2,       AF,       AFH,      ALFAST,   AUX,
                1        BETAF,    BSUM,     CIGN,     CON1,     CSUBP,    CSP,
                2        CSP,      DELU1,    DZERO,    EF,       EUX,      EPS,
                3        GAMMA,    GMW,      HDN,      HUP,      KAP1,     KAP2,
                4        KFF,      PMW,      POWD,     POWIGN,   PSTART,   PSTOP,
                5        QAP,      QFF,      QFUEL,    QL,       QPF,      R,
                6        RAP,      RF,       RHOF,     RHOSP,    RHOX,     RUN
000002          COMMON   SUX,      TAP,      TAV,      TF,       TZERO,    XALFA,
                1        ALAMB,    XN1,      XN2,      XNUP,     XNUST,    XNU1,
                2        XSTPF,    XSTPD,    XSTART,   XSTAP
000002          COMMON/DOUBLE/     MUX,      MT,       TS
000002          COMMON/ALL/        P
000004          RHOP = RHOSP
000005          RF1 = MT/RHOP
000007          KAP1 = MUX/RHOX
000011          TIGN = CIGN*(DZERO*0.0001)**(POWD+1.)/P**POWIGN
000023          XDO = RF1*TIGN/(DZERO*0.0001)
000025          VDO = XDO + RF1/KAP1
000027          UDO = AMIN1(1.0,VDO)
000033          DIGN = 2./3.*DZERO*DZERO*(3.0*(UDO*UDO-XDO*XDO) - 2.0*(UDO**3 -
```

```
     1 XDD**3)/(1000 - XDD)*1.0E-8
000046          IF(DIGN) 2,3,3
000050       2  DIGN = 0.0
000051          GO TO 4
000052       3  DIGN = SQRT(DIGN)
000056       4  CONTINUE
000056          DSF = (1.0 - XNU)*DZERO*DZERO*1.0E-8/(6.0*XNU)
000065          BCAL = SQRT(DSF + DIGN*DIGN/4.0)
000070          RETURN
000070          END

SUBPROGRAM LENGTH                       143
UNUSED COMPILER SPACE                   4100


          FUNCTION BROOT(NI)
000002          IF(NI.GT.50) GO TO 60
000005          GO TO (1,2,3,4,5,6,7,8,9,10,11,12,13,14,15,16,17,18,19,20,21,22,23
               1,24,25,26,27,28,29,30,31,32,33,34,35,36,37,38,39,40,41,42,43,44,45
               1,46,47,48,49,50),NI
000072       1  BROOT = 3.83170597
000074          RETURN
000074       2  BROOT = 7.01558667
000076          RETURN
000076       3  BROOT = 10.17346814
000100          RETURN
000100       4  BROOT = 13.32369194
000102          RETURN
000102       5  BROOT = 16.47063005
000104          RETURN
000104       6  BROOT = 19.61585851
000106          RETURN
000106       7  BROOT = 22.76008438
000110          RETURN
000110       8  BROOT = 25.90367208
000112          RETURN
000112       9  BROOT = 29.04682853
000114          RETURN
000114      10  BROOT = 32.18967991
000116          RETURN
000116      11  BROOT = 35.33230755
000120          RETURN
000120      12  BROOT = 38.47476623
000122          RETURN
000122      13  BROOT = 41.61709421
000124          RETURN
000124      14  BROOT = 44.75931900
000126          RETURN
000126      15  BROOT = 47.90146089
000130          RETURN
000130      16  BROOT = 51.04353518
000132          RETURN
000132      17  BROOT = 54.18555364
000134          RETURN
000134      18  BROOT = 57.32752544
000136          RETURN
000136      19  BROOT = 60.46945785
000140          RETURN
```

```
000140      20  BROOT = 65.61135670
000142          RETURN
000142      21  BROOT = 66.75522673
000144          RETURN
000144      22  BROOT = 67.89507184
000146          RETURN
000146      23  BROOT = 73.03689523
000150          RETURN
000150      24  BROOT = 76.17869956
000152          RETURN
000152      25  BROOT = 79.32048718
000154          RETURN
000154      26  BROOT = 82.46225991
000156          RETURN
000156      27  BROOT = 85.60401944
000160          RETURN
000160      28  BROOT = 88.74576714
000162          RETURN
000162      29  BROOT = 91.88750425
000164          RETURN
000164      30  BROOT = 95.02923181
000166          RETURN
000166      31  BROOT = 98.17095073
000170          RETURN
000170      32  BROOT = 101.31266182
000172          RETURN
000172      33  BROOT = 104.45436579
000174          RETURN
000174      34  BROOT = 107.59606326
000176          RETURN
000176      35  BROOT = 110.73775478
000200          RETURN
000200      36  BROOT = 113.87944085
000202          RETURN
000202      37  BROOT = 117.02112190
000204          RETURN
000204      38  BROOT = 120.16279853
000206          RETURN
000206      39  BROOT = 123.30447049
000210          RETURN
000210      40  BROOT = 126.44613870
000212          RETURN
000212      41  BROOT = 129.58780325
000214          RETURN
000214      42  BROOT = 132.72946439
000216          RETURN
000216      43  BROOT = 135.87112236
000220          RETURN
000220      44  BROOT = 139.01277739
000222          RETURN
000222      45  BROOT = 142.15442966
000224          RETURN
000224      46  BROOT = 145.29607934
000226          RETURN
000226      47  BROOT = 148.43772662
000230          RETURN
000230      48  BROOT = 151.57937165
000232          RETURN
```

```
000232      49  BROOT = 154.72101452
000234          RETURN
000234      50  BROOT = 157.86265540
000236          RETURN
000237      60  XN1 = N1
000240          XK = 2.0*3.14159265*(1.0 + 4.0*XN1)
000243          BROOT = XN1*3.14159265*(1.0 + 1.0/(4.0*XN1)) - 3.0/XK +
               1 12.0/XK**3
000255          RETURN
000255          END

SUBPROGRAM LENGTH                       366
UNUSED COMPILER SPACE                  3300


                SUBROUTINE BESSEL(X,Y,ANS)
000005          DIMENSION ANS(2)
          C
          C     ON RETURN
          C      ANS(1)= J ZERO (X)
          C      ANS(2)= J ONE  (Y)
          C
000005          IF(X-3.)2,2,4
000007        2 Z=X*X/9.
000011          IF(X)20,20,30
000012       20 ANS(1)=1.
000014          GO TO 6
000014       30 CONTINUE
000014          ANS(1)=(((((.00021*Z-.0039444)*Z+.0444479)*Z-.3163866)*Z+
               *1.2656208)*Z-2.2499997)*Z+1.
000027          GO TO 6
000030        4 Z=3./X
000031          FZERO=(((((.00014476*Z-.00072805)*Z+.00137237)*Z-.00009512)*Z
               *-.0055274)*Z-.77E-6)*Z+.79788456
000045          THZERO=X+(((((.00013558*Z-.00029333)*Z-.00054125)*Z+.00262573)*Z
               *-.00003954)*Z-.04166397)*Z-.78539816
000056          ANS(1)=FZERO*COS(THZERO)/SQRT(X)
000070        6 IF(Y-3.)8,8,10
000073        8 Z=Y*Y/9.
000075          IF(Y)40,40,50
000076       40 ANS(2)=0.
000077          GO TO 80
000100       50 CONTINUE
000100          ANS(2)=(((((.00001109*Z-.00031761)*Z+.00443319)*Z-.03954289)*Z
               *+.21093573)*Z-.56249985)*Z+.5)*Y
000113       80 RETURN
000115       10 Z=3./Y
000116          FONE=(((((-.00020033*Z+.00113653)*Z-.00249511)*Z+.00017105)*Z
               **+.01659667)*Z+1.56E-6)*Z+.79788456
000130          THONE=Y+(((((-.00029166*Z+.00079824)*Z+.00074348)*Z-.00637879)*Z
               *+.00005650)*Z+.12499612)*Z-2.3561945
000145          ANS(2)=FONE*COS(THONE)/SQRT(Y)
000155          RETURN
000155          END
          C     ******                    OUTPUT                    ******

SUBPROGRAM LENGTH                       275
UNUSED COMPILER SPACE                  3600
```

```
                SUBROUTINE OUTPUT(M1,IOX)
00004           REAL KAP1,KAP2,KPF,MOX,MT,KAP1D,KAP2D,KPFD
00004           COMMON    A1,         A2,         AF,         AFM,        ALFAST,     AOX,
                1         BETAF,      BSQR,       CIGN,       CON1,       CSUBP,      CSP,
                2         CSP,        DELD1,      DZERO,      EF,         EOX,        EPS,
                3         GAMMA,      GMW,        HDN,        HDP,        KAP1,       KAP2,
                4         KPF,        PMW,        POWD,       POWIGN,     PSTART,     PSTOP,
                5         QAP,        QFF,        QFUEL,      QL,         QPF,        R,
                6         RAP,        RF,         RHOF,       RHOSP,      RHOX,       RUN
00004           COMMON    SOX,        TAP,        TAV,        TF,         TZERO,      XALFA,
                1         ALAMB,      XN1,        XN2,        XNUP,       XNUST,      XNU1,
                2         XSTPF,      XSTPD,      XSTARD,     XSTAP
00004           COMMON/DOUBLE/        MOX,        MT,         TS
00004           COMMON/ALL/           P
00004           COMMON/XINT/          K
00004           COMMON /RWG/          BETA,       RHOM,       GM
00004           COMMON/BDP1/ TFD(3), GMWD(3), XNU1D(3), XNUPD(3),
                1 PMWD(3), QLD(3), RHOXD(3), AOXD(3), EOXD(3), TAPD(3),
                2 CIGND(3), POWIGD(3), POWDD(3), CONFD(3), TAVD(3),
                3 KPFD(3), KAP1D(3), KAP2D(3), XN1D(3), XN2D(3), XN3D(3),
                4 CSUBPD(3), XLAMBD(3), GAMMAD(3), AFMD(3), EPSD(3), YD(3)
00004           COMMON/DOI/ ALFAI(5,5), SIGMAI(5,5), DBARI(5,5), MODES
00004           DIMENSION BR(30), PT(30), BRA(30), PIA(30)
00004           GO TO (10,20,5,2),M1
00013         2 CONTINUE
00013           WRITE(6,110)
00017       110 FORMAT(1H1,15X,13H FUEL DATA IS,//)
00021           WRITE(6,111) TZERO
00026       111 FORMAT(2X,21H PROP INITIAL TEMP IS,F6.1,/)
00030           WRITE(6,112) XALFA
00035       112 FORMAT(2X,25H MASS FRAC OF OXIDIZER IS ,F5.2,/)
00037           WRITE(6,113) QFUEL
00044       113 FORMAT(2X,29H HEAT OF PYROLYSIS OF FUEL IS,F6.1,/)
00046           WRITE(6,114) RHOF
00053       114 FORMAT(2X,19H DENSITY OF FUEL IS,F5.2,/)
00055           WRITE(6,115) AF
00062       115 FORMAT(2X,30H ARRHENIUS FREQ FAC OF FUEL IS,E9.3,/)
00064           WRITE(6,116) EF
00071       116 FORMAT(2X,29H ACTIVATION ENERGY OF FUEL IS,F7.0,////)
00073           RETURN
00073         5 CONTINUE
00073           WRITE(6,117) IOX
00101       117 FORMAT(2X,16H OXIDIZER NUMBER,I3,5H DATA,//)
00103           WRITE(6,118) QLD(IOX)
00111       118 FORMAT(2X,25H LATENT HEAT OF OXID IS,F6.1,/)
00113           WRITE(6,119) RHOXD(IOX)
00121       119 FORMAT(2X,19H DENSITY OF OXID IS,F5.2,/)
00123           WRITE(6,120) AOXD(IOX)
00131       120 FORMAT(2X,30H ARRHENIUS  REQ FAC OF OXID IS,E9.3,/)
00133           WRITE(6,121) EOXD(IOX)
00141       121 FORMAT(2X,29H ACTIVATION ENERGY OF OXID IS,F7.0,/)
00143           WRITE(6,122) TAPD(IOX)
00151       122 FORMAT(2X,17H AP FLAME TEMP IS,F6.0,/)
00153           WRITE(6,123) CIGND(IOX)
00161       123 FORMAT(2X,29H OXID IGNITION DELAY PARAM IS,F5.0,/)
00163           WRITE(6,124) POWDD(IOX)
00171       124 FORMAT(2X,41H DIAMETER EXP IN OXID IGNIT DELAY TERM IS,F6.3,/)
```

```
00199           WRITE(6,125) POWIGD(10X)
00201     125   FORMAT(2X,34H PRESS EXP IN OX IGN DELAY TERM IS,F6.3,/)
00205           WRITE(6,126) RPFD(10X)
00211     126   FORMAT(2X,31H PRIMARY FLAME RATE CONSTANT IS,F5.1,/)
00215           WRITE(6,127) RAP1D(10X)
00221     127   FORMAT(2X,26H AP FLAME RATE CONSTANT IS,F6.3,/)
00225           WRITE(6,128) XN1D(10X)
00231     128   FORMAT(2X,35H REACTION ORDER OF PRIMARY FLAME IS,F5.1,/)
00235           WRITE(6,129) XN2D(10X)
00241     129   FORMAT(2X,30H REACTION ORDER OF AP FLAME IS,F5.1,/)
00245           WRITE(6,130) CSUBPD(10X)
00251     130   FORMAT(2X,21H AVE HEAT CAPACITY IS,F6.3,/)
00255           WRITE(6,131) XLAMBD(10X)
00261     131   FORMAT(2X,33H THERMAL CONDUCTIVITY OF GASES IS,F8.5,/)
00265           WRITE(6,132) GAMMAD(10X)
00271     132   FORMAT(2X,23H DIFFUSION PARAMETER IS,E9.2,/)
00275           WRITE(6,133) MODES
00300     133   FORMAT(2X,19H NUMBER OF MODES IS,I4,/)
00302           DO 134 IT=1,MODES
00303           WRITE(6,135) SIGMA1(IT,10X)
00313     135   FORMAT(2X,26H STAND DEV OF THIS MODE IS,F6.2)
00315           WRITE(6,136) DBAR1(IT,10X)
00325     136   FORMAT(2X,37H WT MEAN DIAM OF OX1D IN THIS MODE IS,F6.0)
00327           WRITE(6,137) ALPA1(IT,10X)
00337     137   FORMAT(2X,39H MASS FRAC OF THIS OX1D IN THIS MODE IS,F7.3,/)
00341     134   CONTINUE
00343           RETURN
00344      10   BR(K) = R                                                    469 0353
00346           PT(K) = P                                                    469 0354
00350           PTA(K) = PT(K)*14.7
00352           BRA(K) = BR(K)/2.54
00354           KMAX = K                                                     469 0367
00354           K = K + 1                                                    469 0368
00356           RETURN                                                       469 0371
00356      20   CONTINUE
00356           WRITE(6,102)
00362           WRITE(6,104)
00367           DO 69 K = 1, KMAX
00372           WRITE(6,103) PT(K),PTA(K),BR(K),BRA(K)
00407      69   CONTINUE
00411           RETURN
00412     102   FORMAT(8X,4HPRES,5X,4HPRES,7X,2HBR,9X,2HBR)
00412     103   FORMAT (5X,F7.2,2X,F7.1,2(2X,F9.4))
00412     104   FORMAT(8X,4HATMS,5X,4HPSIA,5X,6HCM/SEC,5X,6HIN/SEC/)
00412           END                                                          469 0478

SUBPROGRAM LENGTH                1077
/NUSED COMPILER SPACE            1500
```

```
FUEL DATA IS

PROP INITIAL TEMP IS 300.0

MASS FRAC OF OXIDIZER IS  .70

HEAT OF PYROLYSIS OF FUEL IS 200.0

DENSITY OF FUEL IS 1.27

ARRHENIUS FREQ FAC OF FUEL IS2.700E+03

ACTIVATION ENERGY OF FUEL IS  15000


OXIDIZER NUMBER  1 DATA

LATENT HEAT OF OXID IS   0.0

DENSITY OF OXID IS 1.95

ARRHENIUS FREQ FAC OF OXID IS4.000E+05

ACTIVATION ENERGY OF OXID IS  22000

AP FLAME TEMP IS  1400

OXID IGNITION DELAY PARAM IS  190

DIAMETER EXP IN OXID IGNIT DELAY TERM IS  .800

PRESS EXP IN OX IGN DELAY TERM IS  .750

PRIMARY FLAME RATE CONSTANT IS 20.0

AP FLAME RATE CONSTANT IS 2.150

REACTION ORDER OF PRIMARY FLAME IS  1.8

REACTION ORDER OF AP FLAME IS  1.8

AVE HEAT CAPACITY IS  .300

THERMAL CONDUCTIVITY OF GASES IS  .00030

DIFFUSION PARAMETER IS 7.60E-06

NUMBER OF MODES IS   1

STAND DEV OF THIS MODE IS  1.00
WT MEAN DIAM OF OXID IN THIS MODE IS   200
MASS FRAC OF THIS OXID IN THIS MODE IS   .700
```

PROPELLANT DENSITY = 1.6801

VOLUME FRAC OF VOID = .6031

C FROM VF = C*DZERO**N IS .34455

PRESSURE IS 29.4 THE OXIDIZER BEING CONSIDERED IS 1

DZERO	RATE	TS	XNUST	ALFAST	RHOSP	TF	BETAF	XSTPD	XSTPF	XSTAP	XSTD
199.82	.0993	746	.6031	.7000	1.6801	2545	1.0000	55.87	23.96	191.48	16.38
199.83	.0993	746	.6031	.7000	1.6801	2545	1.0000	55.88	23.95	191.46	16.38
199.85	.0993	746	.6031	.7000	1.6801	2545	1.0000	55.88	23.95	191.45	16.39
199.86	.0993	746	.6031	.7000	1.6801	2545	1.0000	55.89	23.95	191.43	16.39
199.88	.0993	746	.6031	.7000	1.6801	2545	1.0000	55.89	23.95	191.42	16.39
199.90	.0993	746	.6031	.7000	1.6801	2545	1.0000	55.90	23.95	191.41	16.39
199.91	.0993	746	.6031	.7000	1.6801	2545	1.0000	55.90	23.95	191.40	16.39
199.93	.0993	746	.6031	.7000	1.6801	2545	1.0000	55.91	23.95	191.39	16.39
199.94	.0993	746	.6031	.7000	1.6801	2545	1.0000	55.91	23.95	191.38	16.39
199.96	.0993	746	.6031	.7000	1.6801	2545	1.0000	55.92	23.94	191.37	16.40
199.98	.0992	746	.6031	.7000	1.6801	2545	1.0000	55.92	23.94	191.35	16.40
199.99	.0992	746	.6031	.7000	1.6801	2545	1.0000	55.93	23.94	191.34	16.40
200.01	.0992	745	.6031	.7000	1.6801	2545	1.0000	55.93	23.94	191.33	16.40
200.02	.0992	745	.6031	.7000	1.6801	2545	1.0000	55.94	23.94	191.32	16.40
200.04	.0992	745	.6031	.7000	1.6801	2545	1.0000	55.94	23.94	191.31	16.40
200.06	.0992	745	.6031	.7000	1.6801	2545	1.0000	55.95	23.94	191.30	16.40
200.07	.0992	745	.6031	.7000	1.6801	2545	1.0000	55.95	23.94	191.29	16.41
200.09	.0992	745	.6031	.7000	1.6801	2545	1.0000	55.96	23.94	191.27	16.41
200.10	.0992	745	.6031	.7000	1.6801	2545	1.0000	55.96	23.93	191.26	16.41
200.12	.0992	745	.6031	.7000	1.6801	2545	1.0000	55.97	23.93	191.25	16.41
200.14	.0992	745	.6031	.7000	1.6801	2545	1.0000	55.97	23.93	191.24	16.41
200.15	.0992	745	.6031	.7000	1.6801	2545	1.0000	55.98	23.93	191.23	16.41
200.17	.0992	745	.6031	.7000	1.6801	2545	1.0000	55.98	23.93	191.22	16.41
200.18	.0992	745	.6031	.7000	1.6801	2545	1.0000	55.99	23.93	191.21	16.42
200.20	.0992	745	.6031	.7000	1.6801	2545	1.0000	55.99	23.93	191.19	16.42

VALUE OF RATE INTEGRAL = .19350

PRESSURE IS 52.0 THE OXIDIZER BEING CONSIDERED IS 1

DZERO	RATE	TS	XNUST	ALFAST	RHOSP	TF	BETAF	XSTPD	XSTPF	XSTAP	XSTD
199.82	.1172	759	.6031	.7000	1.6801	2545	.6259	62.54	10.12	88.40	16.35
199.83	.1172	759	.6031	.7000	1.6801	2545	.6258	62.54	10.12	88.40	16.36
199.85	.1172	759	.6031	.7000	1.6801	2545	.6257	62.55	10.12	88.40	16.36
199.86	.1172	759	.6031	.7000	1.6801	2545	.6256	62.56	10.12	88.39	16.36
199.88	.1172	759	.6031	.7000	1.6801	2545	.6256	62.56	10.12	88.39	16.36
199.90	.1172	759	.6031	.7000	1.6801	2545	.6255	62.57	10.12	88.39	16.36
199.91	.1172	759	.6031	.7000	1.6801	2545	.6254	62.58	10.12	88.38	16.37
199.93	.1172	759	.6031	.7000	1.6801	2545	.6253	62.58	10.12	88.38	16.37
199.94	.1172	759	.6031	.7000	1.6801	2545	.6252	62.59	10.12	88.38	16.37
199.96	.1172	759	.6031	.7000	1.6801	2545	.6251	62.60	10.12	88.37	16.37
199.98	.1172	759	.6031	.7000	1.6801	2545	.6250	62.60	10.12	88.37	16.37
199.99	.1172	759	.6031	.7000	1.6801	2545	.6249	62.61	10.12	88.37	16.38
200.01	.1172	759	.6031	.7000	1.6801	2545	.6248	62.62	10.12	88.36	16.38
200.02	.1172	759	.6031	.7000	1.6801	2545	.6247	62.62	10.12	88.36	16.38
200.04	.1172	759	.6031	.7000	1.6801	2545	.6246	62.63	10.12	88.36	16.38
200.06	.1172	759	.6031	.7000	1.6801	2545	.6246	62.64	10.12	88.36	16.38
200.07	.1172	759	.6031	.7000	1.6801	2545	.6245	62.64	10.12	88.35	16.39

200.09	.1172	759	.6031	.7000	1.6801	2545	.6244	62.65	10.12	88.55	18.39
200.10	.1172	759	.6031	.7000	1.6801	2545	.6243	62.66	10.11	88.55	18.39
200.12	.1172	759	.6031	.7000	1.6801	2545	.6242	62.66	10.11	88.54	18.39
200.14	.1172	759	.6031	.7000	1.6801	2545	.6241	62.67	10.11	88.54	18.39
200.15	.1172	759	.6031	.7000	1.6801	2545	.6240	62.68	10.11	88.54	18.39
200.17	.1172	759	.6031	.7000	1.6801	2545	.6239	62.68	10.11	88.53	18.40
200.18	.1172	759	.6031	.7000	1.6801	2545	.6238	62.69	10.11	88.53	18.40
200.20	.1172	759	.6031	.7000	1.6801	2545	.6237	62.70	10.11	88.53	18.40

VALUE OF RATE INTEGRAL = .22854

PRESSURE IS 93.2 THE OXIDIZER BEING CONSIDERED IS 1

DZERO	RATE	TS	XNUST	ALFAST	RHOSP	TF	BETAF	XSTPO	XSTPF	XSTAF	XSTO
199.82	.1562	781	.6031	.7000	1.6801	2545	.2853	73.86	4.12	46.87	21.77
199.83	.1562	781	.6031	.7000	1.6801	2545	.2853	73.87	4.12	46.87	21.78
199.85	.1562	781	.6031	.7000	1.6801	2545	.2852	73.88	4.12	46.87	21.78
199.86	.1562	781	.6031	.7000	1.6801	2545	.2852	73.89	4.12	46.86	21.78
199.88	.1562	781	.6031	.7000	1.6801	2545	.2851	73.90	4.12	46.86	21.78
199.90	.1562	781	.6031	.7000	1.6801	2545	.2851	73.90	4.12	46.86	21.79
199.91	.1562	781	.6031	.7000	1.6801	2545	.2850	73.91	4.12	46.86	21.79
199.93	.1562	781	.6031	.7000	1.6801	2545	.2850	73.92	4.12	46.86	21.79
199.94	.1562	781	.6031	.7000	1.6801	2545	.2850	73.93	4.12	46.86	21.79
199.96	.1562	781	.6031	.7000	1.6801	2545	.2849	73.94	4.12	46.85	21.80
199.98	.1562	781	.6031	.7000	1.6801	2545	.2849	73.95	4.12	46.85	21.80
199.99	.1562	781	.6031	.7000	1.6801	2545	.2848	73.96	4.12	46.85	21.80
200.01	.1562	781	.6031	.7000	1.6801	2545	.2848	73.96	4.12	46.85	21.80
200.02	.1562	781	.6031	.7000	1.6801	2545	.2847	73.97	4.12	46.85	21.81
200.04	.1562	781	.6031	.7000	1.6801	2545	.2847	73.98	4.12	46.85	21.81
200.06	.1562	781	.6031	.7000	1.6801	2545	.2846	73.99	4.12	46.84	21.81
200.07	.1562	781	.6031	.7000	1.6801	2545	.2846	74.00	4.12	46.84	21.81
200.09	.1562	781	.6031	.7000	1.6801	2545	.2846	74.01	4.12	46.84	21.82
200.10	.1562	781	.6031	.7000	1.6801	2545	.2845	74.02	4.12	46.84	21.82
200.12	.1562	781	.6031	.7000	1.6801	2545	.2845	74.03	4.12	46.84	21.82
200.14	.1561	781	.6031	.7000	1.6801	2545	.2844	74.03	4.12	46.84	21.83
200.15	.1561	781	.6031	.7000	1.6801	2545	.2844	74.04	4.12	46.84	21.83
200.17	.1561	781	.6031	.7000	1.6801	2545	.2843	74.05	4.12	46.83	21.83
200.18	.1561	781	.6031	.7000	1.6801	2545	.2843	74.06	4.12	46.83	21.83
200.20	.1561	781	.6031	.7000	1.6801	2545	.2843	74.07	4.12	46.83	21.84

VALUE OF RATE INTEGRAL = .30454

PRESSURE IS 165.2 THE OXIDIZER BEING CONSIDERED IS 1

DZERO	RATE	TS	XNUST	ALFAST	RHOSP	TF	BETAF	XSTPO	XSTPF	XSTAF	XSTO
199.82	.2039	802	.6031	.7000	1.6801	2545	.1252	88.11	2.20	24.26	26.17
199.83	.2039	802	.6031	.7000	1.6801	2545	.1251	88.12	2.20	24.25	26.17
199.85	.2039	802	.6031	.7000	1.6801	2545	.1251	88.13	2.20	24.25	26.17
199.86	.2039	802	.6031	.7000	1.6801	2545	.1251	88.14	2.20	24.25	26.17
199.88	.2039	802	.6031	.7000	1.6801	2545	.1251	88.15	2.20	24.25	26.18
199.90	.2039	802	.6031	.7000	1.6801	2545	.1251	88.16	2.20	24.25	26.18
199.91	.2038	802	.6031	.7000	1.6801	2545	.1250	88.17	2.20	24.25	26.18
199.93	.2038	802	.6031	.7000	1.6801	2545	.1250	88.18	2.20	24.25	26.19
199.94	.2038	802	.6031	.7000	1.6801	2545	.1250	88.19	2.20	24.25	26.19
199.96	.2038	802	.6031	.7000	1.6801	2545	.1250	88.20	2.20	24.25	26.19
199.98	.2038	802	.6031	.7000	1.6801	2545	.1250	88.21	2.20	24.25	26.20
199.99	.2038	802	.6031	.7000	1.6801	2545	.1249	88.22	2.20	24.25	26.20

200.01	.2038	802	.6031	.7000	1.6801	2545	.1249	88.24	2.20	24.24	26.20
200.02	.2038	802	.6031	.7000	1.6801	2545	.1249	88.25	2.20	24.24	26.21
200.04	.2038	802	.6031	.7000	1.6801	2545	.1249	88.26	2.20	24.24	26.21
200.06	.2038	802	.6031	.7000	1.6801	2545	.1249	88.27	2.20	24.24	26.21
200.07	.2038	802	.6031	.7000	1.6801	2545	.1248	88.28	2.20	24.24	26.21
200.09	.2038	802	.6031	.7000	1.6801	2545	.1248	88.29	2.20	24.24	26.22
200.10	.2038	802	.6031	.7000	1.6801	2545	.1248	88.30	2.20	24.24	26.22
200.12	.2038	802	.6031	.7000	1.6801	2545	.1248	88.31	2.20	24.24	26.22
200.14	.2038	802	.6031	.7000	1.6801	2545	.1248	88.32	2.20	24.24	26.23
200.15	.2038	802	.6031	.7000	1.6801	2545	.1248	88.33	2.20	24.24	26.23
200.17	.2038	802	.6031	.7000	1.6801	2545	.1247	88.34	2.20	24.24	26.23
200.18	.2038	802	.6031	.7000	1.6801	2545	.1247	88.35	2.20	24.24	26.24
200.20	.2037	802	.6031	.7000	1.6801	2545	.1247	88.36	2.20	24.23	26.24

VALUE OF RATE INTEGRAL = .53769

PRESSURE IS 294.0 THE OXIDIZER BEING CONSIDERED IS 1

DZERO	RATE	TS	XNUST	ALFAST	RMOSP	TF	BETAF	XSTPO	XSTPF	XSTAF	XSTO
199.82	.2620	819	.6031	.7000	1.6801	2545	.0499	105.88	1.00	11.56	31.71
199.83	.2619	819	.6031	.7000	1.6801	2545	.0499	105.87	1.00	11.56	31.71
199.85	.2619	819	.6031	.7000	1.6801	2545	.0498	105.88	1.00	11.56	31.71
199.86	.2618	819	.6031	.7000	1.6801	2545	.0498	105.89	1.00	11.56	31.71
199.88	.2618	819	.6031	.7000	1.6801	2545	.0498	105.90	1.00	11.55	31.72
199.90	.2618	819	.6031	.7000	1.6801	2545	.0498	105.92	1.00	11.55	31.72
199.91	.2618	819	.6031	.7000	1.6801	2545	.0498	105.93	1.00	11.55	31.72
199.93	.2618	819	.6031	.7000	1.6801	2545	.0498	105.94	1.00	11.55	31.73
199.94	.2618	819	.6031	.7000	1.6801	2545	.0498	105.95	1.00	11.55	31.73
199.96	.2618	819	.6031	.7000	1.6801	2545	.0498	105.96	1.00	11.55	31.74
199.98	.2618	819	.6031	.7000	1.6801	2545	.0498	105.98	1.00	11.55	31.74
199.99	.2618	819	.6031	.7000	1.6801	2545	.0498	105.99	1.00	11.55	31.74
200.01	.2618	819	.6031	.7000	1.6801	2545	.0498	106.00	1.00	11.55	31.75
200.02	.2617	819	.6031	.7000	1.6801	2545	.0498	106.01	1.00	11.55	31.75
200.04	.2617	819	.6031	.7000	1.6801	2545	.0497	106.03	1.00	11.55	31.75
200.06	.2617	819	.6031	.7000	1.6801	2545	.0497	106.04	1.00	11.55	31.76
200.07	.2617	819	.6031	.7000	1.6801	2545	.0497	106.05	1.00	11.55	31.76
200.09	.2617	819	.6031	.7000	1.6801	2545	.0497	106.06	1.00	11.55	31.76
200.10	.2617	819	.6031	.7000	1.6801	2545	.0497	106.07	1.00	11.55	31.77
200.12	.2617	819	.6031	.7000	1.6801	2545	.0497	106.09	1.00	11.55	31.77
200.14	.2617	819	.6031	.7000	1.6801	2545	.0497	106.10	1.00	11.55	31.78
200.15	.2617	819	.6031	.7000	1.6801	2545	.0497	106.11	1.00	11.55	31.78
200.17	.2617	819	.6031	.7000	1.6801	2545	.0497	106.12	1.00	11.55	31.78
200.18	.2616	819	.6031	.7000	1.6801	2545	.0497	106.13	1.00	11.55	31.79
200.20	.2616	819	.6031	.7000	1.6801	2545	.0497	106.15	1.00	11.54	31.79

VALUE OF RATE INTEGRAL = .51068

PRESSURE IS 320.4 THE OXIDIZER BEING CONSIDERED IS 1

DZERO	RATE	TS	XNUST	ALFAST	RMOSP	TF	BETAF	XSTPO	XSTPF	XSTAF	XSTO
199.82	.3209	834	.6031	.7000	1.6801	2545	.0193	123.91	.44	5.23	37.40
199.83	.3207	834	.6031	.7000	1.6801	2545	.0193	123.89	.44	5.22	37.39
199.85	.3207	834	.6031	.7000	1.6801	2545	.0193	123.91	.44	5.22	37.40
199.86	.3207	834	.6031	.7000	1.6801	2545	.0193	123.92	.44	5.22	37.40
199.88	.3207	834	.6031	.7000	1.6801	2545	.0193	123.94	.44	5.22	37.41
199.90	.3207	834	.6031	.7000	1.6801	2545	.0193	123.95	.44	5.22	37.41
199.91	.3207	834	.6031	.7000	1.6801	2545	.0193	123.96	.44	5.22	37.41

199.93	.3207	854	.6031	.7000	1.6801	2545	.0193	123.96	.44	5.22	37.42
199.94	.3206	854	.6031	.7000	1.6801	2545	.0193	123.99	.44	5.22	37.42
199.96	.3206	854	.6031	.7000	1.6801	2545	.0193	124.00	.44	5.22	37.43
199.98	.3206	854	.6031	.7000	1.6801	2545	.0193	124.02	.44	5.22	37.43
199.97	.3206	854	.6031	.7000	1.6801	2545	.0193	124.03	.44	5.22	37.44
200.01	.3206	854	.6031	.7000	1.6801	2545	.0193	124.05	.44	5.22	37.44
200.02	.3206	854	.6031	.7000	1.6801	2545	.0193	124.06	.44	5.22	37.44
200.04	.3206	854	.6031	.7000	1.6801	2545	.0193	124.07	.44	5.22	37.45
200.06	.3205	854	.6031	.7000	1.6801	2545	.0193	124.09	.44	5.22	37.45
200.07	.3205	854	.6031	.7000	1.6801	2545	.0193	124.10	.44	5.22	37.46
200.09	.3205	854	.6031	.7000	1.6801	2545	.0193	124.12	.44	5.22	37.46
200.10	.3205	854	.6031	.7000	1.6801	2545	.0193	124.13	.44	5.22	37.47
200.12	.3205	854	.6031	.7000	1.6801	2545	.0193	124.14	.44	5.22	37.47
200.14	.3205	854	.6031	.7000	1.6801	2545	.0193	124.16	.44	5.22	37.47
200.15	.3205	854	.6031	.7000	1.6801	2545	.0193	124.17	.44	5.22	37.48
200.17	.3204	854	.6031	.7000	1.6801	2545	.0192	124.19	.44	5.22	37.48
200.18	.3204	854	.6031	.7000	1.6801	2545	.0192	124.20	.44	5.22	37.49
200.20	.3204	854	.6031	.7000	1.6801	2545	.0192	124.21	.44	5.22	37.49

VALUE OF RATE INTEGRAL = .62545

PRESSURE IS 932.0 THE OXIDIZER BEING CONSIDERED IS 1

DZERO	RATE	TS	XNUST	ALFAST	RHOSP	TF	BETAF	XSTPO	XSTPF	XSTAF	XSTO
199.82	.3786	846	.6031	.7000	1.6801	2545	.0072	141.17	.18	2.23	42.89
199.83	.3785	846	.6031	.7000	1.6801	2545	.0072	141.16	.18	2.22	42.89
199.85	.3785	846	.6031	.7000	1.6801	2545	.0072	141.18	.18	2.22	42.89
199.86	.3785	846	.6031	.7000	1.6801	2545	.0072	141.19	.18	2.22	42.90
199.88	.3784	846	.6031	.7000	1.6801	2545	.0072	141.21	.18	2.22	42.90
199.90	.3784	846	.6031	.7000	1.6801	2545	.0072	141.22	.18	2.22	42.91
199.91	.3784	846	.6031	.7000	1.6801	2545	.0072	141.24	.18	2.22	42.91
199.93	.3784	846	.6031	.7000	1.6801	2545	.0072	141.25	.18	2.22	42.92
199.94	.3784	846	.6031	.7000	1.6801	2545	.0072	141.27	.18	2.22	42.92
199.96	.3784	846	.6031	.7000	1.6801	2545	.0072	141.28	.18	2.22	42.93
199.98	.3783	846	.6031	.7000	1.6801	2545	.0072	141.30	.18	2.22	42.93
199.99	.3783	846	.6031	.7000	1.6801	2545	.0072	141.32	.18	2.22	42.93
200.01	.3783	846	.6031	.7000	1.6801	2545	.0072	141.33	.18	2.22	42.94
200.02	.3783	846	.6031	.7000	1.6801	2545	.0072	141.35	.18	2.22	42.94
200.04	.3783	846	.6031	.7000	1.6801	2545	.0072	141.36	.18	2.22	42.95
200.06	.3783	846	.6031	.7000	1.6801	2545	.0072	141.38	.18	2.22	42.95
200.07	.3782	846	.6031	.7000	1.6801	2545	.0072	141.39	.18	2.22	42.96
200.09	.3782	846	.6031	.7000	1.6801	2545	.0072	141.41	.18	2.22	42.96
200.10	.3782	846	.6031	.7000	1.6801	2545	.0072	141.43	.18	2.22	42.97
200.12	.3782	846	.6031	.7000	1.6801	2545	.0072	141.44	.18	2.22	42.97
200.14	.3782	846	.6031	.7000	1.6801	2545	.0072	141.46	.18	2.22	42.98
200.15	.3781	846	.6031	.7000	1.6801	2545	.0072	141.47	.18	2.22	42.98
200.17	.3781	846	.6031	.7000	1.6801	2545	.0072	141.49	.18	2.22	42.99
200.18	.3781	846	.6031	.7000	1.6801	2545	.0072	141.50	.18	2.22	42.99
200.20	.3781	846	.6031	.7000	1.6801	2545	.0072	141.52	.18	2.22	43.00

VALUE OF RATE INTEGRAL = .73763

PRESSURE IS 1652.3 THE OXIDIZER BEING CONSIDERED IS 1

DZERO	RATE	TS	XNUST	ALFAST	RHOSP	TF	BETAF	XSTPO	XSTPF	XSTAF	XSTO
199.82	.4295	856	.6031	.7000	1.6801	2545	.0027	138.73	.07	.92	48.48
199.83	.4294	856	.6031	.7000	1.6801	2545	.0027	138.73	.07	.92	48.48

199.85	.4294	856	.6031	.7000	1.6801	2545	.0027	158.75	.07	.92	48.48
199.86	.4293	856	.6031	.7000	1.6801	2545	.0027	158.77	.07	.92	48.49
199.88	.4293	856	.6031	.7000	1.6801	2545	.0027	158.78	.07	.92	48.49
199.90	.4293	856	.6031	.7000	1.6801	2545	.0027	158.80	.07	.92	48.50
199.91	.4293	856	.6031	.7000	1.6801	2545	.0027	158.82	.07	.92	48.51
199.93	.4293	856	.6031	.7000	1.6801	2545	.0027	158.83	.07	.92	48.51
199.94	.4292	856	.6031	.7000	1.6801	2545	.0027	158.85	.07	.92	48.52
199.96	.4292	856	.6031	.7000	1.6801	2545	.0027	158.87	.07	.92	48.52
199.98	.4292	856	.6031	.7000	1.6801	2545	.0027	158.89	.07	.92	48.53
199.99	.4292	856	.6031	.7000	1.6801	2545	.0027	158.90	.07	.92	48.53
200.01	.4292	856	.6031	.7000	1.6801	2545	.0027	158.92	.07	.92	48.54
200.02	.4292	856	.6031	.7000	1.6801	2545	.0027	158.94	.07	.92	48.54
200.04	.4291	856	.6031	.7000	1.6801	2545	.0027	158.95	.07	.92	48.55
200.06	.4291	856	.6031	.7000	1.6801	2545	.0027	158.97	.07	.92	48.55
200.07	.4291	856	.6031	.7000	1.6801	2545	.0027	158.99	.07	.92	48.56
200.09	.4291	856	.6031	.7000	1.6801	2545	.0027	159.00	.07	.92	48.56
200.10	.4291	856	.6031	.7000	1.6801	2545	.0027	159.02	.07	.92	48.57
200.12	.4290	856	.6031	.7000	1.6801	2545	.0027	159.04	.07	.92	48.57
200.14	.4290	856	.6031	.7000	1.6801	2545	.0027	159.06	.07	.92	48.58
200.15	.4290	856	.6031	.7000	1.6801	2545	.0027	159.07	.07	.92	48.58
200.17	.4290	856	.6031	.7000	1.6801	2545	.0027	159.09	.07	.92	48.59
200.18	.4290	856	.6031	.7000	1.6801	2545	.0027	159.11	.07	.92	48.59
200.20	.4289	856	.6031	.7000	1.6801	2545	.0027	159.12	.07	.92	48.60

VALUE OF RATE INTEGRAL = .85734

PRESSURE IS 2940.0 THE OXIDIZER BEING CONSIDERED IS 1

DZERO	RATE	TS	XNUST	ALFAST	RMUSP	TF	BETAF	XSTPO	XSTPF	XSTAF	XSTO
199.82	.4737	864	.6031	.7000	1.6801	2545	.0010	175.25	.03	.37	53.74
199.83	.4736	864	.6031	.7000	1.6801	2545	.0010	175.24	.03	.37	53.74
199.85	.4735	864	.6031	.7000	1.6801	2545	.0010	175.25	.03	.37	53.74
199.86	.4735	864	.6031	.7000	1.6801	2545	.0010	175.27	.03	.37	53.75
199.88	.4735	864	.6031	.7000	1.6801	2545	.0010	175.29	.03	.37	53.76
199.90	.4735	864	.6031	.7000	1.6801	2545	.0010	175.31	.03	.37	53.76
199.91	.4735	864	.6031	.7000	1.6801	2545	.0010	175.33	.03	.37	53.77
199.93	.4734	864	.6031	.7000	1.6801	2545	.0010	175.35	.03	.37	53.77
199.94	.4734	864	.6031	.7000	1.6801	2545	.0010	175.37	.03	.37	53.78
199.96	.4734	864	.6031	.7000	1.6801	2545	.0010	175.39	.03	.37	53.79
199.98	.4734	864	.6031	.7000	1.6801	2545	.0010	175.41	.03	.37	53.79
199.99	.4734	864	.6031	.7000	1.6801	2545	.0010	175.43	.03	.37	53.80
200.01	.4733	864	.6031	.7000	1.6801	2545	.0010	175.45	.03	.37	53.80
200.02	.4733	864	.6031	.7000	1.6801	2545	.0010	175.47	.03	.37	53.81
200.04	.4733	864	.6031	.7000	1.6801	2545	.0010	175.49	.03	.37	53.82
200.06	.4733	864	.6031	.7000	1.6801	2545	.0010	175.51	.03	.37	53.82
200.07	.4733	864	.6031	.7000	1.6801	2545	.0010	175.53	.03	.37	53.83
200.09	.4732	864	.6031	.7000	1.6801	2545	.0010	175.55	.03	.37	53.83
200.10	.4732	864	.6031	.7000	1.6801	2545	.0010	175.57	.03	.37	53.84
200.12	.4732	864	.6031	.7000	1.6801	2545	.0010	175.59	.03	.37	53.85
200.14	.4732	864	.6031	.7000	1.6801	2545	.0010	175.61	.03	.37	53.85
200.15	.4732	864	.6031	.7000	1.6801	2545	.0010	175.63	.03	.37	53.86
200.17	.4731	864	.6031	.7000	1.6801	2545	.0010	175.64	.03	.37	53.86
200.18	.4731	864	.6031	.7000	1.6801	2545	.0010	175.66	.03	.37	53.87
200.20	.4731	864	.6031	.7000	1.6801	2545	.0010	175.68	.03	.37	53.87

VALUE OF RATE INTEGRAL = .92265

PRES ATMS	PRES PSIA	BR CM/SEC	BR IN/SEC

2.00	29.4	.0992	.0391
3.54	52.0	.1172	.0461
6.34	93.2	.1562	.0615
11.24	165.2	.2039	.0803
20.00	294.0	.2619	.1031
35.40	520.4	.3207	.1263
63.40	932.0	.3783	.1489
112.40	1652.5	.4294	.1691
200.00	2940.0	.4732	.1863

SECURITY CLASSIFICATION OF THIS PAGE (When Data Entered)

REPORT DOCUMENTATION PAGE

READ INSTRUCTIONS BEFORE COMPLETING FORM

1. REPORT NUMBER: AFOSR - TR - 76 - 1099
2. GOVT ACCESSION NO.
3. RECIPIENT'S CATALOG NUMBER

4. TITLE (and Subtitle): MEAN FLOW/ACOUSTIC INTERACTIONS AND STATISTICAL ANALYSIS OF STEADY STATE COMBUSTION OF NON-METALLIZED COMPOSITE SOLID PROPELLANTS.

5. TYPE OF REPORT & PERIOD COVERED: FINAL rept. 1 May 74 - 30 Jun 76

6. PERFORMING ORG. REPORT NUMBER: U-76-18

7. AUTHOR(s): R. L. CLICK

8. CONTRACT OR GRANT NUMBER(s): F44620-74-C-0080

9. PERFORMING ORGANIZATION NAME AND ADDRESS:
THIOKOL CORPORATION
HUNTSVILLE DIVISION
HUNTSVILLE, ALABAMA 35807

10. PROGRAM ELEMENT, PROJECT, TASK AREA & WORK UNIT NUMBERS: 681308; AT-9711-01; 61102F; 9711-01

11. CONTROLLING OFFICE NAME AND ADDRESS:
AIR FORCE OFFICE OF SCIENTIFIC RESEARCH/NA
BLDG 410
BOLLING AIR FORCE BASE, D C 20332

12. REPORT DATE: 1976

13. NUMBER OF PAGES: 114

14. MONITORING AGENCY NAME & ADDRESS (if different from Controlling Office)

15. SECURITY CLASS. (of this report): UNCLASSIFIED

15a. DECLASSIFICATION/DOWNGRADING SCHEDULE

16. DISTRIBUTION STATEMENT (of this Report)

Approved for public release; distribution unlimited.

17. DISTRIBUTION STATEMENT (of the abstract entered in Block 20, if different from Report)

18. SUPPLEMENTARY NOTES

19. KEY WORDS (Continue on reverse side if necessary and identify by block number)
MONODISPERSE BDP COMBUSTION MODEL
HYDRAULIC T-BURNER ANALOG
NON-NEUTRAL PRESSURE-TIME HISTORY
POLYDISPERSE COMBUSTION MODEL
HETEROGENEOUS PROPELLANTS

20. ABSTRACT (Continue on reverse side if necessary and identify by block number)
A statistical frame work capable of extending any monodisperse combustion model (steady or nonsteady) to propellants with mixed, polydisperse oxidizer was developed. The BDP model was modified to conform to the ensemble averaging requirements of the method and embedded therein. Methods to include ellipsoidal particles and additives were explored and omissions in the BDP model were corrected. An operational FORTRAN IV code is available for polydisperse, additive free AP propellants. A hydraulic analog of a T-burner was constructed and employed to explore vent flow phenomena. Results show flow downstream of vent is a Karman

DD FORM 1 JAN 73 1473 EDITION OF 1 NOV 65 IS OBSOLETE

UNCLASSIFIED

SECURITY CLASSIFICATION OF THIS PAGE (When Data Entered)

401 944

vortex street created by periodic flow separation/attachment on alternate sides of vent as burner flow oscillates. Examination of Culick's one-dimensional theory has shown that vent gain prediction is a result of an improper boundary condition; proper condition yields null vent condition. A consistent method to deduce performance data from motor test data when pressure, time history is non-neutral was derived.